Cosmochemical study on the heterogeneity and diversity of nucleosynthetic components in the early solar system inferred from Ba and Sr isotopic analyses of primitive planetary materials

(始原惑星物質中の Ba および Sr 同位体分析からみた初期太陽系の原子核合成成分の不均質性と多様性に関する宇宙化学的研究)

SAKUMA, Keisuke

(佐久間　圭佑)

Cosmochemical study on the heterogeneity and diversity of nucleosynthetic components in the early solar system inferred from Ba and Sr isotopic analyses of primitive planetary materials

SAKUMA, Keisuke

Department of Earth and Environmental Sciences,

Graduate School of Environmental Studies, Nagoya University

始原惑星物質中の Ba および Sr 同位体分析からみた初期太陽系の原子核合成成分の不均質性と多様性に関する宇宙化学的研究

名古屋大学大学院環境学研究科地球環境科学専攻

佐久間　圭佑

Abstract

Isotopic compositions of several elements in the primitive planetary materials have been used to understand the cosmochemical evolution processes of the early solar system. High-precision isotopic data of carbonaceous chondrites have provided information of nucleosynthetic isotopic anomalies. Ba and Sr are suitable elements for the isotopic study to infer the origin and diversity of nucleosynthetic components because of their specific nuclear signatures. Ba and Sr have several stable isotopes, and are composed of s-, r- and p-process nucleosynthetic components. Additionally, ^{135}Ba and ^{87}Sr include radiogenic components decayed from ^{135}Cs ($t_{1/2}$ = 2.3 Ma) and ^{87}Rb ($t_{1/2}$ = 48.8 Ga), respectively. Therefore, Ba and Sr isotopic data of primitive planetary materials provide information about the evaluation of isotopic heterogeneity in the early solar system and the chronological approaches based on the ^{135}Cs–^{135}Ba and ^{87}Rb–^{87}Sr decay systems. In this study, isotopic analyses of Ba and Sr, and quantitative analyses of Rb, Sr, Cs, Ba and rare earth element (REE) abundances from the chemical separates obtained from sequential acid leaching experiments of five carbonaceous chondrites, Cold Bokkeveld, Murray, Nogoya, NWA 4428, and Tagish Lake, were performed to discuss the heterogeneity and diversity of nucleosynthetic components in the early solar system.

The Ba and Sr isotopic data from the whole rocks of carbonaceous chondrites often show a slight difference in their isotopic compositions compared with those of terrestrial materials (nucleosynthetic isotopic anomalies). On the other hand, the Ba and Sr isotopic data from most of the chemical separates show larger nucleosynthetic isotopic anomalies than those of the whole rocks. These Ba and Sr isotopic data set suggest a

heterogeneous distribution of several nucleosynthetic components in the early solar system. The sequential acid-leaching experiment is a useful approach to extract multiple fractions from the meteorite sample, which cannot be detected from the analyses of the whole rock samples.

The Ba isotopic data for the acid residues show a series of remarkably isotopic deficits of ^{130}Ba, ^{132}Ba, ^{135}Ba, ^{137}Ba, and ^{138}Ba, which suggests the enrichments of s-process isotopes caused by the presence of presolar SiC grains. Furthermore, the correlation between the isotopic data for ^{135}Ba, ^{137}Ba, and ^{138}Ba for the acid residues in Cold Bokkeveld, Murray, and Nogoya suggested the contribution of n-process nucleosynthetic components. In order to discuss the ^{135}Cs isotopic abundance, two new models were proposed in which the contribution of s- and n-process nucleosynthetic components is subtracted from the isotopic compositions of the acid residues. The correlation of the maximum value of ^{135}Ba isotopic data obtained from the model with Cs/Ba ratio provides the upper limit of the ^{135}Cs isotopic abundance (^{135}Cs/^{133}Cs), as (2.28 ± 0.43/2.28 ± 0.41) × 10^{-4} for Cold Bokkeveld, (1.40 ± 1.21/1.39 ± 0.85) × 10^{-4} for Murray, and (4.32 ± 0.68/4.31 ± 0.65) × 10^{-4} for Nogoya, respectively.

CONTENTS

CHAPTER 1

General Introduction

1.1 Isotopic studies of primitive planetary materials

Meteorites are important in understanding the origin and early planet evolution processes in the solar system, and are valuable materials that can be directly treated as extraterrestrial samples. Despite their diversity, the primitive meteorites, that have experienced little differentiation or metamorphosis, are thought to retain information of the early solar system. Therefore, a number of studies have been conducted on the mineral composition, chemical composition, and isotopic composition in meteoritic samples.

Elements of the solar system are composed of several nucleosynthetic components that existed before the formation of the solar system. These diverse components with different isotopic compositions depending on their origin were homogenized during the evolution process after the formation of the early solar system. However, recent high-precision isotopic data of several elements of primitive planetary materials have confirmed a slight difference in their isotopic compositions compared with those of terrestrial materials, which are recognized as nucleosynthetic isotopic anomalies (Cr, Sr, Ba, Nd and Sm and so on: Andreasen and Sharma, 2006; 2007; Carlson et al., 2007; Trinquier et al., 2007; Moynier et al., 2012; Bermingham et al., 2016). These results suggest that the primitive planetary materials retain the isotopic heterogeneity of the early solar system.

Considering the circumstances of the early solar system, the isotopic compositions in the primitive planetary materials may be affected by the presence of

radionuclides having half-lives ($t_{1/2}$) of less than 100 million years (Ma) and are now completely decaying. ^{129}I ($t_{1/2}$ =16 Ma) was detected for the first time as evidence of extinct nuclide in meteorite samples based on the isotopic excess of ^{129}Xe (Reynolds, 1960). The extinct nuclides have been used as valuable tools to consider the early solar system chronology (e.g., Fujiya et al., 2012, 2013). Because radionuclides decay with their half-lives, the primitive planetary material is the most suitable sample to detect isotopic evidence for the presently extinct nuclides. To discuss the estimation of isotopic abundances of decay of extinct nuclides, it is necessary to prove as isotopic excess components of daughter nuclides which show a quantitative correlation with elemental data including parent nuclides and daughter nuclides. High-precision isotopic analysis by mass spectrometry is a useful method for detecting small isotopic excess components associated with the decay of small amounts of extinct nuclides in the early solar system, and enables quantitative discussion of the abundance of extinct nuclides.

Comprehensive measurements of the elemental abundances and the isotopic compositions of multiple elements in primitive planetary materials make it possible to systematically discuss the origin of the isotopic variations.

1.2 Isotopic studies of Ba

1.2.1 Nuclear signature of Ba isotopes

Barium is a suitable element for the isotopic studies to understand the homogeneous or heterogeneous conditions of nucleosynthetic components in the early solar system because of its specific nuclear signature. A part of the nuclear chart around Ba isotopes is shown in Fig. 1. Elements heavier than Fe are synthesized mainly by neutron capture reactions. The neutron capture reactions are classified into the s-process

(slow neutron capture) and r-process (rapid neutron capture). In addition, there is a p-process (photo-dissociation of nuclides) as a process for synthesizing proton-rich isotopes with low isotopic abundance. Barium has seven stable isotopes with mass numbers 130, 132, 134, 135, 136, 137 and 138. ^{130}Ba and ^{132}Ba with low isotopic abundance (< 1%) are the p-process isotopes. ^{134}Ba and ^{136}Ba are the s-process isotopes. ^{135}Ba, ^{137}Ba, and ^{138}Ba are the s- and r-process isotopes. In addition, radiogenic ^{135}Ba components decayed from presently extinct ^{135}Cs ($t_{1/2}$ = 2.3 Ma) may also affect the isotopic abundance of ^{135}Ba. Isotopic analyses of Ba in primitive planetary materials led to the evaluation of isotopic heterogeneity in the solar system and may be applied to the chronological study based on the ^{135}Cs–^{135}Ba decay system.

Ba isotopic data of primitive planetary materials showed isotopic anomalies of ^{135}Ba correlated with ^{137}Ba, suggesting the heterogeneous distribution of the nucleosynthetic components of s-process isotopes in the early solar system (Hidaka et al., 2003; Andreasen and Sharma, 2007; Carlson et al., 2007; Qin et al., 2011; Hidaka and Yoneda, 2011, 2013; Bermingham et al., 2014, 2016). The Ba isotopic data of chemical separates obtained by sequential acid-leaching experiments of CI and CM chondrites showed larger isotopic anomalies of Ba than those of whole rocks (WRs) (Hidaka et al., 2003; Hidaka and Yoneda, 2011; Qin et al., 2011). In particular, the remarkable isotopic anomalies of the acid residues in CM chondrites are isotopic evidence for the enrichment of s-process isotopes caused by the presence of presolar SiC grains (Ott and Begemann, 1990; Zinner et al., 1991; Prombo et al., 1993). These results revealed the isotopic heterogeneity of Ba in the primitive planetary materials.

Advances in mass spectrometric technology over the past decade have made it possible to perform high-precision Ba isotopic analyses having the analytical

uncertainties of $\varepsilon < 0.1$ which is nearly ten times better than those in previous studies (Hidaka et al., 2001, 2003; Hidaka and Yoneda, 2011, 2013). As a result, it became possible to detect several isotopic variations even in the WR of primitive planetary materials without any chemical separation (Andreasen and Sharma, 2006, 2007; Carlson et al., 2007; Bermingham et al., 2016). Unlike the isotopic composition of WR in carbonaceous chondrites, the Ba isotopic composition of WR of enstatite chondrites, ordinary chondrites, achondrites (eucrites, angrites, Martian meteorite), and lunar materials was found to be indistinguishable from those of terrestrial materials (Andreasen and Sharma, 2007; Carlson et al., 2007; Bermingham et al., 2016; Brennecka and Kleine, 2017). In the Ba isotopic compositions of chemical separates of ordinary and carbonaceous chondrites other than CI and CM chondrites, the magnitude of their isotopic anomaly is smaller than that of CI and CM chondrites (Hidaka et al., 2003; Hidaka and Yoneda, 2011; Qin et al., 2011). Unlike CI and CM chondrites, these chondrites had experienced thermal metamorphism on meteorite parent bodies. In other words, the thermal metamorphic event may be one of the factors that homogenized the isotopic composition in the primitive planetary materials. The results of Ba isotopic analysis of differentiated meteorites suggest that the information of isotopic anomalies caused by the additional nucleosynthesis components may have disappeared by the differentiation process of these parent bodies (Hidaka et al., 2003; Hidaka and Yoneda, 2016). These results suggest that CI and CM chondrites, which have experienced mainly aqueous alteration, may provide important information for evaluating the heterogeneity of nucleosynthetic components in the early solar system.

Although many cases of Ba isotopic anomalies have been reported mainly due to the contribution of the s-process nucleosynthetic component (Hidaka et al., 2003;

Andreasen and Sharma, 2007; Carlson et al., 2007; Qin et al., 2011; Hidaka and Yoneda, 2011, 2013; Bermingham et al., 2014, 2016), there are several cases of Ba isotopic anomalies due to other minor contributions. McCulloch and Wasserburg (1978a) reported the r-process isotopic anomalies from FUN (fractionation and unknown nuclear effects) inclusions in the Allende meteorites. Lewis et al. (1991) also reported the r-process isotopic anomalies from the nanodiamonds in the Allende meteorites. In recent years, isotopic analyses of individual presolar SiC grains have been carried out to provide a wealth of information in the cosmochemical and astrophysical research fields, including information on stellar nucleosynthesis and evolution, and the inventory of presolar grains (e.g. Hoppe et al., 2010). As a result, it was found that there were various degrees of isotope variation in each presolar SiC grain (Pellin et al., 2000, 2006; Liu et al., 2015; Stephan et al., 2018). In particular, presolar X grains, which are a minor type of presolar SiC grains, had a very specific isotopic composition. X grains are thought to come from type II Supernova (SNeII), called n-process components (Ranen and Jacobsen, 2006). X grains account for 1–2% of all presolar SiC grains (Hoppe et al., 2010). The isotopic signature of n-process components indicates a neutron burst signature (Pellin et al., 2006). The Ba isotopic data for these presolar X grains showed significant isotopic excesses of ^{137}Ba on ^{138}Ba (Pellin et al., 2000, 2006; Stephan et al., 2018). A coupled isotopic excess of ^{137}Ba and ^{138}Ba was also reported in the WR of carbonaceous chondrites (Ranen and Jacobsen, 2006), suggesting the isotopic anomalies due to the contribution of the n-process component. Later, however, Andreasen and Sharma (2007) pointed out that the isotopic anomalies may have been caused by analytical problems.

1.2.2 Isotopic studies of the extinct nuclide of ^{135}Cs

Evaluation of the isotopic abundances of ^{135}Cs in the early solar system is still debated in the cosmochemical and astrophysical research fields. Extinct nuclides heavier than iron are considered to be synthesized mainly the r-process, which is one of the main nucleosynthetic processes of the elements that make up the solar system. Based on a uniform galactic production (UP) model proposed by previous studies (e.g. Wasserburg et al., 1996; Busso et al., 1999), there is a rough correlation and discontinuity between the abundances of extinct nuclides and their half-lives. This result suggests that the r-process nuclides have multiple origins. In particular, the formation mechanism of these nuclides may be different between lighter and heavier nuclides around the mass number 140 (Wasserburg et al., 1996; Busso et al., 1999). Because ^{135}Cs is an extinct nuclide with a mass number close to 140, ^{135}Cs may have contributions from multiple r-process nucleosynthetic components. In addition, considering that ^{135}Cs is a nuclide that can be synthesized in the s-process, Hidaka and Yoneda (2013) pointed out that its initial abundance may be higher than that expected from the UP model. Therefore, it is important to estimate the abundance of ^{135}Cs based on chemical and isotopic data of the primitive planetary materials.

McCulloch and Wasserburg (1978a) firstly reported the possible abundance of ^{135}Cs from the isotopic deficit of ^{135}Ba in one of the Allende inclusions. Pioneer worker (Hidaka et al., 2001) reported isotopic excesses of ^{135}Ba correlated with high Cs/Ba elemental ratio, suggesting isotopic evidence of extinct nuclide ^{135}Cs. This study used a sequential acid-leaching experiment to collect chemical separates having high Cs/Ba elemental ratio (Cs/Ba = 19.8; Cs/Ba = 0.0799: CI, Anders and Grevesse, 1989) in alkali-rich H chondrite (Beardsley). Subsequently, although the same leaching experimental method was applied to carbonaceous chondrite to search for isotopic evidence of ^{135}Cs

based on the isotopic excess of ^{135}Ba correlated with a high Cs/Ba elemental ratio, it was difficult to find evidence of radiogenic components of ^{135}Ba (Hidaka et al., 2003; Hidaka and Yoneda, 2011, 2013). In previous studies, the Cs/Ba elemental ratio of the primitive planetary materials is low, and even chemical separates recovered by the acid-leaching experiment could not find a high Cs/Ba elemental ratio in those of carbonaceous chondrites (Cs/Ba < 0.300, Hidaka et al., 2003; Hidaka and Yoneda, 2011) as seen in the H chondrite. As a result, although there are various studies on Ba isotopes in WRs and chemical separates of early condensates (McCulloch and Wasserburg, 1978a; Hidaka et al., 2001; Brennecka et al., 2013; Hidaka and Yoneda, 2013; Bermingham et al., 2014), various types of carbonaceous chondrites (Hidaka et al., 2003; Hidaka and Yoneda, 2011; Bermingham et al., 2016), ordinary chondrite (Hidaka et al., 2001; Bermingham et al., 2016), and differentiated meteorites (Hidaka et al., 2003; Bermingham et al., 2016; Brennecka and Kleine, 2017), the initial abundance of ^{135}Cs is still unknown.

1.3 Isotopic studies of Sr

In a similar fashion to Ba, Sr isotopic data of primitive planetary materials have been used to discuss the evolution process in the early solar system. Sr has four stable isotopes: ^{84}Sr is the p-process isotope, ^{86}Sr and ^{87}Sr are s-process isotopes, and ^{88}Sr is s- and r-process isotopes. In addition, ^{87}Sr includes a radiogenic component that was derived from the decay of ^{87}Rb ($t_{1/2}$ = 48.8 Ga). In previous studies, the ^{87}Rb–^{87}Sr decay system had been applied to the chronological study in the cosmochemical field (e.g., Kaushal and Wetherill, 1970; Mittlefehldt and Wetherill, 1979; MacDougall et al., 1984; Macdougall, 2000). In recent years, high-precision Sr isotopic analysis of primitive planetary materials found a variation of ^{84}Sr/^{88}Sr (Andreasen and Sharma, 2007; Moynier et al., 2012). Sr

isotopic data for the WRs of carbonaceous chondrites showed an isotopic excess of ^{84}Sr. Sr isotopic data for the chemical separates of CI and CM chondrites and the Tagish Lake meteorite (C2-ungrouped) showed larger nucleosynthetic isotopic anomalies than those of the WR samples (Paton et al., 2013; Qin et al., 2011; Yokoyama et al., 2015). Furthermore, isotopic excess of ^{84}Sr of Ca- and Al-rich inclusions (CAIs) in the Allende meteorite has a higher than those of carbonaceous chondrites (Moynier et al., 2012; Hans et al., 2013). Sr isotopic data for acid residues in the CI and CM chondrites and the Tagish Lake meteorite showed significant negative isotopic anomalies of ^{84}Sr (Qin et al., 2011; Yokoyama et al., 2015; Burkhardt et al., 2019), suggesting the presence of presolar SiC grains (Podosek et al., 2004; Liu et al., 2015). Recent studies on the isotopic composition of presolar SiC grains have reported not only the s-process nucleosynthetic components having a significant isotopic deficit of ^{84}Sr (Liu et al., 2015), but also the X grains having a significant isotopic excess of ^{88}Sr (Pellin et al., 2000, 2006; Stephan et al., 2018). These results suggest a heterogeneous distribution of Sr isotope in the early solar system.

On the other hand, because the Sr isotopic data were normalized to ^{88}Sr/^{86}Sr = 8.375209 for the correction of instrumental mass fractionation, the variation of ^{84}Sr/^{86}Sr in primitive planetary materials may not only be from the heterogeneity of p-process isotope (^{84}Sr), but also from apparent isotopic anomalies affecting the normalized ratio (^{88}Sr/^{86}Sr). For this reason, it is difficult to elucidate the origin of the isotopic anomaly in the Sr isotope alone (Papanastassiou and Wasserburg, 1978; Andreasen and Sharma, 2007), but the combination of Sr and Ba isotopic data enables complementary consideration of the origin of their isotopic anomalies.

1.4 Nuclear reactions in planetary materials associated with cosmic-ray irradiation

The surface parts of planetary materials without atmosphere are exposed to cosmic rays. Cosmic rays are classified into galactic cosmic rays (GCRs) and solar cosmic rays (SCRs) based on their origins. These cosmic rays interact with the surface of planetary material, leading to nuclear spallation reactions and neutron capture reactions in which the surrounding nuclei capture secondarily generated neutrons. The effects of these nuclear reactions had been found to show a significant variation of isotopic composition in some elements.

Bermingham et al. (2016) conducted Ba isotopic analyses of WRs of various meteorite samples and discussed the effects of cosmic-ray irradiation. Considering the Ba isotopic data, neutron capture reaction cross section of Ba and the cosmic ray exposure (CRE) age for each sample, the isotopic anomalies by the nuclear reactions with cosmic-ray irradiation could not be detected in the measured Ba isotopic data. However, remarkable variations in the Sr and Ba isotopic compositions have been reported from the results of isotopic analysis of extraterrestrial materials experienced to intense cosmic-ray irradiation (Hidaka and Yoneda, 2014, 2017). Hidaka and Yoneda (2014) found systematic isotopic excesses in ^{84}Sr, ^{130}Ba, ^{132}Ba, ^{136}Ce, ^{138}Ce, and ^{144}Sm on the surface parts of the Kapoeta meteorite, which is known as a solar-gas rich meteorite (Caffee and Nishiizumi, 2001) and may be experienced early intense irradiation by SCRs (Hidaka and Yoneda, 2009). They mentioned that the isotopic anomalies may be due to the nuclear reaction associated with intense cosmic-ray irradiation from the young sun.

Nuclear reactions by the interaction between cosmic-ray and primitive planetary materials are considered as one of the formation processes of extinct nuclides, such as ^{10}Be, in the early solar system (Mckeegan et al., 2000). Because evidence for the existence of the extinct radionuclides has been found in *in-situ* analyses of some CAIs, the effects

of nuclear reactions associated with intense cosmic-ray irradiation from the young sun may be one factor of the origins of isotopic anomalies in the primitive planetary materials. Consideration the isotopic data of ^{84}Sr, ^{130}Ba, and ^{132}Ba from primitive planetary materials may provide information to discuss the contribution of intense cosmic-ray irradiation from the young sun in terms of variations in these isotopic compositions.

1.5 Research objectives and thesis structure

The purpose of this study is to elucidate the heterogeneity and diversity of nucleosynthetic components in primitive planetary materials. While Ba is a suitable element for assessing isotopic heterogeneity in the early solar system, previous cosmochemical studies on Ba isotope have some fundamental problems.

The Ba isotopic compositions of the primitive planetary materials may be affected by the contribution of the additional nucleosynthetic components in the early solar system, the contribution of the radiogenic ^{135}Ba components decayed from ^{135}Cs, and the nuclear reaction with the cosmic-ray irradiation. Therefore, it is necessary to measure all seven stable Ba isotopes to consider Ba isotopic anomalies in the primitive planetary materials, but the measurement of all Ba isotopes in samples have not been carried out even in recent studies (Bermingham et al., 2016; Brennecka and Kleine, 2017).

As noted above, because the ^{135}Ba isotopic abundances in primitive planetary materials may contain the isotopic excess of ^{135}Ba derived from ^{135}Cs, the quantitative estimation of the contribution of ^{135}Cs contained in the Ba isotopic data should be considered using complementary isotopic data and elemental concentration data including daughter and parent nuclides of the samples. However, the quantitative analysis of Cs has not been carried out in most previous Ba isotopic studies (Andreasen and

Sharma, 2007; Bermingham et al., 2014, 2016), and it is impossible to quantitatively estimate the radiogenic isotopic excess of ^{135}Ba depending on the elemental abundance of Cs. In this study, therefore, the abundance of ^{135}Cs is discussed based on the Cs/Ba elemental ratios and Ba isotopic data in the sample.

In this thesis, I report herewith the elemental abundances and isotopic compositions of Ba and Sr in the chemical separates from carbonaceous chondrites, and attempt a detailed discussion of the heterogeneity and diversity of nucleosynthetic components in the early solar system. I also discuss the estimate of the ^{135}Cs abundance in the early solar system and the possibility of isotopic anomalies caused by ancient SCR irradiation from the young Sun.

CHAPTER 2

Samples and Experimental method

2.1 Samples

Five carbonaceous chondrites, three CM chondrites (Cold Bokkeveld, Murray, and Nogoya), one CM anomalous chondrite (NWA 4428), and one C2-ungrouped chondrite (Tagish Lake), were used in this study. A common feature of these chondrites is the presence of secondary minerals, such as serpentines, oxides, and calcites, which is evidence for aqueous alteration on the parent bodies (Tomeoka and Buseck, 1985; Zolensky et al., 1989; Brown et al., 2000; Zolensky et al., 2002). Details of these samples used are shown in Table 1.

2.1.1 Cold Bokkeveld

The Cold Bokkeveld meteorite fell in 1838 to Cape Province, South Africa. A petrological study (Rubin et al., 2007) showed evidence that this meteorite experienced intense aqueous alteration on the meteorite parent body, and the petrological type of this meteorite is classified as 2.2. The weathering grade of this meteorite is low among CM chondrites (W0-1, Rubin et al., 2007). The CRE age of this meteorite is 0.32 ± 0.04 Ma, which is typical of CM chondrites (Heymann and Anders, 1967).

2.1.2 Murray

The Murray meteorite fell in 1950 to Kentucky, United States. The petrological study (Rubin et al., 2007) has classified the petrological type of this meteorite as 2.4/2.5,

which means a low degree of aqueous alteration on the meteorite parent body. The weathering grade of this meteorite varies (W1~2, Rubin et al., 2007), with some samples being affected by terrestrial weathering. The Murray has the longer CRE age (2~ 6 Ma) than typical of CMs, and may have a complicated cosmic-ray irradiation history (Herzog et al., 1997). In addition, a previous study of elemental and isotopic abundances of the noble gases in the chondrules in Murray showed that the CRE history of chondrule is more complex than that of the whole rock, suggesting the possibility of excess irradiation record by SCR (Das and Murty, 2009).

2.1.3 Nogoya

The Nogoya meteorite fell in 1879 to Entre Rios, Argentina. The petrological study (Rubin et al., 2007) showed that this meteorite was classified into the petrological type of 2.2, which means that it experienced intense aqueous alteration on the meteorite parent body. The weathering grade is the lowest value (W0, Rubin et al., 2007). The CRE age of this meteorite is 0.14 ± 0.04 Ma (Heymann and Anders, 1967), which is the shortest CRE age used in this study.

2.1.4 North West Africa 4428 (NWA 4428)

The NWA 4428 is a meteorite that has not been approved by the Meteorological Society. This meteorite was found in Northwest Africa (CM2 anomalous).

2.1.5 Tagish Lake

The Tagish Lake meteorite fell in 2000 to Tagish Lake, which spans British Columbia from the Yukon Territory in Canada (Brown et al., 2000). From a chemical and

isotopic standpoint (Brown et al., 2000; Friedrich et al., 2002), the Tagish Lake meteorite shows similarities to CI and CM chondrites. On the other hand, the Tagish Lake meteorite has lower density and higher porosity than CI and CM chondrite, and is identified as a C2-ungrouped chondrite (Zolensky et al., 2002). Based on the Re-Os systematics and platinum group element measurements, Brandon et al. (2005) pointed out that the Tagish Lake meteorite may originate from the same parent body as CI and CM chondrites, but the relationship between three carbonaceous chondrites is still unclear (Hiroi et al., 2001; Vernazza et al., 2013). From the spectroscopic studies, the Tagish Lake meteorite may be originated from a D-class asteroid (Hiroi et al., 2001), and there are reports that the parent body of the Tagish Lake meteorite is different from that of CM chondrite (Vernazza et al., 2013). The Tagish Lake meteorite has the CRE age of 5.5 ± 0.7 Ma (Nakamura et al., 2003).

2.2 Experimental method

2.2.1 Acid-leaching experiments

Each of the powdered samples weighing 400 to 1000 mg was used in this study. To assess the origin of isotopic anomalies in primitive planetary materials, a sequential acid-leaching experiment was performed based on the previous study (Hidaka et al., 2001). The majority of each of the powdered samples (~90%) was leached using 5 mL of 0.1 M CH_3COOH-CH_3COONH_4, 0.1 M HCl, 2 M HCl, and aqua regia, successively. The amounts of reagents described above are for the Tagish Lake (< 400 mg), and in the case of CM chondrites (500~900 mg), 10 mL of the reagents were used. In each leaching procedure, the sample was ultrasonicated for 1 hour, and kept at room temperature for 23 hours. The acid residue and another aliquot of the powdered sample (< 100 mg) were

decomposed by HF–$HClO_4$ for 5 days at 130–150℃. Each fraction was dried and redissolved with 2 M HCl of 1–5 mL. These samples of five leaching fractions and whole rock were designated as L1, L2, L3, L4, L5, and WR, respectively. The sample of individual leaching fraction was divided into two portions: a major portion (~90%) for Sr and Ba isotopic analyses by thermal ionization mass spectrometry (TIMS) and another minor portion (~10%) for the determination of elemental abundances of Rb, Sr, Cs, Ba and rare earth elements (REEs) by inductively coupled plasma mass spectrometry (ICP–MS). Fig. 2 shows the experimental scheme of the sequential acid-leaching experiment and chemical separation procedure.

2.2.2 Chemical separates

Major portions of L1–L5 and WR fractions were used for the isotopic studies after chemical separation with conventional resin chemistry (Hidaka and Yoneda, 2014). Table 2 shows the scheme of the chemical separation and purification for Sr and Ba. Each sample solution was passed through a column packed with cation exchange resin (AG50WX8, 200–400 mesh, H^+ form, 50 mm length × 4.0 mm diameter). The column was washed with 3.5 mL of 2 M HCl to remove the major elements. Then, the column was washed with 3.5 mL of 2 M HCl to elute Sr fraction. Finally, the column was washed with 3 mL of 2 M HNO_3 to elute the Ba fraction. For further purification of Sr and Ba fractions, each fraction was passed through a column packed with a Sr resin (Eichrom, Sr resin, particle size of 100–150 μm, 50 mm length × 4.0 mm diameter). For Sr fraction, the column was washed with 2.5 mL of 3 M HNO_3, and was washed with 3 mL of ultrapure water to elute the Sr fraction. For Ba fraction, the column was washed with 3.5 mL of 3 M HNO_3, and was washed with 6.5 mL of 7.5 M HNO_3 to elute the Ba fraction.

2.3 Analytical procedure

2.3.1 Isotopic analyses by TIMS

Isotopic measurements of Ba and Sr were carried out by a thermal ionization mass spectrometer (TRITON–Plus) at Department of Science and Engineering, Tsukuba research departments, National Museum of Nature and Science in this study. The TRITON–Plus was equipped with nine Faraday cup collectors linked to 10^{11} Ω resistors. Data correction was performed in static mode with the amplifier rotation system to cancel out amplifier gains. Isotopic measurements consist of 10 cycles as 1 block. For each isotopic measurement, the peak center was performed for 30 seconds at the start of the measurement, and the baseline measurement and the lens focus were performed every at 5 blocks. Table 3 shows the Faraday cup configuration and zoom optics for Ba and Sr isotopic measurements by the TRITON–Plus.

The Ba fraction was redissolved in 1–2 μl of ultrapure water, depending on the sample size. For Ba isotopic measurements, the Ba fraction was loaded on the outer filament of a double Re filament assembly, without any activators. Barium isotopic analyses were performed to monitor the seven Ba isotopes, ^{130}Ba, ^{132}Ba, ^{134}Ba, ^{135}Ba, ^{136}Ba, ^{137}Ba, and ^{138}Ba, in addition, to monitor ^{139}La and ^{140}Ce for evaluation of isobaric interferences of ^{138}La, ^{136}Ce, and ^{138}Ce in the Ba mass spectra. During any analyses in this study, detectable interferences from La and Ce were not found. The integration time for Ba isotopic measurement was 8.389 seconds having 3 seconds of idle time. A $^{138}Ba^{+}$ ion beam of (1.0–24) × 10^{-11} A was obtained for more than 1 hour from individual fractions. All Ba isotopic data were referenced to ^{136}Ba. Ba isotopic data were normalized by ^{134}Ba/^{136}Ba = 0.307776 (Hidaka et al., 2003; Hidaka and Yoneda, 2011, 2013, 2014)

to correct for instrumental mass fractionation using the exponential law. The correction coefficient f_e used in the exponential law is obtained as the following equation:

$$f_e = \frac{(^{134}\mathrm{Ba}\ /^{136}\mathrm{Ba}\ )_{\mathrm{measured}}}{0.307776}$$

The measured isotopic data (^{i}Ba/^{136}Ba) were corrected for instrumental mass fractionation based on the exponential law and f_e using the following equation.

$$\left(\frac{^{i}\mathrm{Ba}}{^{136}\mathrm{Ba}}\right)_{\mathrm{corrected}} = \left(\frac{^{i}\mathrm{Ba}}{^{136}\mathrm{Ba}}\right)_{\mathrm{measured}} \Big/ f_e^{\frac{\ln(\ ^{i}\mathrm{M}\ /^{136}\mathrm{M}\ )}{\ln(^{134}\mathrm{M}\ /^{136}\mathrm{M}\ )}}$$

Where i is the mass number of the Ba isotope (130, 132, 135, 137, and 138), ^{i}M is the mass of isotopes.

On the other hand, some studies were normalized using ^{134}Ba/^{138}Ba isotopic ratios, and ^{134}Ba/^{138}Ba ratios were used to correct the mass fractionation effects during mass spectrometry of the isotopic data (McCulloch and Wasserburg, 1978; Lewis et al., 1991; Bermingham et al., 2016). The isotopic data have also confirmed the Ba isotopic anomalies, and the homogeneity of nucleosynthetic components in the early solar system was discussed based on the results. However, it is impossible to consider the isotopic anomaly of ^{138}Ba because the normalization has been carried out using ^{134}Ba isotope synthesized from the s-process and ^{138}Ba isotope synthesized from s- and r-processes. In this study, all Ba isotopic data have been normalized to ^{134}Ba/^{136}Ba, which are isotopes synthesized only from s-process, as in many recent studies (Hidaka et al., 2003; Andreasen and Sharma, 2007; Carlson et al., 2007; Qin et al., 2011; Hidaka and Yoneda,

2011, 2013; Brennecka et al., 2013; Bermingham et al., 2014; Brennecka and Kleine, 2017). Therefore, if any isotopic anomalies are observed in measured Ba isotopic data, it is possible to consider the contribution of the relative nuclear components to s-process isotopes. It is also possible that the ^{135}Ba isotopic excess decayed from ^{135}Cs can be detected as an isotopic excess of the only ^{135}Ba which is correlated with the Cs/Ba ratio.

The Sr fraction was redissolved in 1–2 μl of ultrapure water, depending on the sample size. For Sr isotopic measurements, the Sr fraction was loaded on a single Re filament. The sample on Re filament was overcoated with 1.0 μl of a Ta_2O_5 activator. Sr isotopic analyses were performed to monitor the four Sr isotopes, ^{84}Sr, ^{86}Sr, ^{87}Sr, and ^{88}Sr, together with ^{85}Rb to evaluate the isobaric interference of ^{87}Rb for ^{87}Sr. The integration time for Sr isotopic measurement was 16.777 seconds having 3 seconds of idle time. An $^{88}Sr^{+}$ ion beam of (0.16–23) × 10^{-11} A was obtained for more than 1 hour from individual fractions. All Sr isotopic data were referenced to ^{86}Sr. Sr isotopic data were normalized by $^{88}Sr/^{86}Sr$ = 8.375209 to correct for instrumental mass fractionation using the exponential law.

In this study, a standard Sr solution produced by NIST SRM-987 and standard Ba solution produced by SPEX CertiPrep were used for Sr and Ba isotopic analyses.

2.3.2 Quantitative analysis by ICP–MS

An ICP-MS (Agilent 7700cx) was used for quantitative analysis of Rb, Sr, Cs, Ba, and REEs in individual chemical separates and the WRs at Nagoya University in this study. The minor portion of each sample solution was completely evaporated and then redissolved using 5 mL of 2% HNO_3. Each sample solution was appropriately diluted for quantitative analysis of trace elemental abundances. The calibration curve method was

used for the determination of trace elements. In the determination of REEs, the interference from Ba and lighter REEs (La, Ce, Pr, Nd, Sm, Eu, Gd, and Tb) oxides to heavier REEs was corrected. In this study, a correction value for the interference of oxides was obtained using standard materials. Based on the values, the determination of REEs in the samples was carried out.

CHAPTER 3

Results

3.1 Elemental abundances of chemical separates and whole rocks of carbonaceous chondrites

The data of elemental abundances of Rb, Sr, Cs, Ba, and REEs in the L1–L5 and WR of all five carbonaceous chondrites are listed in Table 4. The “sum” is the data of elemental abundances for the whole rock based on the sum of the data of elemental abundances for each chemical fraction (see in Table 4). Fig. 3 shows the CI-chondrite normalized REE patterns of each sample in this study. Comparing the sum of the elemental abundances with the measured WRs, these values are in good agreement (see in Table 4, Fig. 3), which suggests that all the components contained in carbonaceous chondrites in this study were completely dissolved by the sequential acid-leaching experiment.

The WR analysis of NWA 4428 showed enrichment of Sr and Ba (Sr, CI × 5.8 ppm; Ba, CI × 16.2 ppm). The REE pattern of NWA 4428 showed an enrichment in the light REEs (LREEs, La–Sm), which are unusual in common CM meteorites, suggesting the addition of terrestrial contaminants by weathering after their fall onto Earth (see in Fig. 3). The REE pattern of WR of Murray showed the enrichment in LREE compared with that of some carbonaceous chondrites, such as Cold Bokkeveld and Nogoya. The Tagish Lake of WR had enrichments of Sr and Ba (see in Table 4), which is higher than those of Cold Bokkeveld and Nogoya. The Murray and Tagish Lake meteorites showed various degrees of weathering grade (Friedrich et al., 2002; Rubin et al., 2007). Judging

from the weathering grade and enrichments of LREEs, Sr, and Ba, the chemical compositions of Murray and Tagish Lake used in this study may be affected by terrestrial weathering.

It is known that most REEs are enriched in refractory inclusions. Because the condensation temperature of Eu and Yb are lower than those of the other REEs, the REE pattern of the refractory inclusions like a hibonite shows negative Eu and Yb anomalies (Ireland et al., 1988). In particular, the REE pattern of the ultra-refractory component in the Murchison showed strongly large negative Eu and Yb anomalies, and an enrichment in heavy REEs (HREEs), suggesting a fractionation between LREEs and HREEs occurred during chemical processing (Boynton et al., 1980). In carbonaceous chondrites, Ca-phosphate is known as a specific mineral with enriched REEs (Ebihara and Honda, 1987), which also shows enrichment in Eu (Ebihara and Honda, 1987; Zhang et al., 2016). The REE pattern may be used to identify the geochemical features and environmental situations during their formation and to elucidate the evolution processes that might be reflected in the main components of the individual leaching fractions. Besides, because the ^{84}Sr excess of CAIs showed higher than that of WR of carbonaceous chondrites (Moynier et al., 2012; Hans et al., 2013), the estimation of the chemical separates in which CAIs were dissolved from the REE pattern may provide a hint for consideration of the isotopic data.

The leaching fractions L3 and L5 in all four CMs showed a higher REE content than the other fractions. The REE patterns of L3 showed the highest REE contents with a positive Eu anomaly (see in Fig. 3), suggesting the dissolution of REE-rich minerals in L3, like apatite (Ebihara and Honda, 1987; Zhang et al., 2016). In addition, the REE patterns of L5 showed the depletion of LREEs compared with HREEs (see in Fig. 3), a

large negative anomaly of Eu, and a small depletion in Yb relative to Tm and Lu, suggesting that one of the main components in L5 is the refractory inclusion (Boynton et al., 1980). The REE pattern of the acid residue in NWA 4428 also shows the negative anomalies of Eu and Yb, suggesting that the refractory inclusion is one of the main components of the acid residue in a desert meteorite in this study.

Assuming that refractory inclusions are dissolved in L5, Sr and Ba elemental abundances can be calculated from the elemental abundances of the refractory inclusions (Sr = 129 ppm, Ba = 39.9 ppm; Grosmann et al., 1977) and the modal abundance of refractory inclusion in the CM chondrite (1.21 vol%; Hezel et al., 2008). Our estimates provide the elemental abundances of Sr (1470 ppb (Cold Bokkeveld), 929 ppb (Murray), 1160 ppb (Nogoya)) and Ba (456 ppb (Cold Bokkeveld), 287 ppb (Murray), 357 ppb (Nogoya)). Except for the estimated Ba elemental abundance of L5 in Murray, others are higher than the measured Sr and Ba content of L5 (Table 4). These results suggest the heterogeneous existence of CAIs in the CM matrices, which are consistent with the results in previous studies that vol% of CAIs in CM vary widely in the range from 0.016% to 3.8% (Norton and McSween, 2007; Hezel et al., 2008). Comparing the results with the measured elemental abundance data of L5, vol% of CAIs in individual samples in this study can estimate 0.13–0.21% for the Cold Bokkeveld, 0.89–4.20% for the Murray, and 0.28–0.30% for the Nogoya.

The REE patterns of all fractions of Tagish Lake showed a flat pattern without Eu anomaly (see in Fig. 3). In addition, the REE concentrations of the acid residue in Tagish Lake are lower than those of CM chondrites. The difference in the concentrations of REEs in the acid residues of CM chondrites and Tagish Lake can be explained by the difference in the abundance of the CAIs in these meteorites. Because the presence of CAIs

is rare in Tagish Lake compared with CM (Brown et al., 2000), the REE pattern of acid residue in the Tagish Lake suggests that the CAIs may not be present in the samples used in this study. As another interpretation, the CAIs in Tagish Lake have been severely altered, and most of these are replaced by secondary minerals (Brown et al., 2000; Zolensky et al., 2002). This suggests that the CAIs having Eu anomaly were destroyed by aqueous alteration and that their rare earth elements may be redistributed in the meteorite parent body. This interpretation is also plausible to explain the difference between the REE pattern of CMs and that of Tagish Lake (see in Fig. 3).

3.2 Isotopic data of carbonaceous chondrites

Isotopic data of Ba and Sr from the chemical separates (L1–L5) and WR of all carbonaceous chondrites are shown in Tables 5 and 6, respectively. The data are expressed in ε units, which is the deviations of the isotopic ratios between samples and the standard materials, as defined by the following equations;

$$\varepsilon\ {}^{i}\mathrm{Ba} = \left\{ \frac{({}^{i}\mathrm{Ba}/{}^{136}\mathrm{Ba})_{\mathrm{sample}}}{({}^{i}\mathrm{Ba}/{}^{136}\mathrm{Ba})_{\mathrm{standard}}} - 1 \right\} \times 10^{4}$$

$$\varepsilon\ {}^{j}\mathrm{Sr} = \left\{ \frac{({}^{j}\mathrm{Sr}/{}^{86}\mathrm{Sr})_{\mathrm{sample}}}{({}^{j}\mathrm{Sr}/{}^{86}\mathrm{Sr})_{\mathrm{standard}}} - 1 \right\} \times 10^{4}$$

Where ${}^{i}\mathrm{Ba}/{}^{136}\mathrm{Ba}$ and ${}^{j}\mathrm{Sr}/{}^{86}\mathrm{Sr}$ are the isotopic ratios of the standard materials and samples, i and j are the mass number of the Ba isotope (130, 132, 135, 137, and 138) and Sr isotope (84 and 87), respectively.

In this study, the Faraday cup installed in the mass spectrometer (TIMS) used for isotopic analysis was adjusted during the measurement period from April 2016 to June

2019. Isotopic deviation of Ba and Sr were determined using the values of the standard materials during each sample measurement period. The averages of Sr isotopic ratio of the standard material for each period were $^{87}Sr/^{86}Sr_{NIST}$ = 0.710258 ± 8, 2SE = 11 ppm (n = 6) (before adjustment), $^{87}Sr/^{86}Sr_{NIST}$ = 0.710252 ± 5, 2SE = 7 ppm (n = 16) (after adjustment), and $^{87}Sr/^{86}Sr_{NIST}$ = 0.710254 ± 8, 2SE = 11 ppm (n = 22) (within the measurement period). Since these values could not be distinguished within the range of external precision (2SE), all measured Sr isotopic ratios through the period in this study can be compared with each other without any further numerical bias. Sr and Ba isotopic data of standard materials during the measurement period were shown in Tables S1 and S2, and Fig. S1.

3.2.1 Isotopic data of Ba

The Ba isotopic deviation patterns, which consist of the measured isotopic deviations of L1–L5 and WR of all five carbonaceous chondrites, are shown in Fig. 4. The patterns of the WR of Cold Bokkeveld and Tagish Lake had positive isotopic anomalies of ^{135}Ba and ^{137}Ba ($\varepsilon^{135}Ba$ = 0.24–0.45, $\varepsilon^{137}Ba$ = 0.17–0.19). The Ba isotopic data for the WR for CI and CM often showed positive or negative isotopic anomalies of ^{135}Ba correlated with ^{137}Ba ($0 < \varepsilon^{135}Ba, \varepsilon^{137}Ba < 1$, $-1 < \varepsilon^{135}Ba, \varepsilon^{137}Ba < 0$) (Hidaka et al., 2001, 2003; Andreasen and Sharma, 2007; Carlson et al., 2007; Hidaka and Yoneda, 2011, 2013; Bermingham et al., 2014, 2016), which were similar to Ba isotopic data for the WR of Cold Bokkeveld and Tagish Lake in this study.

On the other hand, most Ba isotopic deviation patterns of L1–L5 of all of five carbonaceous chondrites showed significant and large deviations compared with those of WR. Most patterns of the L1–L4 fractions showed variable isotopic excesses of ^{130}Ba,

^{132}Ba, ^{135}Ba, ^{137}Ba, and ^{138}Ba, while those of all L5 fractions showed isotopic deficits of ^{130}Ba, ^{132}Ba, ^{135}Ba, ^{137}Ba, and ^{138}Ba (see in Fig. 4). In previous Ba isotopic studies in chemical separates in the Murchison (CM) meteorite (Qin et al., 2011), the Ba isotopic data of the acid residue in CM showed large negative isotopic anomalies of ^{130}Ba, ^{132}Ba, ^{135}Ba, ^{137}Ba, and ^{138}Ba because of the enrichment of presolar SiC grains, which is a representative carrier of s-process isotopes (Ott and Begemann, 1990; Zinner et al., 1991; Prombo et al., 1993). The isotopic data sets of several chemical phases using sequential acid-leaching of primitive planetary materials suggested a heterogeneous distribution of s-process nucleosynthetic components of Ba isotopes in the early solar system. The acid-leaching experiment in carbonaceous chondrites can reveal information for isotopic heterogeneity of Ba that could not be found in the WRs (Hidaka et al., 2003; Hidaka and Yoneda, 2011).

In most of the Ba isotopic deviation patterns, the degree of isotopic deviation decreases along with the mass number (ε^{135}Ba > ε^{137}Ba > ε^{138}Ba), possibly because of a depletion of s-process nucleosynthetic components (see in Fig. 4). However, all Ba isotopic deviation patterns could not be explained only by the contribution of s-process nucleosynthetic components. The Ba isotopic deviation pattern of the WR of Murray having deficits of ^{137}Ba and ^{138}Ba was different from those of Cold Bokkeveld, which is a typical pattern showing the contribution of the s-process nucleosynthetic components. This pattern was similarly observed in the WR of Sayama (Hidaka et al., 2003). The Ba isotopic deviation pattern of the WR of Nogoya had excesses of ^{135}Ba and ^{137}Ba, and slight deficits of ^{130}Ba and ^{132}Ba, suggesting not only the depletion of s-process isotopes but also the depletion of ^{130}Ba and ^{132}Ba. Although these results suggest the deficit of p-process isotopes, they are inconclusive because of the large analytical uncertainties.

Furthermore, the Ba isotopic deviation pattern of the L4 in Murray showed a large isotopic excess of ^{130}Ba and an isotopic excess of ε^{137}Ba that was larger than that of ε^{135}Ba (see in Fig. 4), which was different from those typical for CMs. These results suggest that additional nucleosynthetic components, other than those derived from the s-process, were involved in the isotope anomalies.

All Ba isotopic deviations of WR and L1–L5 of NWA 4428 were less than those of other CMs ($-2 < \varepsilon < +1$). While the deviations of ^{130}Ba and ^{132}Ba were within the external errors in all fractions, the Ba isotopic data of L2 and L3 showed small ^{135}Ba excesses, and ^{137}Ba and ^{138}Ba deficits. This pattern was similarly observed in the chemical separates of Karonda (Hidaka and Yoneda, 2011), which may be attributed to the addition of Ba due to contamination on the terrestrial weathering. Considering the high Ba elemental abundances of WR in NWA 4428 (38.2 ppm), the Ba isotopic composition of NWA 4428 may be close to the terrestrial values due to the addition of terrestrial components by terrestrial weathering.

3.2.2 Isotopic data of Sr

The isotopic deviations of ^{84}Sr for the individual fractions of carbonaceous chondrites are shown in Fig. 5. The Sr isotopic data for three of five carbonaceous chondrites, Cold Bokkeveld, Murray, and Nogoya showed an isotopic excess of ^{84}Sr ($+0.34 < \varepsilon^{84}\mathrm{Sr} < +0.46$) in the WRs. In previous studies of ^{84}Sr isotopic variations in carbonaceous chondrites (Moynier et al., 2012; Yokoyama et al., 2015), the Sr isotopic data for the WR samples of the carbonaceous chondrites showed slightly isotopic excesses of ε^{84}Sr ($\varepsilon^{84}\mathrm{Sr} < 1$) that were consistent with our data.

On the other hand, the Sr isotopic data for the L1–L5 in carbonaceous chondrites

showed variable isotopic anomalies of $\varepsilon^{84}Sr$ in the range of $-5 < \varepsilon^{84}Sr < +7$, which were significantly larger variations than that of WRs. Therefore, as with the Ba isotopic results, the Sr isotopic data of chemical separates of carbonaceous chondrites using acid-leaching experiments provide information about Sr isotopic heterogeneities in the primitive planetary materials. In particular, isotopic data of the acid residues (L5) in all CMs showed an isotopic deficit of ^{84}Sr in the range of $-5 < \varepsilon^{84}Sr < -2$, which is isotopic evidence for the enrichment of s-process nucleosynthetic components due to the presence of acid-resistant presolar SiC grains (Podosek et al., 2004; Liu et al., 2015). On the other hand, isotopic data of acid residue in Tagish Lake could be detected no isotopic anomalies due to the large analytical uncertainty (see in Fig. 5).

The Sr isotopic data of the leachates (L1–L4) in all five carbonaceous chondrites showed variable isotopic excesses of $\varepsilon^{84}Sr$ in the rage of $0 < \varepsilon^{84}Sr < 7$ (see in Fig. 5). Most of the data showed isotopic excesses of $\varepsilon^{84}Sr$ in the rage of $0 < \varepsilon^{84}Sr < 2$, which consistent with previous data collected from leachates of other CM2 chondrites ($0 < \varepsilon^{84}Sr < 2$) (Qin et al., 2011; Yokoyama et al., 2015; Burkhardt et al., 2019). However, $\varepsilon^{84}Sr$ isotopic data of L4 in Nogoya ($\varepsilon^{84}Sr = 7.35 \pm 0.51$) were found to be significantly higher than those of previous studies. Although the isotopic excess of $\varepsilon^{84}Sr$ (1.23 ± 0.35) in CAIs is higher than that of WRs in carbonaceous chondrites (Hans et al., 2013), the isotopic excess of L4 in Nogoya cannot be explained by the presence of CAIs. The processes that lead to the isotopic excess of ^{84}Sr are the enrichments of the r-process isotopic component (Papanastassiou and Wasserburg, 1978), and spallogenic products induced from the intense irradiation by SCR from the early Sun (Hidaka and Yoneda, 2014).

Isotopic data for the L4, L5, and WR of Tagish Lake could not detect isotopic anomalies due to the large analytical uncertainty (see in Fig. 5). On the other hand,

isotopic data of the other chemical separates (L1, L2 and L3) of Tagish Lake showed isotopic excesses of ^{84}Sr, which were similar to those of CMs. Isotopic data for the L5 and WR of NWA 4428 showed isotopic deficits of ^{84}Sr, while the other chemical separates showed no ε^{84}Sr anomalies within the range of analytical uncertainties (see in Fig. 5). These results were not commonly observed in the other CMs. The ^{84}Sr isotopic data of WR (ε^{84}Sr = −0.63 ± 20) was indistinguishable from those of the terrestrial materials (ε^{84}Sr = −0.18 ± 30, −0.25 ± 22 [Paton et al., 2013], –0.29 ± 17 [Yokoyama et al., 2015]). Judging from the high Sr concentration of NWA 4428 (46 ppm) relative to the other two CM chondrites, Cold Bokkeveld and Nogoya in this study (8–9 ppm), the Sr isotopic composition of the WR of NWA 4428 may be a mixture of the terrestrial component having negative isotopic anomalies of ^{84}Sr and typical CM chondrites having positive isotopic anomalies of ^{84}Sr. This interpretation is plausible with the results of isotopic data other than acid residues that show no isotopic anomalies of ^{84}Sr.

The ^{87}Sr/^{86}Sr isotopic ratios in the carbonaceous chondrites showed a large variation in the range from 0.702536 to 0.782063 (see in Table 6), and there was a slightly positive correlation with the ^{87}Rb/^{86}Sr ratio for each isotope data, which may indicate ^{87}Sr isotopic excesses derived from decayed ^{87}Rb. The ^{87}Rb–^{87}Sr evolution diagram for L1–L5 and WR of all carbonaceous chondrites used in this study and data from previous studies (Qin et al., 2011; Yokoyama et al., 2015) are shown in Fig. 6. The solid line in the figure is a 4.568 Ga-old reference line with an initial ^{87}Sr/^{86}Sr ratio of 0.698975 (Hans et al., 2013). In the figure, the data points of L1 of Cold Bokkeveld, Murray, and Nogoya, and the data points of L2 of Tagish Lake are plotted on or close to the line. However, other data points are plotted outside the line. The low correlation between the ^{87}Rb/^{86}Sr ratio and ^{87}Sr/^{86}Sr isotopic ratio of acid leachates in carbonaceous chondrites has also

been reported in previous studies (Qin et al., 2011; Yokoyama et al., 2015; Burkhardt et al., 2019).

All data points of the NWA 4428 analyses are plotted outside the reference line (see in Fig. 4). Previous studies (Hans et al., 2013; Ferdous et al., 2017) reported that the ^{87}Rb–^{87}Sr decay system in desert meteorites is often disturbed by terrestrial weathering. Ferdous et al. (2017) reported that the $^{87}Sr/^{86}Sr$ isotopic ratio was close to the terrestrial seawater ($^{87}Sr/^{86}Sr$ = ~0.7090) due to the terrestrial weathering. In this study, the ^{87}Rb–^{87}Sr decay system in NWA 4428 might have been affected by the terrestrial weathering in desert because: (1) data points of WR, L1, L2, L3, and L4 were plotted above the reference line (see in Fig. 4), suggesting a decrease of the Rb/Sr ratio accompanied by the addition of Sr (46 ppm), possibly after the fall; (2) the variation of $^{87}Sr/^{86}Sr$ was less than the variations of other data for carbonaceous chondrites, suggesting a two-component mixture of $^{87}Sr/^{86}Sr$ data for the meteorite components and the additional terrestrial components having a $^{87}Sr/^{86}Sr$ = ~0.710.

3.2.3 The weighted averages of isotopic data of Sr and Ba

Based on the elemental and isotopic data in Tables 4 and 5, the weighted averages (WAs) of isotopic deviations were calculated for each sample, which are shown in Table 6. By comparing these results (WA) with isotopic data of WR for each sample, I confirmed the reliability of sequential acid-leaching experiments conducted in this study. As shown in Table 6, the WAs of isotopic deviations of the ^{84}Sr in Cold Bokkeveld, Nogoya, and Tagish Lake, and the WA of the Ba in Tagish Lake were indistinguishable with those of WR within the analytical uncertainties. On the other hand, the WAs of isotopic deviations of ^{84}Sr of Nogoya and NWA 4428 were slightly different from those

of the WRs. Furthermore, the Ba isotopic deviations of WAs were different from those of the WRs of all CM chondrites. In addition, the isotopic excesses of ^{135}Ba, ^{137}Ba, and ^{138}Ba of WA in Cold Bokkeveld and Nogoya showed larger than those of WR (see in Table 6), which indicates the possibility of the presence of undissolved components during the acid-leaching experiment. The degree of the isotopic excess due to the undissolved presolar SiC grains correlated with the amount of the used samples: e.g., approximately 600–800 mg were used for the sequential acid-leaching experiments, which is more than the ~100 mg used for the WR analyses.

Overall, the isotopic data for the measured WRs and the calculated WAs were very similar to those of the WRs of CMs in the previous studies ($0 < \varepsilon^{84}Sr < 1$, Moynier et al., 2012; Yokoyama et al., 2015; $0 < \varepsilon^{135}Ba, \varepsilon^{137}Ba < 1$, Hidaka et al., 2003; Andreasen and Sharma, 2007; Carlson et al., 2007; Hidaka and Yoneda, 2011). The results of this study reveal that the Sr and Ba isotopic compositions of WRs of carbonaceous chondrites consist of several isotopic heterogeneous components. A sequential acid-leaching experiment could chemically separate several components with various isotopic compositions constituting meteoritic samples, which is one of the effective approaches to evaluate the isotopic heterogeneity in meteorite samples.

CHAPTER 4

Discussion

4.1 Isotopic variation of Ba

Ba isotopic data normalized to $^{134}Ba/^{136}Ba$ have been efficiently used to find several kinds of isotopic anomalies (Hidaka et al., 2003; Andreasen and Sharma, 2007; Carlson et al., 2007; Qin et al., 2011; Hidaka and Yoneda, 2011, 2013; Bermingham et al., 2014). In order to discuss the origin of isotopic anomalies of Ba and Sr, a quantitative evaluation of the contribution of several nucleosynthetic components is required from the measured Ba and Sr isotopic data in this study. Furthermore, I would like to refer to the initial abundance of ^{135}Cs and the possible contribution of nuclear reactions associated with cosmic-ray irradiation.

As shown in Fig. 4, the Ba isotopic data of the acid residue of NWA 4428 showed isotopic deviations patterns suggesting the enrichment of s-process nucleosynthetic components similar to those of other CMs. However, the magnitude of the isotopic deviations was less than those in the other CMs, and the Ba isotopic deviation patterns of other chemical separates (L1–L4) and WR of NWA 4428 showed different from those of the other CMs (see in Fig. 4). Among the Ba isotopes, ^{130}Ba and ^{132}Ba are not sufficient to assess the contribution of isotopic anomalies because of their large analytical uncertainties. Considering the enrichments of Ba content in WR of NWA 4428 compared to those of other CM (see in Table 5), terrestrial weathering may also affect the Ba isotopic composition of NWA 4428. In this study, assuming that all $^{134}Ba/^{136}Ba$ are constant, the Ba isotope ratio is corrected for the instrumental mass fractionation. For this reason, there

is a possibility that apparent isotopic anomalies occur due to a change in the $^{134}Ba/^{136}Ba$ ratio. Assuming that the Ba isotopic data of NWA 4428 consists of a mixture of typical CM and additional components of the terrestrial materials, I calculated isotopic data of additional components based on mass balance using the following equation:

$$(\varepsilon^{i}Ba)_{NWA} = \left(\frac{C_{CM}}{C_{NWA}}\right) \times (\varepsilon^{i}Ba)_{CM} + \left\{\frac{(C_{NWA}) - (C_{CM})}{C_{NWA}}\right\} \times (\varepsilon^{i}Ba)_{a.c}$$

Where i is the mass number of the Ba isotope (i =130, 132, 135, 137, and 138), $C_{CM,}$ and C_{NWA} are Ba contents of typical CM and NWA 4428, $(^{i}Ba)_{NWA,}$ $(^{i}Ba)_{CM,}$ and $(^{i}Ba)_{a.c,}$ are isotopic data of measured, typical CM, and additional components, respectively. Typical CM data were taken from Cold Bokkeveld based on the similarity of element concentrations and isotopic compositions of the CMs in previous studies (Hidaka et al., 2003; Hidaka and Yoneda, 2011; Bermingham et al., 2016).

Fig. 7 shows the Ba isotopic deviation patterns of the additional components of NWA 4428, and apparent Ba isotopic deviation pattern based on estimated values of the Ba isotopic anomalies caused by false correction of the instrumental mass fractionation (A–E, A–C: $^{134}Ba/^{136}Ba > 0.307776$, D–E: $^{134}Ba/^{136}Ba < 0.307776$). As shown in Fig. 7, the apparent Ba isotopic deviation pattern showed isotopic anomalies of ^{135}Ba inversely correlated with ^{137}Ba and ^{138}Ba. Isotopic deviation pattern of L2 is a good agreement with that of the apparent isotopic deviation pattern, suggesting isotopic data of NWA 4428 consist of a mixture of Ba isotopic composition of typical CM and additional components of the terrestrial materials having $^{134}Ba/^{136}Ba$ ratio higher than the normalization value ($^{134}Ba/^{136}Ba > 0.307776$). The isotopic composition of NWA 4428 is useful for isotopic data on the effects of terrestrial weathering, but may not be suitable for elucidating the

origin of isotopic anomalies in the early solar system, which will be discussed later. Therefore, isotopic data for NWA 4428 were excluded from further discussion.

4.1.1 Correlation between isotopic anomalies of ^{135}Ba, ^{137}Ba, and ^{138}Ba

Because Ba isotopic anomalies due to the contribution of s-process nucleosynthetic components showed clearly linked isotopic variation of ^{135}Ba, ^{137}Ba and ^{138}Ba, the correlation between isotopic anomalies of ^{135}Ba, ^{137}Ba, and ^{138}Ba is useful for the evaluation of isotopic anomalies due to the contribution of nucleosynthetic components (Hidaka et al., 2003; Hidaka and Yoneda, 2011, Qin et al., 2011). Figs. 8(a) and (b) show the correlation diagrams for ε^{135}Ba vs. ε^{137}Ba and ε^{138}Ba vs. ε^{137}Ba from the individual chemical separates of the four carbonaceous chondrites used in this study, i.e., Cold Bokkeveld, Murray, Nogoya, and Tagish Lake, and from previous data (Hidaka et al., 2003; Hidaka and Yoneda, 2011; Qin et al., 2011). To compare the measured isotopic data with the ideal s-process components (Ott and Begemann, 1990; Zinner et al., 1991; Prombo et al., 1993), reference isotopic data were calculated based on the s-process-enriched components. The Ba isotopic data for presolar SiC grains were cited from references (Ott and Begemann, 1990; Zinner et al., 1991; Prombo et al., 1993). The shaded zones in Figs. 8 indicate the reference Ba isotopic data assuming the contribution of the s-process component. For comparison, the solid line in Figs. 8 represents the ideal isotopic data mixed between the solar component and the additional nucleosynthetic component based on the stellar model (^{135}Ba:^{137}Ba:^{138}Ba = 34.8:31.9:33.4; Bisterzo et al., 2015).

As shown in Figs. 8(a) and (b), most data points of L1–L5 and WR in carbonaceous chondrites are plotted in the shaded zone. This result is consistent with

previous studies (Hidaka et al., 2001, 2003; Hidaka and Yoneda, 2011), which suggests that most data can be attributed mainly to the s-process nucleosynthetic components. However, all data points (see in Figs. 8(a) and (b)) were not plotted in the shaded zone and the solid lines, which suggest that the measured isotopic data could not be explained solely by the contribution of s-process nucleosynthetic components.

There are four possible minor contributions of isotopic anomalies in primitive planetary materials. The first possibility is isotopic anomalies caused by the presence of carriers of the r-process nucleosynthetic components. Previous studies have reported r-process isotopic anomalies based on the Ba isotopic analysis of the FUN inclusion (McCulloch and Wasserburg, 1978a) and nanodiamond (Lewis et al., 1991) in the Allende meteorites. However, the assessment of ^{138}Ba isotopic anomalies is unclear because all isotopic data were referenced to ^{138}Ba, and ^{134}Ba/^{138}Ba ratio is used to correct the instrumental isotopic mass fractionation. In addition, because most of the Ba isotopic anomalies in CAIs indicate mainly the contribution of the s-process nucleosynthetic components (Brennecka et al., 2013; Bermingham et al., 2014), the contribution of minor components of isotopic anomalies of FUN inclusions are considered to be small. The Ba isotopic data of nanodiamonds in Allende also showed r-process isotopic anomalies (ε^{135}Ba = 12.2 and ε^{137}Ba = 6.0, Lewis et al., 1991). Considering the amount of nanodiamond in the carbonaceous chondrite (~500 ppm, Amari et al., 1994) and the concentration of Ba in the nanodiamond (14 ppb, Lewis et al., 1991), the effect of nanodiamonds on Ba isotopic anomalies in all fractions is less than ε^{135}Ba = 0.002, which is negligible as a contribution of isotopic anomalies.

Next, the second possibility is the contribution of the ^{138}Ba isotopic excess associated with an addition of radiogenic ^{138}Ba decayed from ^{138}La ($t_{1/2}$ = 105 Ga)

(Brennecka et al., 2013). However, the estimation of the radiogenic components of ^{138}Ba from the La/Ba elemental ratios in the L5 (La/Ba = 0.123~1.00) provides the (^{138}Ba*/^{138}Ba) = 4.4 × 10^{-9} to 3.5 × 10^{-8}, which is not resolvable by our mass spectrometric techniques used in this study.

The third possibility is the contribution of presolar X grains (n-process components) having a large isotopic excess of ^{138}Ba (Pellin et al., 2000, 2006; Stephan et al., 2018). Since the X grains are a minor type of presolar SiC grains, it is reasonable to assume that they contribute to the isotopic data of acid residue. However, in previous studies, the Ba isotopic data of acid residues in CI and CMs showed large isotopic deficits of ^{135}Ba, ^{137}Ba, and ^{138}Ba, which suggests the presence of acid-resistant presolar SiC grains as the carrier for s-process nucleosynthetic components (Ott and Begemann, 1990). The data points of acid residue in Tagish Lake are plotted on the shaded zone (see in Figs. 8(a) and (b)), which suggests the enrichment of the s-process isotopes as well as these previous studies (Hidaka et al., 2003; Hidaka and Yoneda, 2011; Qin et al., 2011). However, the isotopic data of the acid residues in Cold Bokkeveld, Murray, and Nogoya, in this study, show an isotopic excess of ^{138}Ba in the shaded zone (see in Fig. 8(b)), suggesting the contribution of n-process components. Hoppe et al. (2010) found presolar X grains in the size range of 0.2–0.5μm are about 2 times higher than micrometer-sized grains, and argued SNeII, on average, may produce smaller presolar grains than those of carriers of s-process nucleosynthetic components. Considering that the isotopic data of presolar SiC grains used in this study were classified into sub-micrometer/micrometer-sized grains (approximately 0.4–6.0 μm; Ott and Begemann, 1990; Zinner et al., 1991; Prombo et al., 1993) during the extraction process, the isotopic data of bulk acid residues in this study may suggest the contribution of the isotopic data of presolar SiC grains of

the carrier of s-process nucleosynthetic components, and the isotopic data of presolar X grains, which is on average a small grains size.

Lastly, the fourth possibility is the ^{135}Ba isotopic excess associated with an addition of extinct nuclide ^{135}Cs decayed to ^{135}Ba. The contribution of radiogenic components of ^{135}Ba in the isotopic anomalies of L5 can be estimated by subtracting the contribution of several nucleosynthetic components.

In this study, I propose two models for the estimation of ^{135}Cs isotopic abundance from measured Ba isotopic data for the L5 fraction. I assume that all Ba isotopes of the acid residues are a mixture of s- and n-process components and the radiogenic components of ^{135}Ba derived from decayed ^{135}Cs.

4.1.2 Inventories of the Ba isotopic deviation caused by the s- and n-process components and ^{135}Cs

The isotopic data of ε^{135}Ba, ε^{137}Ba and ε^{138}Ba are as follows:

$$\varepsilon^{135}\mathrm{Ba} = (\varepsilon^{135}\mathrm{Ba})_s + (\varepsilon^{135}\mathrm{Ba})_n + (\varepsilon^{135}\mathrm{Ba})^{135}\mathrm{Cs}$$

$$\varepsilon^{137}\mathrm{Ba} = (\varepsilon^{137}\mathrm{Ba})_s + (\varepsilon^{137}\mathrm{Ba})_n$$

$$\varepsilon^{138}\mathrm{Ba} = (\varepsilon^{138}\mathrm{Ba})_s + (\varepsilon^{138}\mathrm{Ba})_n$$

where the suffixes, s, n, and ^{135}Cs indicate the contribution of the s- and n-process components and the decay of ^{135}Cs, respectively. In this study, the contributions of the r-process nucleosynthetic component and the radiogenic component of ^{138}Ba decayed from ^{138}La are negligible (see text in section 4.1.1) and therefore excluded from the equations.

Model 1. The subtraction of s- and n-process components based on ^{137}Ba and ^{138}Ba isotopic data

Based on the measured $(\varepsilon^{137}Ba)_s$ and $(\varepsilon^{137}Ba)_n$ obtained by Appendix.1, ^{135}Ba isotopic data could be subtracted from the s- and n-process components of the measured Ba isotopic components. Because the isotopic data for s- and n-process components (Zinner et al., 1991; Prombo et al., 1993; Stephan et al., 2018) provided $(\varepsilon^{135}Ba)_s/(\varepsilon^{137}Ba)_s$ = 1.50–1.90, and $(\varepsilon^{135}Ba)_n/(\varepsilon^{137}Ba)_n$ = –1.90, the contribution of s- and n-process components to the ^{135}Ba isotopic data can be subtracted from the following equation.

$$(\varepsilon^{135}Ba)_{correct} = (\varepsilon^{135}Ba)_{measured} - (1.50 - 1.90) \times (\varepsilon^{137}Ba)_{s(L5)} - (-1.90) \times (\varepsilon^{137}Ba)_{n\,(L5)}$$

Model 2. Matrix calculation based on measured Ba isotopic data

With this assumption, I perform a matrix analysis to estimate the ^{135}Cs isotopic abundances based on the measured Ba isotopic data for L5 (Hidaka and Yoneda, 2011). The detailed calculation process is shown in the Appendix. 2.

4.1.3 Estimation of isotopic abundances of ^{135}Cs

From the maximum value of ^{135}Ba isotopic data after the subtraction of s- and n-process components from the measured Ba isotopic data (Table 7), I estimated the upper limit of isotopic data of radiogenic ^{135}Ba in the L5. As shown in Table 7, the maximum values of ε^{135}Ba isotopic data obtained for model 1 and model 2 were in good agreement, but there was a difference in the degrees of their uncertainties due to error propagation.

The upper limit of isotopic abundance of ^{135}Cs in L5 was estimated based on two models. A correlation diagram between the Cs/Ba elemental ratio and the calculated upper

limits of radiogenic ε^{135}Ba, (ε^{135}Ba*), in the L5 of Cold Bokkeveld, Murray, and Nogoya using models 1 and 2 is shown in Fig. 9(a). These data points show the isotopic excesses of (ε^{135}Ba*) that positively correlated with the Cs/Ba ratio. The data points of Murray showed a slightly isotopic excess of ^{135}Ba with a Cs/Ba ratio (see in Fig. 9(a)) and slopes of (1.66 ± 1.44/1.67 ± 1.02) × 10^{-4}corresponding to the ^{135}Cs/^{133}Cs isotopic abundances of (1.40 ± 1.21/1.39 ± 0.85) × 10^{-4}. Interestingly, the data points of Cold Bokkeveld and Nogoya showed a large isotopic excess of ^{135}Ba with a high Cs/Ba ratio (see in Fig. 9(a)) and slopes of (2.72 ± 0.51/2.72 ± 0.49) × 10^{-4} (Cold Bokkeveld) and (5.15 ± 0.81/5.14 ± 0.77) × 10^{-4} (Nogoya) corresponding to the ^{135}Cs/^{133}Cs isotopic abundances of (2.28 ± 0.43/2.28 ± 0.41) × 10^{-4} and (4.32 ± 0.68/4.31 ± 0.65) × 10^{-4}, respectively. These ^{135}Cs/^{133}Cs ratios were within the range of previously estimated ^{135}Cs/^{133}Cs ratio (initial abundance of ^{135}Cs/^{133}Cs from 2.8 × 10^{-6} to 6.8 × 10^{-4} (McCulloch and Wasserburg, 1978; Hidaka et al., 2001, 2003; Hidaka and Yoneda, 2011, 2013; Brennecka and Kleine, 2017)).

The ^{135}Cs–^{135}Ba decay system is expected to be applied as the most sensitive chronometry to the aqueous alteration on the early solar planetary materials because Cs is highly reactive with water (Hidaka and Yoneda, 2013). However, the REE pattern of the L5 fractions of Cold Bokkeveld, Murray, and Nogoya suggested the presence of CAIs (see in Fig. 3). Therefore, the isotopic abundance of ^{135}Cs in the L5 of CMs seem to indicate the initial abundance of solar system materials at CAIs formation, rather than the timing of the aqueous alteration on primitive planetary materials in the early solar system. The abundance of ^{135}Cs estimated from the results of CAIs in previous studies (McCulloch and Wasserburg, 1978; Hidaka et al., 2001) was 1.6–4.8 × 10^{-4}, which is in good agreement with the estimates obtained from our results.

In general, the Cs/Ba ratios of refractory inclusions are low (Cs/Ba < 0.00888,

Hidaka et al., 2001) because of the large difference of condensation temperature between Cs (799K) and Ba (1455K) (Lodders, 2003). On the other hand, the Cs/Ba ratio of L5 in this study showed a wide range from 0.017 to 0.37, which is higher than that of bulk CAIs. One reason why the Cs/Ba ratio is significantly higher than that of bulk CAIs may be the presence of minerals other than CAIs with high Cs/Ba ratios. In addition, this result can be interpreted as reflecting that the sequential acid-leaching experiment is an effective method to recover chemical separates with Cs/Ba ratio higher than that of the bulk sample (Hidaka et al., 2001, 2003; Hidaka and Yoneda, 2011, 2013). The Cs/Ba ratios of the acid residue obtained from the sequential acid-leaching experiment of Murchison (Hidaka et al., 2003) and chondrules in CM (Hidaka and Yoneda, 2013) are as high as those of acid residues in this study (Cs/Ba = 0.14 [Hidaka et al., 2003], 0.13 [Hidaka and Yoneda, 2013]).

In the Ba isotopic data of chemical separates other than L5 of CMs and WR in Cold Bokkeveld, Murray, Nogoya, and Tagish Lake, the contribution of the additional nucleosynthetic component was subtracted, and an attempt was made to estimate the isotopic abundance of radiogenic ^{135}Ba. As shown in Figs. 8(a) and (b), most of the data points are plotted in the shaded zone suggesting the contribution of s-process nucleosynthetic components. Assuming that the isotopic compositions of ^{135}Ba included the contribution of the s-process nucleosynthetic components and the radiogenic component of ^{135}Ba, (ε^{135}Ba*), the contribution of the s-process component was subtracted from measured Ba isotopic data using the following equation:

$$(\varepsilon^{135}\mathrm{Ba}^*) = (\varepsilon^{135}\mathrm{Ba}) - (\varepsilon^{137}\mathrm{Ba}) \times f$$

where f is an isotopic ratio of $^{135}Ba/^{137}Ba$ given by the additional s-process nucleosynthetic components (Ott and Begemann, 1990; Prombo et al., 1993). As shown in Fig 8(a), the $^{135}Ba/^{137}Ba$ isotopic ratio of additional nucleosynthetic components is from 1.50 to 1.90, as estimated from the isotopic data from presolar SiC grains (Zinner et al., 1991; Prombo et al., 1993).

A correlation diagram between the Cs/Ba elemental ratio and calculated ^{135}Ba, ($\varepsilon^{135}Ba^*$), of the chemical separates other than L5 of CMs and WR of Cold Bokkeveld, Murray and Nogoya, and Tagish Lake is shown in Fig. 9(b). As shown in Fig. 9(b), there is a no correlation between $^{133}Cs/^{136}Ba$ and ($\varepsilon^{135}Ba^*$) from the chemical separates and WR of CMs and Tagish Lake, which has been also reported in other CI and CMs (Hidaka et al., 2003; Hidaka and Yoneda, 2011). This result suggests that Cs, which is highly reactive with water, was distributed heterogeneously with aqueous alteration on the meteorite parent body. Among the CM chondrites, the Cold Bokkeveld and Nogoya experienced relatively intense aqueous alteration on the meteorite parent body (Rubin et al., 2007). It is appropriate to consider that there is no correlation between the data points of Cold Bokkeveld and Nogoya as a large disturbance of the decay system due to the high responsiveness of Cs to aqueous activity. This result is consistent with Sayama meteorite having a petrographic signature of intense aqueous alteration (Yoneda et al., 2001) did not show a positive correlation (Hidaka et al., 2003, 2015). Considering that the Tagish Lake also has the petrological feature that provides evidence for intense aqueous alteration (Zolensky et al., 2002; Nakamura et al., 2003), it is reasonable that there is no positive correlation of the ($\varepsilon^{135}Ba^*$) with $^{133}Cs/^{136}Ba$ ratio of Tagish Lake.

Another possible interpretation is the disturbance of the ^{135}Cs–^{135}Ba decay system associated with terrestrial weathering. The Tagish Lake meteorites used in this

study showed higher Ba concentrations (11 ppm) than those of other CMs (approximately 2.7 ppm), which suggests the addition of Ba associated with the terrestrial weathering. Therefore, the Cs–Ba decay system may have been disturbed by terrestrial weathering. Although a positive correlation was confirmed in the data points of Murray (Hidaka and Yoneda, 2011), no correlation is confirmed in the sample of this study. Considering that the Ba concentration of the whole rock sample in this study (5.3 ppm) is higher than that in the previous study (3.1 ppm), the ^{135}Cs–^{135}Ba decay system may have been disturbed by terrestrial weathering. This is consistent with the results of trace element analysis (see text in section 3.1).

Hidaka and Yoneda (2011) pointed out that the Ba isotopic composition of the CM chondrites may include not only the s-process nucleosynthetic component but also the contribution of several additional nucleosynthetic components, one of which is the possibility of negative isotopic anomalies of ^{135}Ba. As shown in Fig. 9(b), although the contribution of the n-process nucleosynthetic components showed small isotopic deficits of ^{135}Ba, it is not appropriate to consider acid resistant presolar SiC grains as a candidate for the contribution of isotopic anomalies of the acid soluble components. These results suggest that the Ba isotopic anomalies may be attributed to additional nucleosynthetic components other than the s- and n-process.

Although there are several studies on extinct ^{135}Cs in the early solar system (McCulloch and Wasserburg, 1978a; Hidaka et al., 2001; Hidaka and Yoneda, 2011, 2013; Bermingham et al., 2014, 2016; Brennecka and Kleine, 2017), the estimated ^{135}Cs isotopic abundance ranges from 2.8×10^{-6} to 6.8×10^{-4} but is still disputed. Because Cs is highly reactive with water, the ^{135}Cs–^{135}Ba decay system may provide chronological information about aqueous activity on the meteorite parent body in the early solar system.

Based on the ^{53}Mn–^{53}Cr decay system obtained from the analysis of carbonates in carbonaceous chondrites (Fujiya et al., 2012, 2013), an aqueous alteration that occurred on the carbonaceous chondrite parent bodies was estimated to be 4.3–5.7 Ma after the formation of CAIs. Taking into account the ^{135}Cs isotopic abundances ($2.8 \times 10^{-6} \sim 6.8 \times 10^{-4}$, Hidaka and Yoneda, 2013; Brennecka and Kleine, 2017), the age of carbonate formation and measured Cs/Ba elemental ratios of acid leachates and WR of carbonaceous chondrites, the radiogenic ^{135}Ba components decayed from presently extinct ^{135}Cs of each leaching fraction in carbonaceous chondrites are estimated to be $\varepsilon^{135}Ba$ = 0.000073–2.9. Considering the analytical precision for Ba isotopic measurements in our current techniques and ^{135}Ba isobaric interference from the s-process nucleosynthetic component, a chemical phase with a higher Cs/Ba ratio (Cs/Ba > 1), like a chemical separate in alkali-rich H chondrite (Cs/Ba = 19.8, Hidaka et al., 2001), is required to directly detect the contribution of radiogenic ^{135}Ba isotopic excesses.

The uniform galactic production (UP) model proposed in previous studies (e.g. Wasserburg et al., 1996; Busso et al., 1999) has been used to interpret the abundance of extinct radioactive isotopes in the early solar system. The diversity of these nucleosynthetic components has been discussed based on the correlation between the average ratio of extinct short-lived radioactive isotopes (R) to their stable reference isotopes (S) in the early solar system ($(N_R/N_S)_{ESS}$) normalized to their nucleosynthetic production ratios (P_R/P_S) and the mean life (τ) of extinct short-lived radioactive isotopes (Wasserburg et al., 1996; Busso et al., 1999; Jacobsen, 2005; Hidaka and Yoneda, 2013; Brennecka and Kleine, 2017), given by the following equation:

$$((N_R/N_S)_{ESS})/(P_R/P_S) = (\tau)/T \cdot (1-e^{-T/(\tau)}) \approx (\tau)/T$$

Where T is the duration time of nucleosynthesis. The decay of radionuclides in the interstellar medium that formed the solar system depends on the residence time of matter in molecular clouds. Therefore, it is necessary to consider the time interval (ΔT) between the formation of the solar system by the presolar interstellar medium.

Based on previous studies (Harper, 1996; Wasserburg et al., 1996; Busso et al., 1999; Jacobsen, 2005; Hidaka and Yoneda, 2013), Fig. 10 shows the correlation diagram between the average ratios of extinct short-lived radioactive isotopes to their stable reference isotopes in the early solar system normalized by the production ratios of these isotopes and the mean lifetimes of their short-lived radioactive isotopes on a logarithmic scale. In Fig. 10, the pattern of short-lived radionuclides in the average interstellar medium is a black line with a gradient of 1. These extinct nuclides with the half-lives of ~0.1 Ma (^{41}Ca) to ~100 Ma (^{146}Sm) that existed in the early solar system are not expected to have a single origin but to have multiple origins. According to previous studies (Jacobsen, 2005; Jacobsen and Ranen, 2006; Hidaka and Yoneda, 2013), these extinct nuclides can be roughly divided into the following three groups by using a dashed line representing the residence time of the matter in the molecular cloud of the approximately $\Delta T = 6 \times 10^7$ years in the UP model of $T = 10^{10}$ years in Fig. 10: (i) ^{53}Mn, ^{182}Hf, ^{244}Pu, and ^{146}Sm plotted near the dashed line suggest similar origins and injection into the interstellar medium. (ii) ^{129}I and ^{107}Pd are plotted below the dashed line and are considered to have a different origin from the former. (iii) ^{41}Ca, ^{26}Al, and ^{60}Fe are plotted above the dashed line and suggest the effects of contamination by nucleosynthetic components originating from young stars incorporated into the protosolar molecular cloud.

One important point is that there may be multiple contributions to the

nucleosynthesis of the r-process, one producing a nuclide with a mass number less than 140 and the other producing a nuclide with a mass number heavier than 140 (Wasserburg et al., 1996). Since ^{135}Cs is the mass number near the boundary between the nucleosynthesis of these r-processes, ^{135}Cs may have multiple sources of r-process nucleosynthesis. Furthermore, ^{135}Cs can be synthesized not only in r-process but also by the s-process. Hidaka and Yoneda (2013) reported the estimated abundance of ^{135}Cs (^{135}Cs/^{133}Cs = 6.8 × 10^{-4}) based on elemental and isotopic data of chemical separates in the acid leaching experiment in chondrules in CM chondrites, and have argued that the abundance of ^{135}Cs in the early solar system may be higher than that estimated by the UP model. On the other hand, Brennecka and Kleine (2017) estimated the upper limit of the low ^{135}Cs abundance (^{135}Cs/^{133}Cs = 2.8 × 10^{-6}) based on Ba isotopic data and Cs/Ba elemental ratios of differentiated meteorites (eucrites and angrites), and argued that ^{135}Cs consists of contributions from a single nucleosynthetic source. An important point in both discussions is whether the abundance of ^{135}Cs is greater or less than ^{135}Cs/^{133}Cs = ~10^{-5} in the early solar system (Brennecka and Kleine, 2017). In the case of (^{135}Cs/^{133}Cs > ~10^{-5}), the contribution of multiple nucleosynthetic components is necessary to explain the abundance of ^{135}Cs/^{133}Cs. In the case of (^{135}Cs/^{133}Cs < ~10^{-5}), the contribution of a single nucleosynthetic component can explain the abundance.

I discuss the nucleosynthetic source of ^{135}Cs based on the upper limit of the estimated value of ^{135}Cs/^{133}Cs in this study. Based on the elemental and isotopic data of the acid residues of CM chondrites in this study, the upper limits of the abundance of ^{135}Cs (^{135}Cs/^{133}Cs) were estimated to be (2.28 ± 0.43/2.28 ± 0.41) × 10^{-4} (Cold Bokkeveld), (1.40 ± 1.21/1.39 ± 0.85) × 10^{-4} (Murray), and (4.32 ± 0.68/4.31 ± 0.65) × 10^{-4} (Nogoya), respectively. The estimated values of these ^{135}Cs/^{133}Cs obtained in this

study cannot be explained by the contribution of a single nucleosynthetic component alone, suggesting the contribution of multiple nucleosynthetic components. One of the scenarios to interpret these multiple nucleosynthesis components is the contribution of various r-process nucleosynthesis components. As another interpretation, considering that these elemental and isotopic data are derived from acid residues including presolar SiC grains in the CM chondrites, the estimated abundances of ^{135}Cs in this study can be considered to reflect the contribution of the nucleosynthetic components of the s-process and the r-process.

4.1.4 Isotopic anomalies of ^{130}Ba and ^{132}Ba.

Most L1–L5 fractions in five of four carbonaceous chondrites, Cold Bokkeveld, Murray, Nogoya, and Tagish Lake had variable isotopic anomalies of ^{130}Ba and ^{132}Ba (see in Table 5 (b)). The measured isotopic anomalies of ^{130}Ba correlated with ^{132}Ba in this study and showed the same degree of isotopic anomalies as those observed in the previous study (Qin et al., 2011). This suggests that the apparent isotopic anomalies were caused by the false correction of the instrumental mass fractionation in association with the addition of s-process isotopes. According to the ^{134}Ba/^{136}Ba isotopic data (approximately 0.3338) (Prombo et al., 1993; Stephan et al., 2018) and to the Ba contents in the presolar grains (approximately 6 ppm) (Amari et al., 1994), the normalization value of ^{134}Ba/^{136}Ba would have shifted to approximately 0.307800 for Cold Bokkeveld, 0.307777 for Murray, 0.307787 for Nogoya, and 0.307776 for Tagish Lake. The apparent isotopic anomalies of ^{130}Ba and ^{132}Ba using the corrected normalization reflecting the enrichment of s-process isotopes produced a maximum of ε^{130}Ba = 8.77 and ε^{132}Ba = 5.80, respectively, which were too small to explain the measured isotopic anomalies in the data for ε^{130}Ba and

ε^{132}Ba (see in Table 5 (b)).

For further discussion about the origin of the isotopic anomalies of ^{130}Ba and ^{132}Ba, Fig. 11 shows the comparison of the ^{132}Ba/^{130}Ba ratios of this study and the previous study (Prombo et al., 1993). The calculated ^{132}Ba/^{130}Ba data range from 0.9556 to 0.9577 (see in Fig. 11). In addition, the ^{132}Ba/^{130}Ba ratio reflecting the enrichment of s-process isotopes (Prombo et al., 1993) showed large variation in the range from 0.9450 to 0.9637. Because the previous studies mainly focused on the s-process isotopes, these p-process isotopes with low isotopic abundance were not described in detail (Ott and Begemann, 1990; Prombo et al., 1993). Furthermore, there was a variation in the p-process isotope ratio (see in Fig. 11), which suggested a heterogeneous distribution of p-process isotopes in the early solar system, or heterogeneities of p-process isotopes in the presolar SiC grains. The isotope ratios of the L5 fractions showed a large variation of the p-process isotope ratios (0.9577 for Cold Bokkeveld, 0.9568 for Murray, 0.9575 for Nogoya, and 0.9568 for Tagish Lake), which might have been affected by the isotopic variations in the presolar SiC grains. Liu et al. (2015) pointed out that ^{130}Ba and ^{132}Ba were present in presolar SiC grains. On the other hand, the ^{132}Ba/^{130}Ba ratios of the L1–L4 fractions showed variations in the range from 0.9555 to 0.9571, which suggest a heterogeneous distribution of p-process isotopes in the early solar system. Although the isotopic data for acid leachates in this study may be due to isotopic anomalies due to the contribution of presolar silicates that are soluble in acid, there are no reports on Ba isotopic data for these acid soluble presolar materials.

4.2 Isotopic variation of Sr

As shown in Fig. 5, most chemical separates (L1–L5) and WR in carbonaceous

chondrites showed variable isotopic anomalies of ^{84}Sr. The isotopic anomalies of ^{84}Sr do not necessarily reflect the heterogeneity of the p-process isotopes, but may reflect the heterogeneity of the s- or r-process isotopes.

The acid residues (L5) in all of four CMs showed significant isotopic deficits of ^{84}Sr, suggesting the enrichment of s-process isotopes due to the presence of presolar SiC grains. Liu et al. (2015) pointed out that presolar SiC grains, which were carriers of s-process isotopes, might have a significantly large deficit of ε^{84}Sr (ε^{84}Sr < approximately −8000). The n-process components also had a large deficit of ε^{84}Sr (ε^{84}Sr = approximately −5200) (Stephan et al., 2018). However, as mentioned in section 3.1, the REE patterns of the L5 fractions from all four CMs suggested that the refractory inclusion was one of the main components in the L5 fractions (see in Fig. 2). In a previous study, CAIs had a higher excess of ^{84}Sr isotopic abundance (ε^{84}Sr = 1.23 ± 0.35) than WRs belonging to these types of carbonaceous chondrites (Hans et al., 2013). The inventory of ^{84}Sr isotopic deficits stemming only from presolar SiC grains in the L5 fractions can be estimated after subtracting the contribution of the CAIs by the following equation:

$$\varepsilon^{84}Sr_{L5(SiC)} = \varepsilon^{84}Sr_{L5} - \varepsilon^{84}Sr_{CAIs} = \varepsilon^{84}Sr_{L5} - 1.23$$

where $\varepsilon^{84}Sr_{L5(SiC)}$ are isotopic anomalies data due to the contribution of presolar SiC grains in the L5 fraction, $\varepsilon^{84}Sr_{L5}$ are measured ε^{84}Sr isotopic data for the L5 fraction, $\varepsilon^{84}Sr_{CAIs}$ are isotopic anomalies data for CAIs (ε^{84}Sr = 1.23) (Hans et al., 2013). If the data for $\varepsilon^{84}Sr_{L5(SiC)}$ reflected isotopic anomalies due to the contribution of presolar SiC grains, the abundance of presolar SiC grains could be estimated from $\varepsilon^{84}Sr_{L5(SiC)}$. Based on the Sr abundance in the presolar SiC grains (100 ppm) (Amari et al., 1995) and on

$\varepsilon^{84}Sr = -7000$ in presolar SiC grains (Liu et al., 2015; Stephan et al., 2018), I calculated the abundance of presolar SiC grains in Cold Bokkeveld (2.7 ppm), Murray (7.0 ppm), and Nogoya (1.4 ppm), which were consistent with previous results (Amari et al., 1994; Huss et al., 1997).

On the other hand, considering that the presolar SiC grains might also have isotopic anomalies of ^{88}Sr (Liu et al., 2015; Stephan et al., 2018), it is uncertain to estimate the contribution of presolar SiC grains only from the isotopic anomalies of ^{84}Sr. Because the $^{88}Sr/^{86}Sr$ ratio was fixed to 8.375209 for the correction of the instrumental mass fractionation in this study, it is possible that the isotopic anomalies of ^{84}Sr (p-process isotope) were caused by the variation of the $^{88}Sr/^{86}Sr$ normalizing value associated with the addition of s-process isotopes. Based on the content of presolar SiC grains in CMs in this study and on the reference isotopic data for presolar SiC grains (Liu et al., 2015; Stephan et al., 2018), I could confirm that the $\varepsilon^{84}Sr$ shifts from −0.1 to 1.3 (Cold Bokkeveld), from −0.1 to 0.8 (Murray), and from 0 to 0.5 (Nogoya) derived from the change of the normalization factor of $^{88}Sr/^{86}Sr$. It can be concluded that the ^{84}Sr isotopic anomalies in acid residues in CM chondrites reflect not only the contribution of the ^{84}Sr isotopic anomalies of presolar SiC grains and CAIs, but also the apparent isotopic anomalies resulting from the false correction of the mass fractionation.

Positive isotopic anomalies were observed in ^{84}Sr in the most acid-leachates of carbonaceous chondrites. While most of the data show the same degree of the excess as previous studies (Qin et al., 2011; Yokoyama et al., 2015; Burkhardt et al., 2019), Sr isotopic data of L4 of Nogoya showed large deviations from previous studies. The possible explanation for the ^{84}Sr isotopic excesses is the contribution of nucleosynthetic components other than s-process. One of the possibilities is nucleosynthetic origin for p-

process isotopes, which are believed to be synthesized mainly by type II supernovae (SNeII). Although the heterogeneity of p-process isotopes in the early solar system has been reported from the results of isotopic analysis of the primitive planetary materials (McCulloch and Wasserburg, 1978b; Andreasen and Sharma, 2006), p-process isotopic anomalies have rarely been found.

The second possibility is apparent isotopic anomalies of ^{84}Sr accompanied by the enrichment of r-process isotopes. Papanastassiou and Wasserburg (1978) reported a quantitative estimation of the effect of mass fractionation correction caused by the addition of r-process isotopes. They showed that the addition of r-process isotopes resulted in an isotopic excess of ^{84}Sr and a lower $^{87}Sr/^{86}Sr$ isotopic ratio. Assuming the isotopic anomalies due to the r-process, the ^{87}Sr isotope anomalies ($\varepsilon^{87}Sr$) estimated from the measured ^{84}Sr isotope anomalies is approximately –3.5. Considering that the Ba isotopic anomalies in acid leachates are the deficits of s-process isotopes, which is the enrichments of r-process isotopes, the isotopic excess of ^{84}Sr may have occurred in the enrichments of r-process isotopes.

The ^{87}Rb–^{87}Sr decay system of carbonaceous chondrites in this study does not provide any chronological information, which is consistent with the results of previous studies (Mittlefehldt and Wetherill, 1979; Macdougall, 2000; Qin et al., 2011; Yokoyama et al., 2015; Burkhardt et al., 2019). As this interpretation, it is possible that the various phases including Rb and Sr were redistributed by aqueous alterations in the CM and Tagish Lake meteorite parent bodies, and that the inconsistent dissolution of Rb and Sr from these phases occurred during the acid-leaching process. On the other hand, it is known that the CO, CV, and some CM chondrites are plotted on the same Rb–Sr isochron, while CI and some CM chondrites are not plotted on that isochron (Kaushal and Wetherill,

1970; Mittlefehldt and Wetherill, 1979). Considering these results, the information presented by the ^{87}Rb–^{87}Sr decay system of CI and CM chondrites and Tagish Lake is still controversial.

One possibility to be considered in the disturbance of the ^{87}Rb–^{87}Sr decay system is terrestrial weathering, which was confirmed by the ^{87}Rb–^{87}Sr decay system of NWA 4428. As noted at section 3.1, the results of trace elemental analyses of Murray and Tagish Lake suggest the possibility of terrestrial weathering. A reasonable explanation for not providing chronological information of the ^{87}Rb–^{87}Sr decay systems of the Murray and Tagish Lake is the disturbance by terrestrial weathering.

Considering another possibility that the higher Sr isotope ratio of some chemical separates than the that of the WR is due to the contribution of decay of ^{87}Rb (see in Fig. 6), the ^{87}Rb–^{87}Sr decay systems of CM chondrites and Tagish Lake might have been disturbed by late activities on these meteorite parent bodies, such as igneous, aqueous, metamorphic, or impact events. One of the plausible events is an intense impact that destroyed the meteorite parent bodies (Macdougall, 2000). Macdougall et al. (1984) carried out the leaching experiment of carbonate contained in CI chondrite (Orgueil), and pointed out the possibility that very fine soluble materials having an extremely higher $^{87}Sr/^{86}Sr$ isotopic ratio of 0.85337 than those of carbonates existed on the surface of carbonates. Subsequently, Macdougall (2000) performed leaching experiments of the CI chondrite and showed that the chemical separate had a high $^{87}Sr/^{86}Sr$ isotope ratio that did not correlate with the Rb/Sr elemental ratio, suggesting that this result reflects the recent redistribution of these elements and indicates the possibility of chemical fractionation associated with the destruction of the meteorite parent bodies. Considering that the petrological type of all carbonaceous chondrites used in this study is similar to that of the

CI chondrite, disturbances in the ^{87}Rb–^{87}Sr decay system of carbonaceous chondrites that have experienced aqueous alteration on meteorite parent bodies may also be due to recent intense events, like the intense impact that destroyed the meteorite parent bodies, rather than early events in the solar system. This event may have caused disturbances in the ^{135}Cs–^{135}Ba decay system of CM chondrites and Tagish Lake in this study.

As shown in Fig. 6, the data points for L5 in Cold Bokkeveld and Nogoya are not plotted on the ^{87}Rb–^{87}Sr evolution line but are plotted below that line. This suggests the presence of specific materials having isotopic deficits of ^{87}Sr in the L5. Considering elemental and Sr and Ba isotopic data of the L5, acid residues in CM chondrites may include CAIs and presolar SiC grains. Burkhardt et al. (2019) reported that the data for CAIs have Rb/Sr ratios ($^{87}Rb/^{86}Sr = 0.32 \pm 0.06$) comparable to the L5 in this study, and the data point is plotted on the ^{87}Rb–^{87}Sr evolution line. Furthermore, the REE patterns of the CAIs (Burkhardt et al., 2019) showed negative anomalies of Eu and Yb, which were also confirmed in the REE pattern of L5 (see in Fig. 3). On the other hand, considering that presolar SiC grains contained in the L5 showed various isotopic anomalies of ^{87}Sr (Approximately $-4000 < \varepsilon^{87}Sr < +2000$, Liu et al., 2015; Stephan et al., 2018), it is plausible that Sr isotopic data of L5 indicate the ^{87}Sr isotopic anomalies due to the contribution of presolar SiC grains. Further possibilities include the presence of other presolar materials having significant isotopic deficits of ^{87}Sr or apparent isotopic anomalies associated with the presence of presolar materials having significant isotopic excesses of ^{88}Sr.

4.3 Isotopic anomalies caused by SCR irradiation

Because planetary materials have experienced cosmic-ray irradiation, nuclear

reactions occurred by the interaction of cosmic-ray irradiation with surface parts of the materials. A systematic isotopic data set of chemical separates from planetary materials provided a detailed discussion of the CRE history (Hidaka and Yoneda, 2014, 2017). Interestingly, high-precision Sr and Ba isotopic data suggested that the isotopic excesses of ^{84}Sr, ^{130}Ba, and ^{132}Ba reflected possible nuclear reactions due to intense irradiation by SCR from the early Sun (Hidaka and Yoneda, 2014). The Kapoeta meteorite (howardite) is known as a solar-gas rich meteorite and it has a complex irradiation history (Caffee and Nishiizumi, 2001). Hidaka and Yoneda (2009) reported that the neutron capture history of the Kapoeta meteorite suggested the existence of material that had experienced early SCR irradiation. Furthermore, surface parts of the regolith particles in the Kapoeta showed systematic isotopic excesses of ^{84}Sr, ^{130}Ba, ^{132}Ba, ^{136}Ce, ^{138}Ce, and ^{144}Sm, suggesting isotopic excesses due to nuclear reactions caused by ancient SCR irradiation (Hidaka and Yoneda, 2014).

The Murray meteorite is known to have a complex CRE history among CM chondrites (Herzog et al., 1997). A previous study of the elemental and isotopic abundances of the noble gases in chondrules in Murray suggested possible excess irradiation by SCR (Das and Murty, 2009). Therefore, the systematic discussion of isotopic data for ^{84}Sr, ^{130}Ba, and ^{132}Ba in meteoritic samples having a complex exposure history can be used to explore the possible isotopic anomalies due to SCR irradiation.

As shown in Fig. 4, the Ba isotopic deviation pattern in the L4 fraction of Murray had a large isotopic excess of ^{130}Ba, which was slightly higher than that of other CMs and the previous report (Qin et al., 2011). One explanation is that the isotopic anomalies were caused by the nuclear reactions from SCR irradiation. The chondrules contained in Murray may have experienced ancient SCR irradiation (Das and Murty, 2009).

Chondrules are mainly composed of silicates, which are likely to be dissolved in the L5 fractions. The surface materials of chondrules may be dissolved in the L4 fraction with aqua regia before being dissolved in the L5 fraction. Considering that isotopic evidence of nuclear reactions associated with SCR irradiation was detected in the surface parts of Kapoeta (Hidaka and Yoneda, 2014), the ^{130}Ba isotopic excess in the L4 fraction in Murray may suggest the contribution of the nuclear reactions by SCR irradiation. Since the difference of the chemical compositions between chondrules in Murray and the surface parts of Kapoeta meteorite is unclear, it is not possible to quantitatively compare the isotopic data for the L4 fraction in Murray with those of previous studies (Hidaka and Yoneda, 2014). However, considering that the ^{130}Ba isotopic data of L4 were indistinguishable from those of the other fractions of L4 within the analytical uncertainties, there is also the possibility of an isotopic anomaly due to the deficits of s-process nucleosynthetic components as well as other fractions.

4.4 Comparison of elemental and isotopic data between CM chondrites and the Tagish Lake meteorite

Since the Tagish Lake meteorite may originate from the same parent body/ies as CM chondrite (Brandon et al., 2005), the possibility was discussed based on the comparison of the elemental and isotopic data of Tagish Lake and CM chondrites obtained in this study. The REE patterns of all fraction of Tagish Lake show flat pattern without Eu anomaly, which is different from the REE patterns of the chemical separates of the CMs (see in Fig. 3). Considering that Tagish Lake has few CAIs, it is plausible that the REE pattern of Tagish Lake does not have any features suggesting the presence of CAIs in the Tagish Lake. The low abundance of the CAIs in Tagish Lake is different from that

of the CM chondrite, but rather is a feature similar to that of the CI chondrites (Scott and Krot, 2005). This is consistent with previous petrological studies of the Tagish Lake (Brown et al., 2000; Zolensky et al., 2002).

Isotopic data of Sr and Ba for the Tagish Lake meteorites were similar to those for CM (see in Figs. 4 and 5). In particular, the Ba isotopic data of the acid residues in all carbonaceous chondrites confirmed the isotopic anomalies mainly due to the presence of presolar SiC grains. On the other hand, the degree of the isotopic anomalies in the acid residues of Tagish Lake seems to be less than those of other CMs. Considering the WR of Tagish Lake has enrichments of Sr (12 ppm) and Ba (11 ppm) in this study, it is appropriate to interpret that the isotopic compositions of Tagish Lake may be a mixture of the terrestrial materials and typical carbonaceous chondrite.

CHAPTER 5

Summary

The determinations of Ba and Sr isotopic compositions and elemental abundances of Rb, Sr, Cs, Ba, and REEs were carried out in five kinds of carbonaceous chondrites to find cosmochemical evidence of the nucleosynthetic isotopic anomalies in the primitive planetary materials. In order to make a detailed examination of the heterogeneity and diversity of the nucleosynthetic components, analyses of the chemical separate obtained from the sequential acid-leaching experiment were combined with the whole rock sample. The chemical separates obtained by the sequential acid-leaching experiment are suitable for the consideration of several factors contributing to isotopic anomalies in the primitive planetary material that cannot be detected by analyses of whole rock alone.

The Ba isotopic data of WRs of carbonaceous chondrites often show positive isotopic anomalies of ^{135}Ba correlated with ^{137}Ba. In addition, the isotopic anomalies of the chemical separates in the carbonaceous chondrites are significantly larger than those in the WRs. The isotopic data of the acid residues in all carbonaceous chondrites used in this study show significant negative isotopic anomalies of ^{130}Ba, ^{132}Ba, ^{135}Ba, ^{137}Ba, and ^{138}Ba, which represents an enrichment of the presence of a carrier of s-process nucleosynthetic components, such as presolar SiC grains.

Most Ba isotopic deviation patterns of chemical separates and WRs of carbonaceous chondrites show the isotopic anomalies of ε^{135}Ba correlated with ε^{137}Ba and ε^{138}Ba, suggesting the contribution of s-process nucleosynthetic component. However, all

measured Ba isotopic data could not be explained solely by the contribution of s-process nucleosynthetic components. The correlation between the isotopic data for ^{135}Ba, ^{137}Ba, and ^{138}Ba for the acid residues of Cold Bokkeveld, Murray, and Nogoya shows the isotopic anomalies of ^{138}Ba which could not be explained by the contributions of s-process nucleosynthetic components. Taking into account the elemental data for the acid residues, these isotopic anomalies of the acid residues may be attributed to the presolar X grains (n-process component) having a significant isotopic excess of ^{138}Ba.

Assuming that the Ba isotopic compositions of the acid residues in Cold Bokkeveld, Murray, and Nogoya were mixtures of s- and n-process nucleosynthetic components and radiogenic components of ^{135}Ba, I estimate the radiogenic isotopic excess of ^{135}Ba from the measured Ba isotopic data for the L5 fractions from these three CMs. Based on the correlation between the calculated radiogenic ^{135}Ba components and the Cs/Ba elemental ratios of the acid residues in Cold Bokkeveld, Murray, and Nogoya, the estimated values of the ^{135}Cs/^{133}Cs isotopic abundances were $(2.36 \pm 0.44/2.29 \pm 0.42) \times 10^{-4}$, $(1.40 \pm 1.21/1.39 \pm 0.85) \times 10^{-4}$, and $(4.46 \pm 0.69/4.31 \pm 0.65) \times 10^{-4}$, respectively. On the other hand, the ^{135}Cs–^{135}Ba decay system based on data from chemical separates other than L5 of CMs and WRs in all carbonaceous chondrites could not provide any chronological information. This result is considered to be caused by the disturbance of the ^{135}Cs–^{135}Ba decay system due to the high reactivity of Cs, and the Ba isotopic anomalies due to the contribution of several nucleosynthetic components. To find evidence of ^{135}Cs from Ba isotopic data, one needs to find a Cs-rich phase (Cs/Ba > 1). However, finding specific phases having high Cs/Ba elemental ratios in primitive meteorites is currently difficult, and it is necessary to consider the contribution of several additional nucleosynthetic components to discuss the initial abundances of ^{135}Cs using

precise Ba isotopic data.

The isotopic abundance of ^{135}Cs in the early solar system has been used to discuss the diversity of their origins. The r-process may have multiple contributions, one producing nuclides with mass numbers less than 140 and the other producing nuclides with a mass number heavier than 140. Since ^{135}Cs is the mass number near the boundary between the nucleosynthesis of these r-processes, ^{135}Cs may have multiple sources of r-process nucleosynthesis. Furthermore, ^{135}Cs is a nuclide that can be produced not only by r-processes but also by the s-process. An important point in the discussions of the diversity of the nucleosynthetic components of ^{135}Cs in the early solar system is whether isotopic abundances of ^{135}Cs estimated from meteoritic samples is greater or less than ^{135}Cs/^{133}Cs = ~10^{-5} (Brennecka and Kleine, 2017). In this study, the upper limits of the abundance of ^{135}Cs (^{135}Cs/^{133}Cs) were estimated to be (2.28 ± 0.43/2.28 ± 0.41) × 10^{-4} (Cold Bokkeveld), (1.40 ± 1.21/1.39 ± 0.85) × 10^{-4} (Murray), and (4.32 ± 0.68/4.31 ± 0.65) × 10^{-4} (Nogoya), respectively, based on the elemental and isotopic data of the acid residues of three CM chondrites. The estimated values of the ^{135}Cs/^{133}Cs obtained in this study cannot be explained by the contribution of a single nucleosynthetic component alone, and it is necessary to consider the contribution of multiple nucleosynthesis components to explain the estimated values of the ^{135}Cs/^{133}Cs. This interpretation can be attributed to the contribution of the nucleosynthetic components of multiple r-processes or the contribution of the nucleosynthetic components of the s-process.

The conditions required to detect isotopic excess of ^{135}Ba derived from decayed ^{135}Cs by mass spectrometry used in this study are described. Based on previous studies, the estimated abundances of ^{135}Cs were estimated to the range from 5.0 × 10^{-7} to 1.9 × 10^{-4} at the time of aqueous alteration on the carbonaceous chondrite parent bodies in the

early solar system (Fig. 12). Since the Ba isotopic data of the primitive planetary materials showed the isotopic anomalies due to the contribution of the nucleosynthetic components, the materials with a high Cs/Ba ratio are necessary for the detection of the radiogenic ^{135}Ba isotopic excess components. In addition, it is necessary to secure a minimum sample amount (Ba > 200 ng) in order to perform high-precision isotopic analysis by TIMS. One of the candidates for minerals with high Cs/Ba elemental ratio in meteorite samples is evaporate minerals, which is a mineral mainly containing alkali elements. Zolensky et al (1999) reported that halite with sylvite (~ 1 mg), a type of secondary mineral in meteorite samples, shows the elemental abundances of Rb (3.8 ppm) and Sr (0.26 ppm), which is extremely high Rb/Sr > 10. When Cs and Ba are substituted for these alkali concentration data, the amount of sample required for high-precision Ba isotopic analysis using evaporated minerals can be estimated to be about 800 mg, corresponding to 210 ng of Ba.

Ba isotopic data of most L1–L5 in four carbonaceous chondrites, Cold Bokkeveld, Murray, Nogoya, and Tagish Lake, show variable isotopic anomalies of ^{130}Ba and ^{132}Ba. The variations of ^{130}Ba/^{132}Ba in the chemical separate in the carbonaceous chondrites suggest a heterogeneous distribution of p-process isotopes in the early solar system. While the isotopic data of acid residues seem to be the isotopic anomalies associated with the variation of the p-process isotope in presolar SiC grains, the isotopic data for acid-leachates may reflect the contribution of presolar silicates that are soluble in acid.

The chemical separates and WR of carbonaceous chondrites used in this study also show variable isotopic anomalies of ^{84}Sr. Considering the elemental abundances of acid residues in CMs, the isotopic deficits of ^{84}Sr of the L5 fraction suggested the possibility of mixed anomalies stemming from presolar SiC grains and CAIs. However,

some of the apparent isotopic anomalies also resulted from the false correction of the mass fractionation.

The ^{87}Rb–^{87}Sr decay system of carbonaceous chondrites in this study does not provide any chronological information, which is consistent with the results of previous studies. it is possible that the various phases including Rb and Sr were redistributed by aqueous alterations in the CM and the Tagish Lake meteorite parent bodies, and that the incomplete dissolution of Rb and Sr from these phases occurred during the acid-leaching process. Considering another possibility that the higher Sr isotopic ratio of some chemical separates than the that of the WR is due to the contribution of decay of ^{87}Rb, the ^{87}Rb–^{87}Sr decay systems of CM chondrites and Tagish Lake might have been disturbed by late activities on these meteorite parent bodies, such an intense impact event that destroyed the meteorite parent bodies. It is possible that the ^{135}Cs–^{135}Ba decay system, which is an acid-leaching component, is disturbed by the impact events of meteorite parent bodies, as is the case with the ^{87}Rb–^{87}Sr decay system.

The chemical separates of carbonaceous chondrites used in this study show isotopic anomalies of ^{84}Sr, ^{130}Ba, and ^{132}Ba. Although some measured isotopic data showed various degrees of isotopic excesses of ^{84}Sr, ^{130}Ba, and ^{132}Ba, the systematic and significant isotopic anomalies associated with the SCR irradiation (Hidaka and Yoneda, 2014) could not be observed in this study.

Because the Tagish Lake meteorite may originate from the same parent body/ies as the CM chondrite (Brandon et al., 2005), this possibility was discussed based on the comparison of the elemental and isotopic data of Tagish Lake and CM chondrites obtained in this study. Assuming that the difference in REE pattern of acid residues between Tagish Lake and CM chondrites was due to the presence of CAIs, the abundance of CAIs in

Tagish Lake was found to be similar to that of CI chondrite compared to CM chondrite. On the other hand, isotopic data of Sr and Ba for Tagish Lake meteorites were similar to those for CM. In particular, the Ba isotopic data of the acid residues in all carbonaceous chondrites confirmed the isotopic anomalies mainly due to the presence of presolar SiC grains.

Acknowledgments

First of all, I would like to express my deepest gratitude to Prof. Hiroshi Hidaka (Department of Earth and Planetary Sciences, Nagoya University) for his numerous suggestions throughout my research and his reviews of the manuscript. I have learned from him not only gave me a great deal of knowledge and techniques on chemical experiments and mass spectrometry but also how to proceed with study in cosmochemistry.

I would also like to thank Prof. Koshi Yamamoto (Nagoya University), Prof. Masayo Minami (Nagoya University), Dr. Yasuhiro Hirahara (Nagoya University), Dr. Koichi Mimura (Nagoya University) and Dr. Yoshihiro Asahara (Nagoya University) for their various advice on experiment and measurements, and for their fruitful discussion of my research.

I am very grateful to Dr. Shigekazu Yoneda (National Museum of Nature and Science) for his assistance in isotopic measurements by the TIMS and his valuable comments on my research.

I would like to thank all members of the Geochemistry cosmochemistry laboratory at Nagoya University for their various comments on my research.

I would like to express my deep appreciation to my parents, Kazuhisa Sakuma and Akemi Sakuma, for their great support and their understanding of advancing to doctoral programs.

A part of this study was supported financially by a Research Fellowships of Japan Society for the Promotion of Science for Young Scientist from the Japan Society for the Promotion of Science (19J10133).

REFERENCES

Amari, S., Lewis, R. S. and Anders, E. (1994) Interstellar grains in meteorites: I. Isolation of SiC, graphite, and diamond; size distributions of SiC and graphite. *Geochim. Cosmochim. Acta* **58**, 459–470.

Amari, S., Hoppe, P., Zinner, E. and Lewis R. S. (1995) Trace element concentrations in single circumstellar silicon carbide grains from the Murchison meteorite. *Meteoritics* **30**, 679–693.

Anders, E. and Grevesse, N. (1989) Abundances of the elements: meteoritic and solar. *Geochim. Cosmochim. Acta* **53**, 197–214.

Andreasen, R. and Sharma, M. (2006) Solar nebula heterogeneity in p-process samarium and neodymium isotopes. *Sciences* **314**, 806–809.

Andreasen, R. and Sharma, M. (2007) Mixing and homogenization in the early solar system: clues from Sr, Ba, Nd, and Sm isotopes in meteorites. *The Astrophysical Journal* **665**, 874–883.

Bermingham, K. R., Mezger, K., Desch, S., Scherer, E. E. and Horstmann, M. (2014) Evidence for extinct ^{135}Cs from Ba isotopes in Allende CAIs? *Geochim. Cosmochim. Acta* **133**, 463–478.

Bermingham, K. R., Mezger, K., Scherer, E. E., Horan, M. F., Carlson, R. W., Upadhyay, D., Magna, T. and Pack, A. (2016) Barium isotope abundances in meteorites and their implications for early Solar System evolution. *Geochim. Cosmochim. Acta* **175**, 282–298.

Bisterzo, S., Gallino, R., Käppeler, F., Wiescher, M., Imbriani, G., Straniero, O., Cristallo, S., Gorres, J. and deBoer, R. J. (2015) The branchings of the main s-process: their sensitivity to α-induced reactions on ^{13}C and ^{22}Ne and to the uncertainties of the nuclear network. *Monthly Notices of the Royal Astronomical Society* **449**, 506–527.

Bouvier, A. and Wadhwa, M. (2010) The age of the Solar System redefined by the oldest Pb–Pb age of a meteoritic inclusion. *Nature geoscience* **3**, 637.

Boynton, W. V., Frazier, R. M. and Macdougall, J. D. (1980) Identification of an ultra-refractory component in the Murchison meteorite (abstract). In *Lunar and Planetary Science Conference* **11**, (pp. 103–105).

Brandon, A. D., Humayun, M., Puchtel, I. S. and Zolensky, M. E. (2005) Re-Os isotopic systematics and platinum group element composition of the Tagish Lake carbonaceous chondrite. *Geochim. Cosmochim. Acta* **69**, 1619.

Brennecka, G. A., Borg, L. E. and Wadhwa, W. (2013) Evidence for supernova injection into the solar nebula and the decoupling of r-process nucleosynthesis. *Proc.*

Natl. Acad. Sci. **110**, 17241–17246.

Brennecka, G. A. and Kleine, T. (2017) A Low Abundance of ^{135}Cs in the Early Solar System from Barium Isotopic Signatures of Volatile-depleted Meteorites. *The Astrophysical Journal Letters* **837**, L9 (6pp).

Brown, P. G., Hildebrand, A. R., Zolensky, M. E., Grady, M., Clayton, R. N., Mayeda, T. K., Tagliaferri, E., Spalding, R., MacRae, N. D., Hoffman, E. L., Mittlefehldt, D. W., Wacker, J. F., Bird, J. A., Campbell, M. D., Carpenter, R., Gingerich, H., Glatiotis, M., Greiner, E., Mazur, M. J., McCausland P. J., Plotkin, H. and Mazur, T. R. (2000) The fall, recovery, orbit, and composition of the Tagish Lake meteorite: A new type of carbonaceous chondrite. *Science* **290**, 320–325.

Burkhardt, C., Dauphas, N., Hans, U., Bourdon, B. and Kleine, T. (2019) Elemental and isotopic variability in solar system materials by mixing and processing of primordial disk reservoirs. *Geochim. Cosmochim. Acta* **261**, 145–170.

Busso, M., Gallino, R. and Wasserburg, G. J. (1999) Nucleosynthesis in asymptotic giant branch stars: Relevance for galactic enrichment and solar system formation. *Annual Review of Astronomy and Astrophysics* **37**, 239–309.

Caffee, M. W. and Nishiizumi, K. (2001) Exposure history of separated phases from the Kapoeta meteorite. *Meteoritics & Planetary Science* **36**, 429–437.

Carlson, R. W., Boyet, M. and Horan, M. (2007) Chondrite barium, neodymium, and samarium isotopic heterogeneity and early earth differentiation. *Science* **316**, 1175–1178.

Das, J. P. and Murty, S. V. S. (2009) Cosmogenic and trapped noble gases in individual chondrules: Clues to chondrule formation. *Meteoritics & Planetary Science* **44**, 1797–1818.

Ebihara, M. and Honda, M. (1987) Rare earth elements in Ca-phosphates of Allende carbonaceous chondrite. *Meteoritics* **22**, 179–190.

Ferdous, J., Brandon, A. D., Peslier, A. H. and Pirotte, Z. (2017) Evaluating crustal contributions to enriched shergottites from the petrology, trace elements, and Rb-Sr and Sm-Nd isotope systematics of Northwest Africa 856. *Geochim. Cosmochim. Acta* **211**, 280–306.

Friedrich, J. M., Wang, M. S. and Lipschutz, M. E. (2002) Comparison of the trace element composition of Tagish Lake with other primitive carbonaceous chondrites. *Meteoritics & Planetary Science* **37**, 677–686.

Fujiya, W., Sugiura, N., Hotta, H., Ichimura, K. and Sano, Y. (2012) Evidence for the late formation of hydrous asteroids from young meteoritic carbonates. *Nature Commun*. **3**, 627–633.

Fujiya, W., Sugiura, N., Sano, Y. and Hiyagon, H. (2013) Mn–Cr ages of dolomites in CI chondrites and the Tagish Lake ungrouped carbonaceous chondrite. *Earth Planet. Sci. Lett.* **362**, 130–142.

Grossman, L., Ganapathy, R. and Davis, A. M. (1977) Trace elements in the Allende meteorite—III. Coarse-grained inclusions revisited. *Geochim. Cosmochim. Acta* **41**, 1647–1664.

Hans, U., Kleine, T. and Bourdon, B. (2013) Rb-Sr chronology of volatile depletion in differentiated protoplanets: BABI, ADOR and ALL. *Earth Planet. Sci. Lett.* **374**, 204.

Harper, C. L. (1996) Astrophysical site of the origin of the Solar System inferred from extinct radionuclide abundances. *The Astrophysical Journal* 466, 1026–1038.

Herzog, G. F., Vogt, S., Albrecht, A., Xue, S., Fink, D., Klein, J., Middleton, R., Weber, H. W. and Schultz, L. (1997) Complex exposure histories for meteorites with "short" exposure ages. *Meteoritics & Planetary Science* **32**, 413–422.

Heymann, D. and Anders, E. (1967) Meteorites with short cosmic-ray exposure ages, as determined from their Al^{26} content. *Geochim. Cosmochim. Acta* **31**, 1793–1809.

Hezel, D. C., Russell, S. S., Ross, A. J. and Kearsley, A. T. (2008) Modal abundances of

CAIs: Implications for bulk chondrite element abundances and fractionations. *Meteoritics & Planetary Science* **43**, 1879–1894.

Hidaka, H., Ohta, Y., Yoneda, S. and De Laeter J. R. (2001) Isotopic search for live ^{135}Cs in the early solar system and possibility of ^{135}Cs–^{135}Ba chronometer. *Earth Planet. Sci. Lett.* **193**, 459–466.

Hidaka, K., Ohta, Y. and Yoneda, S. (2003) Nucleosynthetic components of the early solar system inferred from Ba isotopic compositions in carbonaceous chondrites. *Earth Planet. Sci. Lett*. **214**, 455–466.

Hidaka, H. and Yoneda, S. (2009) Isotopic evidence of non-thermalized neutron irradiation in solar-gas-rich meteorites: Possibility of the interaction with solar neutrons and activity from the early Sun. *Earth Planet. Sci. Lett.* **285**, 173–178.

Hidaka, H. and Yoneda, S. (2011) Diverse nucleosynthetic components in barium isotopes of carbonaceous chondrites: Incomplete mixing of s-and r-process isotopes and extinct ^{135}Cs in the early solar system. *Geochim. Cosmochim. Acta* **75**, 3687–3697.

Hidaka, H. and Yoneda, S. (2013) Radioactive Cs capture in the early solar system. *Sci. Rep*. **3**, 1330.

Hidaka, H. and Yoneda, S. (2014) Isotopic excesses of proton-rich nuclei related to space weathering observed in a gas-rich meteorite Kapoeta. *The Astrophysical Journal* **786**, 138.

Hidaka, H., Higuchi, T. and Yoneda, S. (2015) Redistribution of alkaline elements in association with aqueous activity in the early solar system. *The Astrophysical Journal* **815**, 76.

Hidaka, H. and Yoneda, S. (2016) Rb-Sr and Cs-Ba Systematics of Eucrites (abstract). In *Annual Meeting of the Meteoritical Society* **79**, 1921.

Hidaka, H. and Yoneda, S. (2017) Systematic Isotopic Variations of Barium, Lanthanum, and Samarium Due to Cosmic-Ray Irradiation in Lunar Surfacial Materials (abstract). In *Lunar and Planetary Science Conference* **48**.

Hiroi, T., Zolensky, M. E. and Pieters, C. M. (2001) The Tagish Lake meteorite: A possible sample from a D-type asteroid. *Science* **293**, 2234–2236.

Hoppe, P., Leitner, J., Gröner, E., Marhas, K. K., Meyer, B. S. and Amari, S. (2010) NanoSIMS studies of small presolar SiC grains: New insights into supernova nucleosynthesis, chemistry, and dust formation. *The Astrophysical Journal* **719**, 1370–1384.

Huss, G. R. (1997) The survival of presolar grains in solar system bodies. In *AIP*

Conference Proceedings (Vol. 402, No. 1, pp. 721–748). AIP.

Ireland, T. R., Fahey, A. J. and Zinner, E. K. (1988) Trace-element abundances in hibonites from the Murchison carbonaceous chondrite: Constraints on high-temperature processes in the solar nebula. *Geochim. Cosmochim. Acta* **52**, 2841–2854.

Jacobsen, S. B. (2005) The birth of the Solar System in a molecular cloud: evidence from the isotopic pattern of short-lived radionuclides in the early Solar System. In Chondrites and the Protoplanetary Disk. *ASP Conference Series* 341. pp. 548–551.

Kaushal, S. K. and Wetherill, G. W. (1970) Rubidium 87–strontium 87 age of carbonaceous chondrites. *Journal of Geophysical Research* 75(2), 463–468.

Lewis, R. S., Huss, G. R. and Lugmair, G. (1991) Finally, Ba & Sr accompanying Xe-HL in diamonds from Allende (abstract). In *Lunar and Planetary Science Conference* 22.

Liu, N., Savina, M. R., Gallino, R., Davis, A. M., Bisterzo, S., Gyngard, F., Ka¨ppeler, F., Cristallo, S., Dauphas, N., Pellin, M. J. and Dillmann, I. (2015) Correlated strontium and barium isotopic compositions of acid-cleaned single mainstream silicon carbides from Murchison. *The Astrophysical Journal* **803**, 12 (23pp).

Lodders, K. (2003) Solar system abundances and condensation temperatures of the elements. *The Astrophysical Journal* **591**, 1220–1247.

Macdougall, J. D., Lugmair, G. W. and Kerridge, J. F. (1984) Early solar system aqueous activity: Sr isotope evidence from the Orgueil CI meteorite. *Nature* **307**, 249.

Macdougall, J. D. (2000) Sr isotopes in the Orgueil CI meteorite: Chronology of early solar system hydrothermal activity. *Journal of Earth System Science* **109**, 187–193.

McCulloch, M. T. and Wasserburg, G. J. (1978a) Barium and neodymium isotopic anomalies in the Allende meteorite. *The Astrophysical Journal Letters* **220**, L15–L19.

McCulloch, M. T. and Wasserburg, G. J. (1978b) More anomalies from the Allende meteorite: Samarium. *Geophysical Research Letters* **5**, 599–602.

McKeegan, K. D., Chaussidon, M. and Robert, F. (2000) Incorporation of short-lived ^{10}Be in a calcium-aluminum-rich inclusion from the Allende meteorite. *Science* **289**, 1334–1337.

Mittlefehldt, D. W. and Wetherill, G. W. (1979) Rb-Sr studies of CI and CM chondrites. *Geochim. Cosmochim. Acta* **43**, 201–206.

Moynier, F., Day, J. M. D., Okui, W., Yokoyama, T., Bouvier, A., Walker, R. J. and Podosek, F. A. (2012) Planetary-scale strontium isotopic heterogeneity and the age of volatile depletion of early solar system materials. *The Astrophysical Journal* **758**, 45.

Nakamura, T., Noguchi, T., Zolensky, M. E. and Tanaka, M. (2003) Mineralogy and noble-gas signatures of the carbonate-rich lithology of the Tagish Lake carbonaceous chondrite: Evidence for an accretionary breccia. *Earth Planet. Sci. Lett.* **207**, 83–101.

Norton, M. B. and McSween, H. Y. (2007) Quantifying the volumetric abundances of the components of the Murray CM chondrite: A preliminary investigation (abstract). In *Lunar and Planetary Science Conference* **38**, 1807.

Ott, U. and Begemann, F. (1990) Discovery of s-process barium in the Murchison meteorite. *The Astrophysical Journal* **353**, L57–L60.

Papanastassiou, D. A. and Wasserburg, G. J. (1978) Strontium isotopic anomalies in the Allende meteorite. *Geophys. Res. Lett*. **5**. 595–598.

Paton, C., Schiller, M. and Bizzarro, M. (2013) Identification of an ^{84}Sr-depleted carrier in primitive meteorites and implications for thermal processing in the solar protoplanetary disk. *The Astrophysical Journal Letters* **763**, L40.

Pellin, M. J., Calaway, W. F., Davis, A. M., Lewis, R. S., Amari, S. and Clayton, R. N. (2000) Toward complete isotopic analysis of individual presolar silicon carbide grains: C, N, Si, Sr, Zr, Mo, and Ba in single grains of Type X (abstract). In *Lunar and Planetary Science Conference* **31**, 1917.

Pellin, M. J., Savina, M. R., Calaway, W. F., Tripa, C. E., Barzyk, J. G., Davis, A. M., Gyngard, F., Amari, S., Zinner, E., Lewis, R. S. and Clayton, R. N. (2006) Heavy metal isotopic anomalies in supernovae presolar grains (abstract). In *Annual Lunar and Planetary Science Conference* **37**, 2041.

Podosek, F. A., Prombo, C. A., Amari, S. and Lewis, R. S. (2004) s-process Sr isotopic compositions in presolar SiC from the Murchison meteorite. *The Astrophysical Journal* **605**, 960–965.

Prombo, C. A., Podosek, F. A., Amari, S. and Lewis, R. S. (1993) s-Process Ba isotopic compositions in presolar SiC from the Murchison meteorite. *The Astrophysical Journal* **410**, 393–399.

Qin, L., Carlson, R. W. and Alexander, C. M. D. (2011) Correlated nucleosynthetic isotopic variability in Cr, Sr, Ba, Sm, Nd and Hf in Murchison and QUE 97008. *Geochim. Cosmochim. Acta* **75**, 7806–7828.

Ranen, M. C. and Jacobsen, S. B. (2006) Barium isotopes in chondritic meteorites: implications for planetary reservoir models. *Science* **314**, 809–812.

Reynolds, J. H. (1960) Isotopic composition primordial xenon. *Phys. Rev. Lett*. **4**, 8–10.

Rubin, A. E., Trigo-Rodríguez, J. M., Huber, H. and Wasson, J. T. (2007) Progressive aqueous alteration of CM carbonaceous chondrites. *Geochim. Cosmochim. Acta* **71**, 2361–2382.

Savina, M. R., Davis, A. M., Tripa, C. E., Pellin, M. J., Clayton, R. N., Lewis, R. S., Amari, C., Gallino, R. and Lugaro, M. (2003) Barium isotopes in individual presolar silicon carbide grains from the Murchison meteorite. *Geochim. Cosmochim. Acta* **67**, 3201–3214.

Scott, E. R. D. and Krot, A. N. (2005) Chondritic meteorites and the high-temperature nebular origins of their components. In *Chondrites and the Protoplanetary Disk,* Vol. 341. (eds. A. N. Krot, E. R. D. Scott, B. Reipurth). ASP Conference Series, pp.15–54.

Stephan, T., Trappitsch, R., Davis, A. M., Pellin, M. J., Rost, D., Savina, M. R., Jadhav, M., Kelly, C. H., Gyngard, F., Hoppe, P. and Dauphas, N. (2018) Strontium and barium isotopes in presolar silicon carbide grains measured with CHILI—two types of X grains. *Geochim. Cosmochim. Acta* **221**, 109–126.

Tomeoka, K. and Buseck, P. R. (1985) Indicators of aqueous alteration in CM carbonaceous chondrites: Microtextures of layered minerals containing Fe, S, O and Ni. *Geochim. Cosmochim. Acta* **49**, 2149–2163.

Trinquier, A., Birck, J. L. and Allègre, C. J. (2007) Widespread ^{54}Cr heterogeneity in the inner solar system. *The Astrophysical Journal* **655**, 1179–1185.

Vernazza, P., Fulvio, D., Brunetto, R., Emery, J. P., Dukes, C. A., Cipriani, F., Witasse, O., Scible, M. J., Zanda, B., Strazzulla, G. and Baragiola, R. A. (2013) Paucity of Tagish Lake-like parent bodies in the Asteroid Belt and among Jupiter Trojans. *Icarus* **225**, 517–525.

Wasserburg, G. J., Busso, M. and Gallino, R. (1996) Abundances of actinides and short-lived nonactinides in the interstellar medium: diverse supernova for the r-processes. *The Astrophysical. Journal* **466**. L109–L113.

Yokoyama, T., Fukami, Y., Okui, W., Ito, N. and Yamazaki, H. (2015) Nucleosynthetic strontium isotope anomalies in carbonaceous chondrites. *Earth Planet. Sci. Lett.* **416**, 46–55.

Yoneda, S., Ebihara, M., Oura, Y., Okada, A., Kusakabe, M., Nakamura, T., Nagao, K. and Naraoka, H. (2001) Sayama meteorite: a new CM chondrite fall in Japan with highly aqueous altered texture (abstract). In *Lunar and Planetary Science Conference* **32**, 2034.

Zhang, A. C., Li, Q. L., Yurimoto, H., Sakamoto, N., Li, X. H., Hu, S., Lin, Y. T. and Wang, R. C. (2016) Young asteroidal fluid activity revealed by absolute age from apatite in carbonaceous chondrite. *Nature communications* **7**, 12844.

Zinner, E., Amari, S. and Lewis, R. S. (1991) s-process Ba, Nd, and Sm in presolar SiC from the Murchison meteorite. *The Astrophysical. Journal* **382**. L47–L50.

Zolensky, M. E., Bourcier, W. L. and Gooding, J. L. (1989) Aqueous alteration on the hydrous asteroids: Results of EQ3/6 computer simulations. *Icarus* **78**, 411–425.

Zolensky, M. E., Bodnar, R. J., Gibson, E. K., Nyquist, L. E., Reese, Y., Shih, C. Y. and Wiesmann, H. (1999) Asteroidal water within fluid inclusion-bearing halite in an H5 chondrite, Monahans (1998). *Science* **285**(5432), 1377-1379.

Zolensky, M. E., Nakamura, K., Gounelle, M., Mikouchi, T., Kasama, T., Tachikawa, O. and Tonui, E. (2002) Mineralogy of Tagish Lake: An ungrouped type 2 carbonaceous chondrite. *Meteoritics & Planetary Science* **37**, 737–761.

APPENDIX

Appendix 1. Calculation of respective contributions of n- and s- process nucleosynthetic components.

Assuming that Ba isotopes of acid residues include s- and n-process components, I attempted to estimate the relative abundances of s- and n-process components in the measured Ba isotopic data. The contributions of n-process components to the Ba isotopic deviations measured in ^{137}Ba and ^{138}Ba isotopic data could be expressed with equations (1) and (2), respectively.

$$(\varepsilon^{137}\mathrm{Ba})_{\mathrm{measured}} = (\varepsilon^{137}\mathrm{Ba})_{\mathrm{s}} + (\varepsilon^{137}\mathrm{Ba})_{\mathrm{n}} \qquad (1)$$

$$(\varepsilon^{138}\mathrm{Ba})_{\mathrm{measured}} = (\varepsilon^{138}\mathrm{Ba})_{\mathrm{s}} + (\varepsilon^{138}\mathrm{Ba})_{\mathrm{n}} \qquad (2)$$

Where suffixes, s, and n is indicate the contribution of s- and n-process components.

In Fig. 8(b), the Ba isotopic data in the shaded zone were expressed by the equation (3) because they were affected only by the s-process component,

$$(\varepsilon^{138}\mathrm{Ba})_{\mathrm{s}} = f_{\text{s-process}} \times (\varepsilon^{137}\mathrm{Ba})_{\mathrm{s}} \qquad (3)$$

Where $f_{\text{s-process}}$ is the isotopic ratio of ^{138}Ba/^{137}Ba given by the additional s-process nucleosynthetic components (Ott and Begemann, 1990; Zinner et al., 1991; Prombo et al., 1993; Savina et al., 2003). The $f_{\text{s-process}}$ estimated from the reference isotopic data for the

presolar SiC grains (Zinner et al., 1991; Prombo et al., 1993) were 0.46– 0.70.

The contribution of the Ba isotopic data affected by the n-process component were estimated by equation (4)

$$(\varepsilon^{138}\mathrm{Ba})_{\mathrm{measured}} = f_{\text{n-process}} \times (\varepsilon^{137}\mathrm{Ba})_{\mathrm{measured}} + \mathrm{b} \qquad (4)$$

where $f_{\text{n-process}}$ is the isotopic ratio of $^{138}\mathrm{Ba}/^{137}\mathrm{Ba}$ given by the additional nucleosynthetic n-process components, and $(\varepsilon^{137}\mathrm{Ba})_{\mathrm{measured}}$ and $(\varepsilon^{138}\mathrm{Ba})_{\mathrm{measured}}$ are isotopic deviations of the measured $^{137}\mathrm{Ba}$ and $^{138}\mathrm{Ba}$ isotopic data from the L5, respectively. The $f_{\text{n-process}}$ showed an $\varepsilon^{138}\mathrm{Ba}/\varepsilon^{137}\mathrm{Ba} = 5.40$ (Stephan et al., 2018). The constant b could be determined from the measured $^{137}\mathrm{Ba}$ and $^{138}\mathrm{Ba}$ isotopic data for L5 and the $f_{\text{n-process}}$ (Cold Bokkeveld: b = 249, Murray: b = 15.7, Nogoya: b = 158).

The maximum and minimum value of $f_{\text{s-process}}$ in L5 was estimated from the upper and lower intersections, respectively, between the line expressed as equation (5) and the shaded zone in Fig. 8(b). The contribution of s-process nucleosynthetic components of L5 ($(\varepsilon^{137}\mathrm{Ba})_{\mathrm{s\ (L5)}}$) were finally expressed through equations (3) and (4).

$$(\varepsilon^{137}\mathrm{Ba})_{\mathrm{s\ (L5)}} = \left\{ \frac{\mathrm{b}}{(f\mathrm{s-process}) - (f\mathrm{n-process})} \right\} \qquad (5)$$

Therefore, the n-process components contained in the measured Ba isotope data of L5 ($(\varepsilon^{137}\mathrm{Ba})_{\mathrm{n\ (L5)}}$) could be estimated by using $(\varepsilon^{137}\mathrm{Ba})_{\mathrm{s\ (L5)}}$ obtained in (5) and equations (1).

Appendix 2. Matrix Calculation for Estimation of ^{135}Cs Using Ba Isotopic Data

I perform a matrix analysis to estimate the ^{135}Cs isotopic abundances based on the measured Ba isotopic data of L5 (Hidaka and Yoneda, 2011).

The equations were expressed in matrix form as follows:

$$\begin{pmatrix} s_{135} & n_{135} & {}^{135}\mathrm{Cs} \\ s_{137} & n_{137} & 0 \\ s_{138} & n_{138} & 0 \end{pmatrix} \begin{pmatrix} x \\ y \\ z \end{pmatrix} = \begin{pmatrix} \varepsilon_{135}\mathrm{Ba} \\ \varepsilon_{137}\mathrm{Ba} \\ \varepsilon_{138}\mathrm{Ba} \end{pmatrix}$$

where s_{135}, s_{137}, and s_{138} in the matrix are $(\varepsilon^{135,137,138}\mathrm{Ba})/(\varepsilon^{137}\mathrm{Ba})$ of s-process nucleosynthetic component (Ott and Begemann, 1990; Prombo et al., 1993), n_{135}, n_{137}, and n_{138} in the matrix are $(\varepsilon^{135,137,138}\mathrm{Ba})/(\varepsilon^{137}\mathrm{Ba})$ of n-process nucleosynthetic component (Stephan et al., 2018), *x, y,* and *z* are the inventory of the Ba isotopic deviations caused by the s- and n-process nucleosynthetic components and isotopic abundance of ^{135}Cs, respectively.

The 3 × 3 matrix was written as follows.

$$\begin{pmatrix} s_{135} & n_{135} & {}^{135}\mathrm{Cs} \\ s_{137} & n_{137} & 0 \\ s_{138} & n_{138} & 0 \end{pmatrix} = \begin{pmatrix} 1.50 \sim 1.90 & -1.90 & 1 \\ 1 & 1 & 0 \\ 0.46 \sim 0.70 & 5.40 & 0 \end{pmatrix}$$

$$\begin{pmatrix} x \\ y \\ z \end{pmatrix} = \begin{pmatrix} s_{135} & n_{135} & {}^{135}\mathrm{Cs} \\ s_{137} & n_{137} & 0 \\ s_{138} & n_{138} & 0 \end{pmatrix}^{-1} \begin{pmatrix} \varepsilon_{135}\mathrm{Ba} \\ \varepsilon_{137}\mathrm{Ba} \\ \varepsilon_{138}\mathrm{Ba} \end{pmatrix}$$

The maximum radiogenic components of ^{135}Ba obtained by modelling are listed

in table 7.

List of Figures

radioactive isotopes to their stable reference isotope in the early solar system normalized by the production ratios of these isotopes and their mean life.

Fig. 11. Calculated $^{132}Ba/^{130}Ba$ ratio from this study and previously reported Ba isotopic data from presolar SiC grains.

Fig. 12. Variation in the isotopic abundance of ^{135}Cs due to the time course after the formation of CAIs.

Fig. s1. $^{87}Sr/^{86}Sr$ isotope ratio during the measurement period.

List of Tables

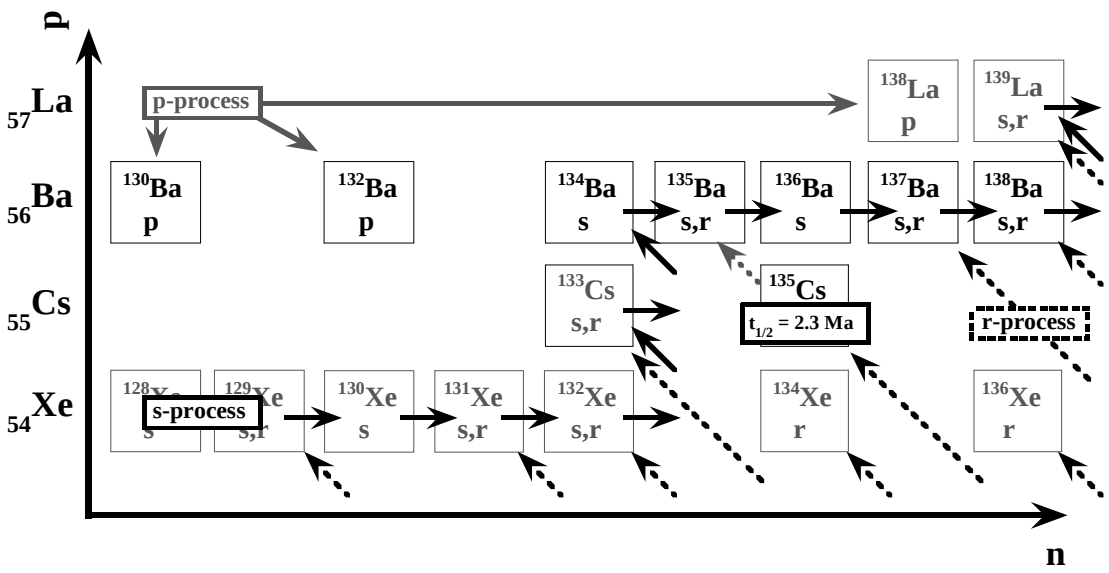

Fig. 1. Nuclear chart around Ba isotopes.

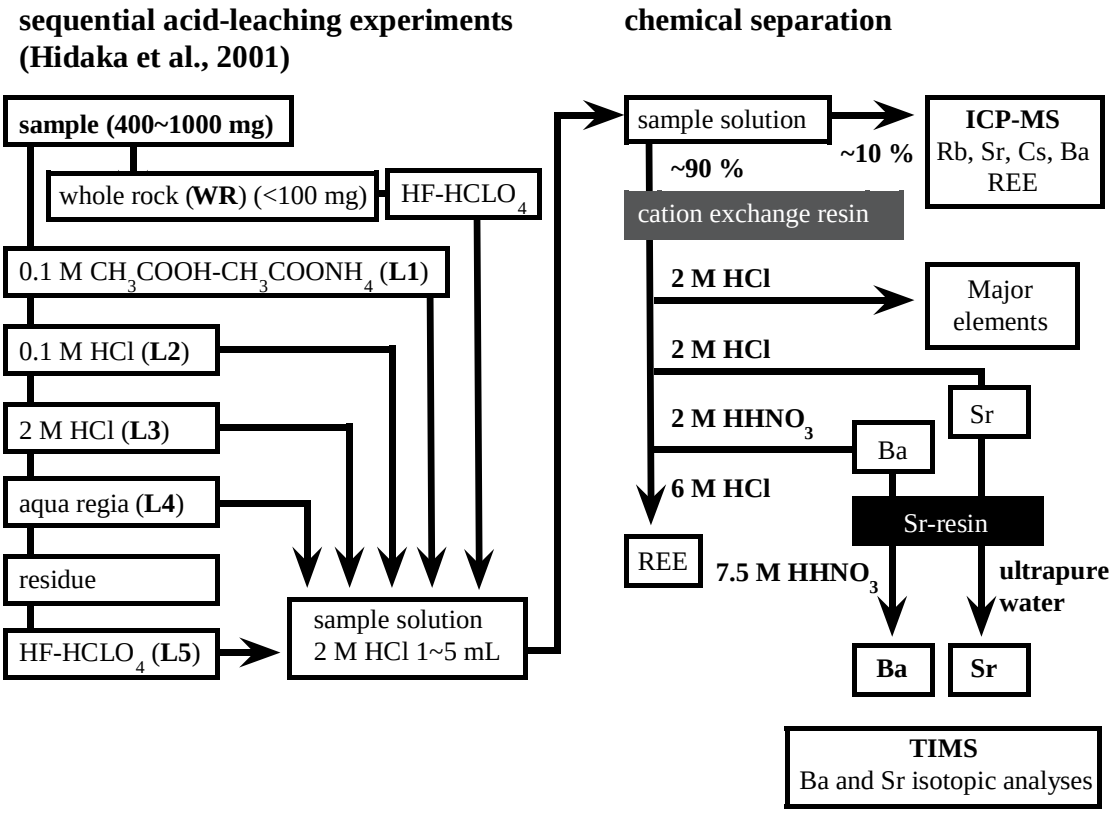

Fig. 2. Experimental scheme of sequential acid-leaching and chemical separation in this study.

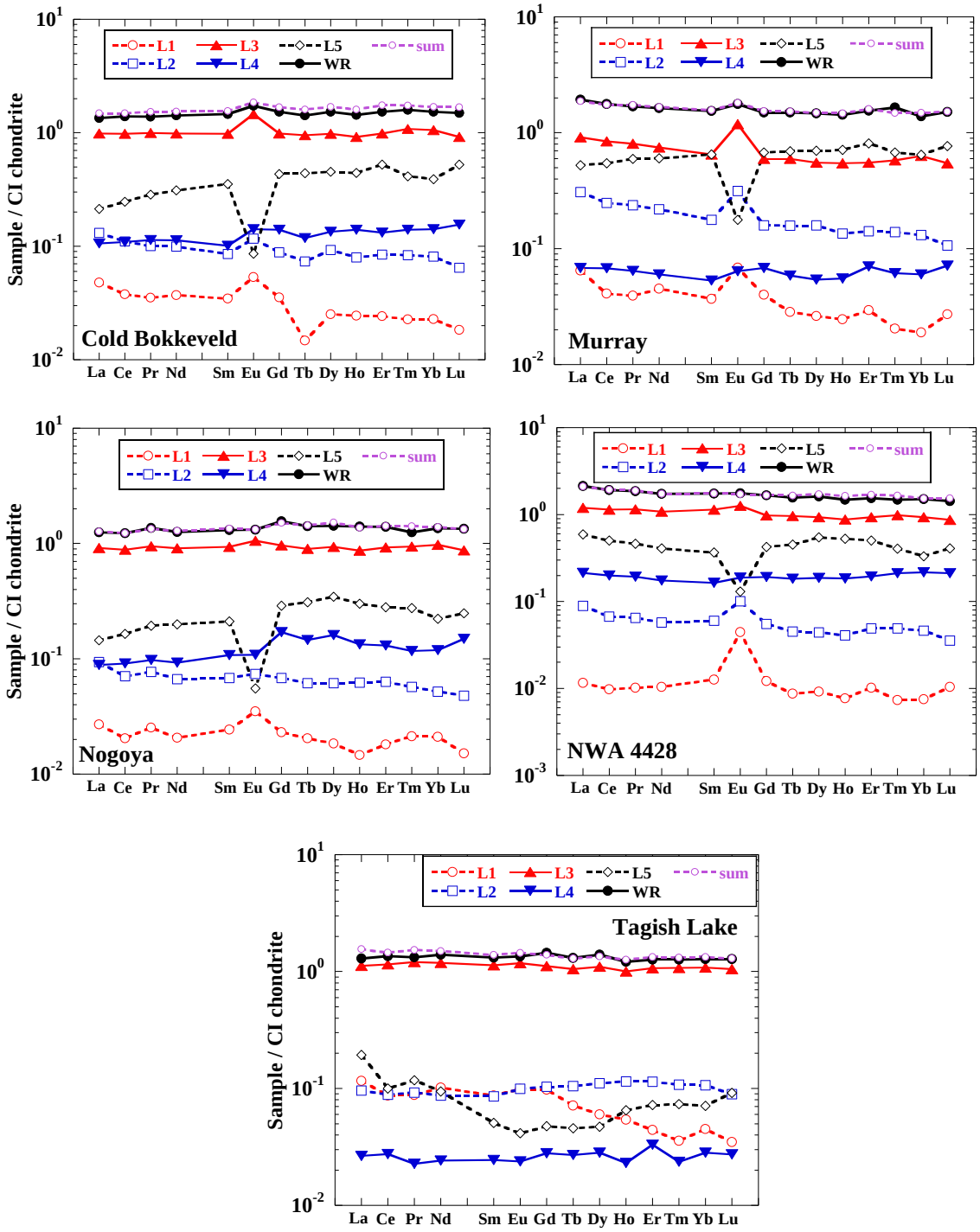

Fig. 3. CI chondrite-normalized REE patterns of L1–L5 and WR of Cold Bokkeveld, Murray, Nogoya, NWA 4428, and Tagish Lake (CI: Andreasen and Grevese, 1989). The data of individual samples from CM chondrites. The "sum" is the elemental abundances of whole rock based on the sum of the measured elemental data for each chemical fraction.

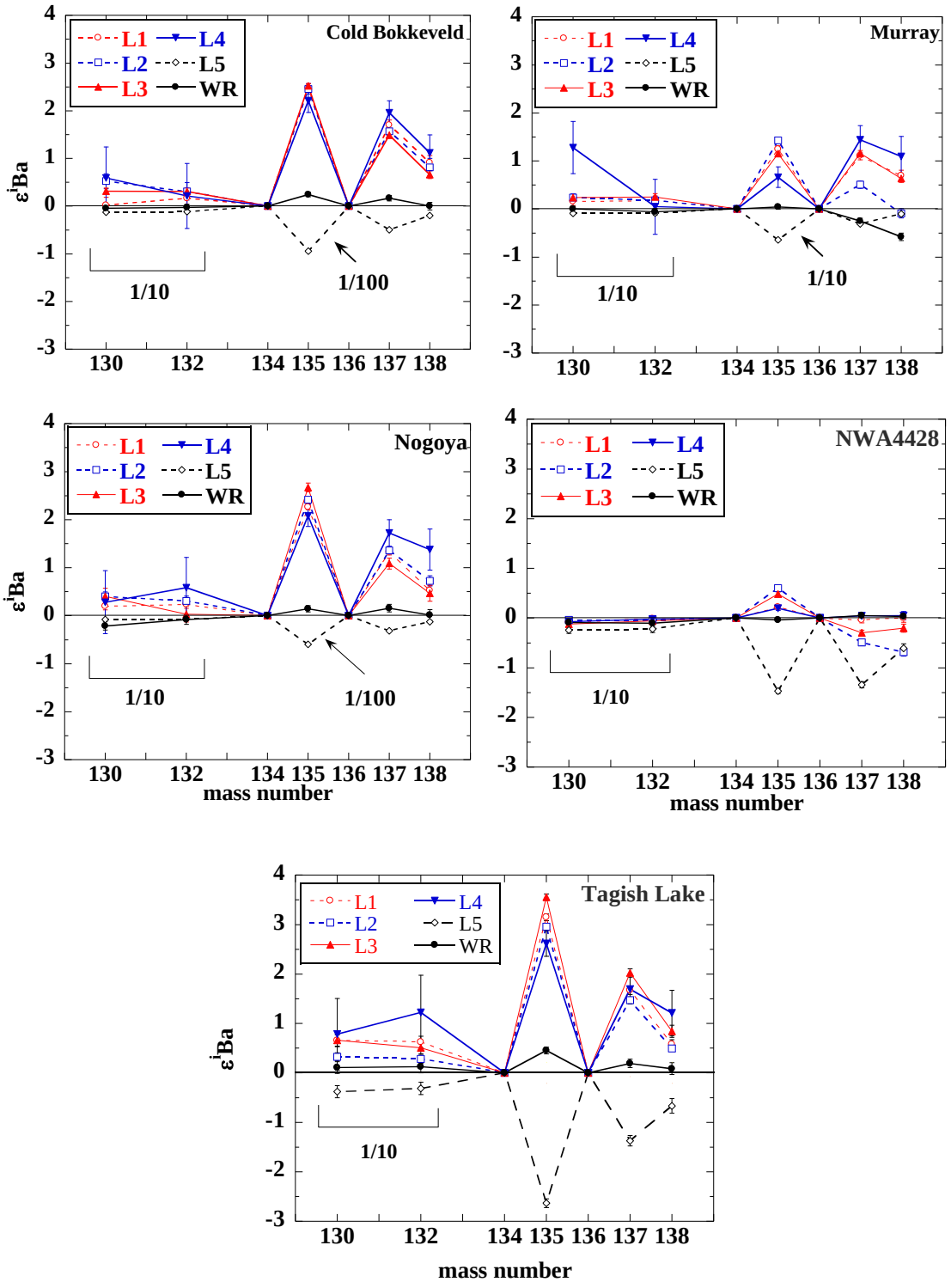

Fig. 4. Ba isotopic deviation patterns of L1–L5 and WR of Cold Bokkeveld, Murray, Nogoya, NWA 4428, and Tagish Lake. The data of ^{130}Ba and ^{132}Ba are plotted in one tenth of the measured values. Analytical errors are shown in 2σ of the means.

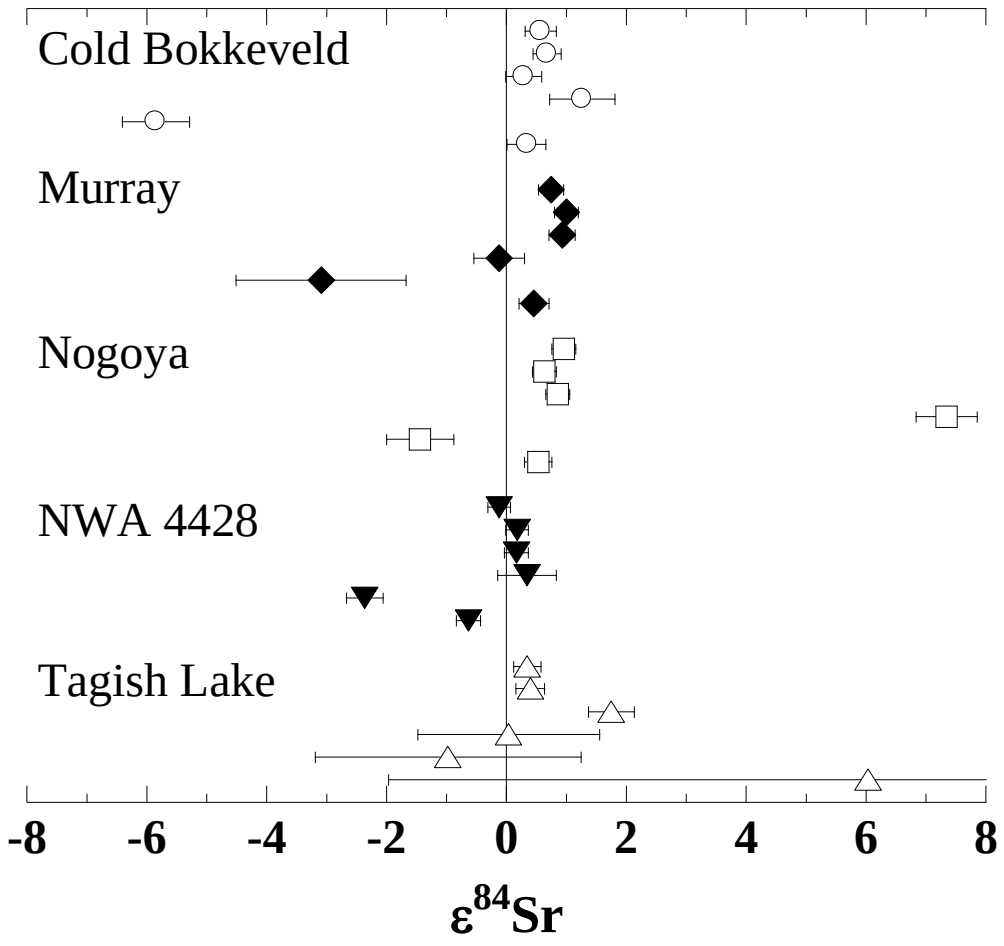

Fig. 5. ^{84}Sr isotopic deviation of L1–L5 and WR of Cold Bokkeveld, Murray, Nogoya, NWA 4428, and Tagish Lake. Analytical errors are shown in 2σ of the means.

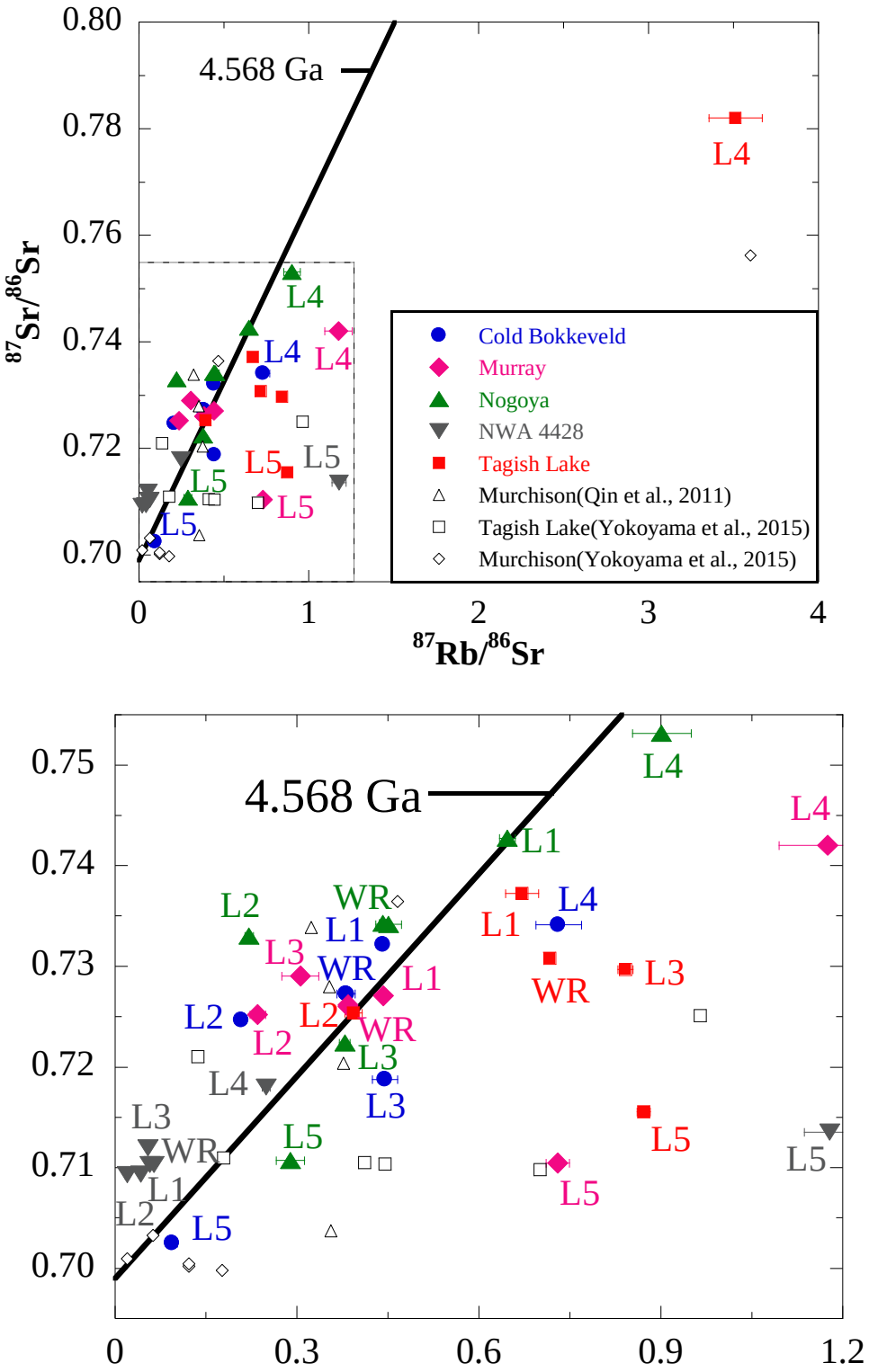

Fig. 6. Isochron diagram for ^{87}Rb–^{87}Sr consisting of the L1–L5 and WR of Cold Bokkeveld, Murray, Nogoya, NWA 4428, and Tagish Lake. The solid line in the figure shows an isochron with an age of 4.568Ga (Bouvier & Wadhwa, 2010). For the comparison in other primitive meteorites experienced aqueous alteration, the data of leaching fraction of CM and TL are also shown in the figure (Murchison, Qin et al., 2011; Yokoyama et al., 2015; TL, Yokoyama et al., 2015).

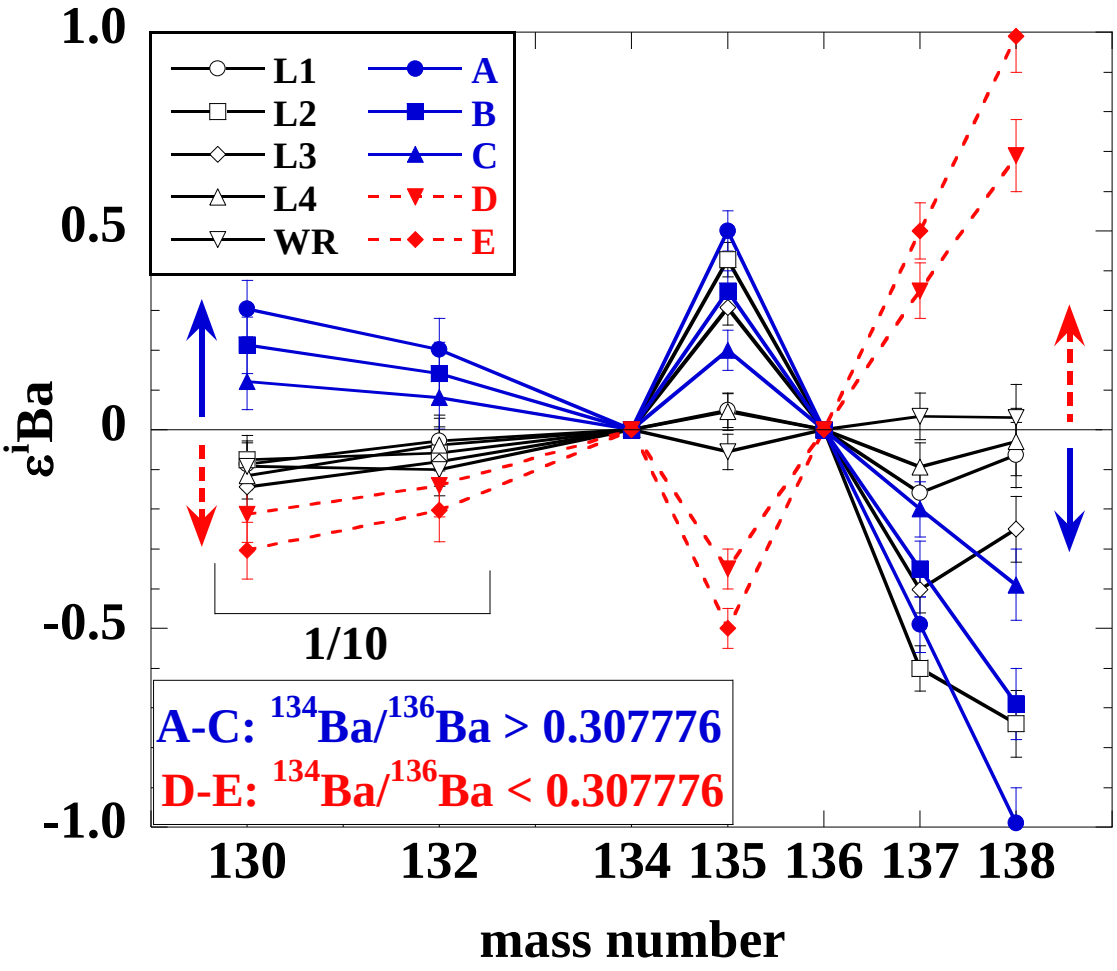

Fig. 7. Ba isotopic deviation pattern of the additional components of chemical separates and WR of NWA 4428, and apparent Ba isotopic deviation pattern based on estimated values of the Ba isotopic anomalies caused by false correction of the instrumental mass fractionation (A–E).

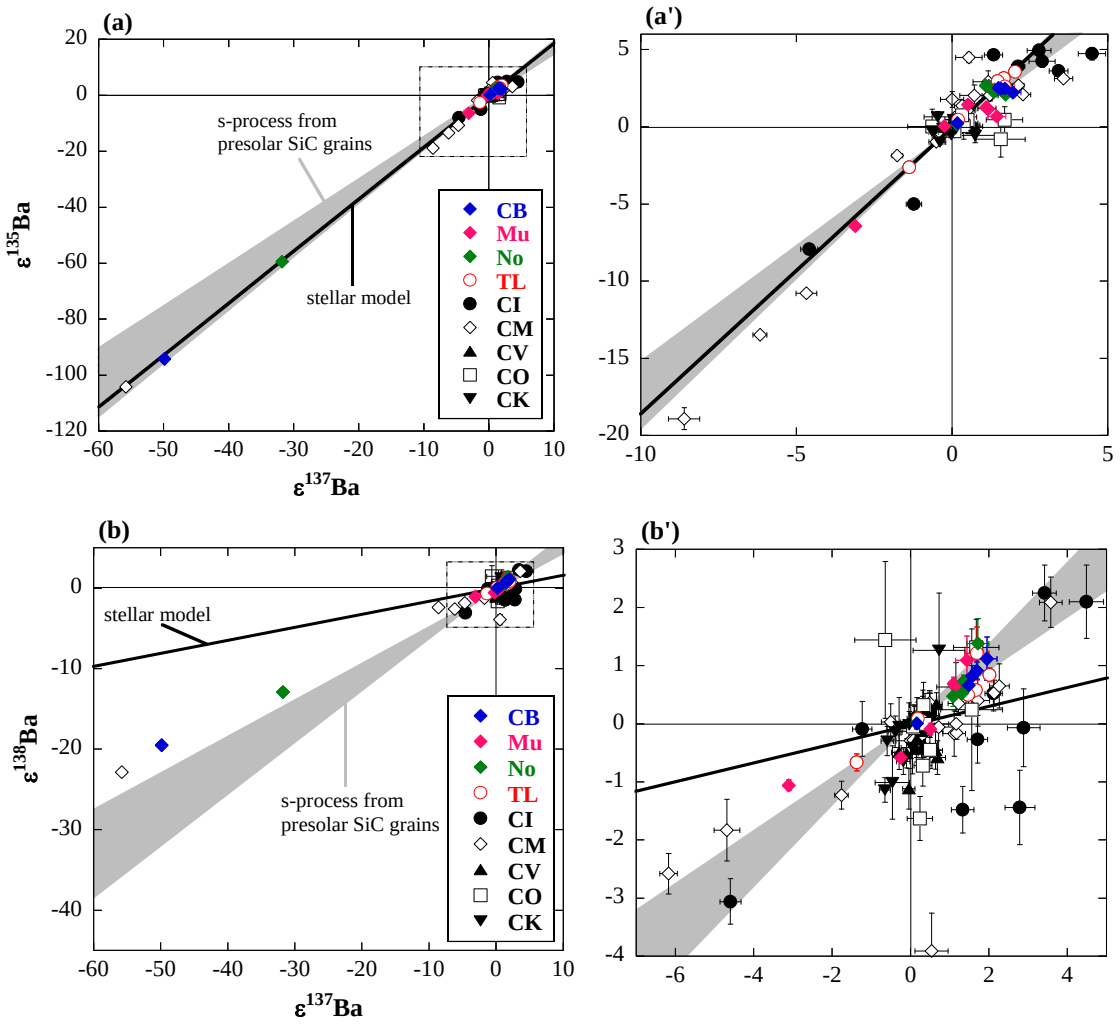

Fig. 8. Correlation diagrams of (a) ε^{135}Ba vs. ε^{137}Ba and (b) ε^{138}Ba vs. ε^{137}Ba for the individual chemical separates of the Cold Bokkeveld, Murray, Nogoya, and Tagish Lake. The gray zones in the figures show two components mixing data between the average of solar system components and s-process components from presolar SiC grains (Ott and Begemann, 1990; Zinner et al., 1991; Prombo et al., 1993). The solid lines in the figures show two components mixing data between the average of solar components and the additional nucleosynthetic component calculated by the stellar model (Bisterzo et al., 2015). For the comparison in other primitive meteorites, the data of chemical separates of carbonaceous chondrites are also shown in the figure (Hidaka et al., 2003; Hidaka and Yoneda, 2011; Qin et al., 2011).

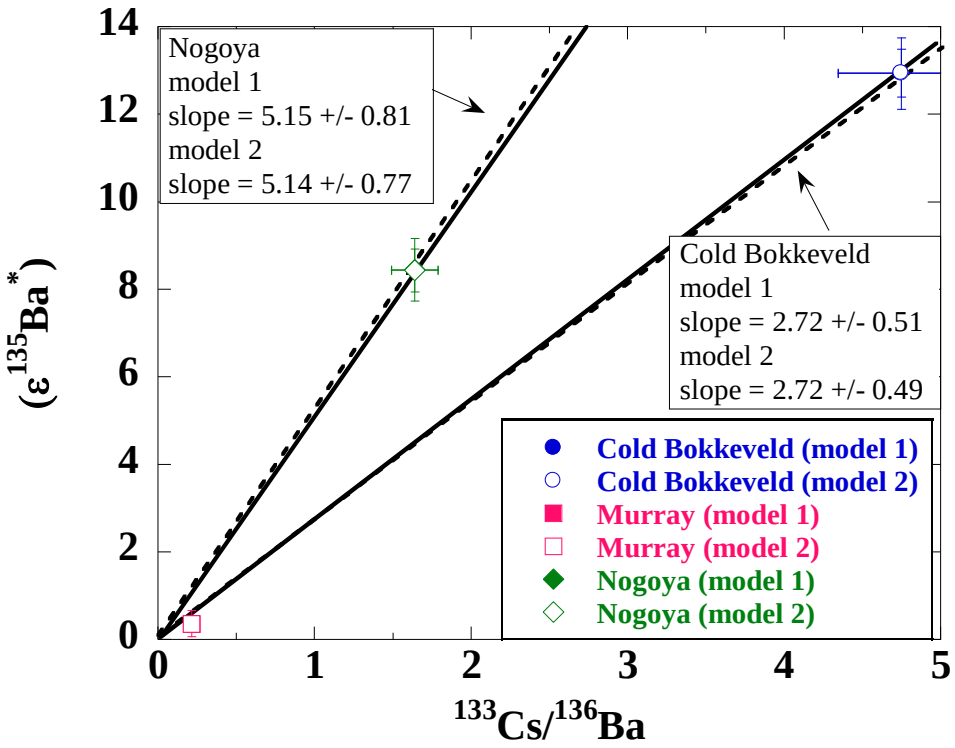

Fig. 9 (a). Isochron diagram for ^{135}Cs–^{135}Ba consisting of the L5 of Cold Bokkeveld, Murray, and Nogoya. The symbols in the figure are given by the ^{133}Cs/^{136}Ba elemental ratio and the highest value $(\varepsilon^{135}Ba)^{*}$ of model 1 (close symbols) and model 2 (open symbols), respectively. The lines in the figure are given by the data points of model 1 (solid lines) and model 2 (dotted lines), respectively.

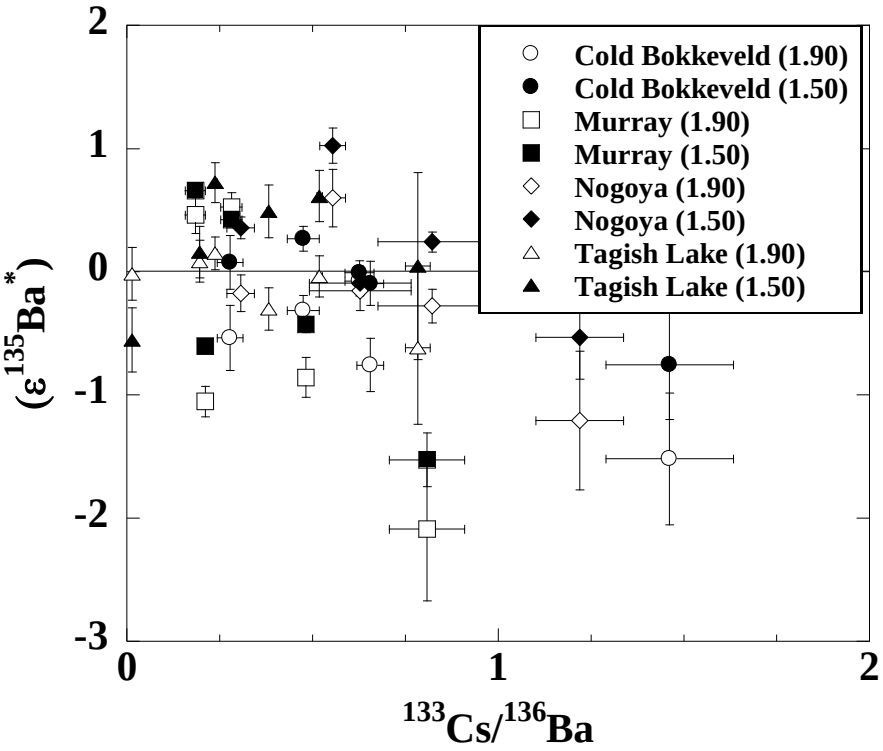

Fig. 9 (b). Isochron diagram for ^{135}Cs–^{135}Ba consisting of chemical separates other than L5 of CMs and WR of Cold Bokkeveld, Murray and Nogoya, and Tagish Lake. While the open symbol of (ε^{135}Ba*) is the calculated value based on the highest ^{135}Ba/^{137}Ba isotopic ratio (1.90) estimated from the isotopic data of the presolar SiC grain, the closed symbol of (ε^{135}Ba*) is the calculated value based on the lowest ^{135}Ba/^{137}Ba isotopic ratio (1.50) estimated from the isotopic data of the presolar SiC grain (Ott and Begemann, 1990; Zinner et al., 1991; Prombo et al., 1993).

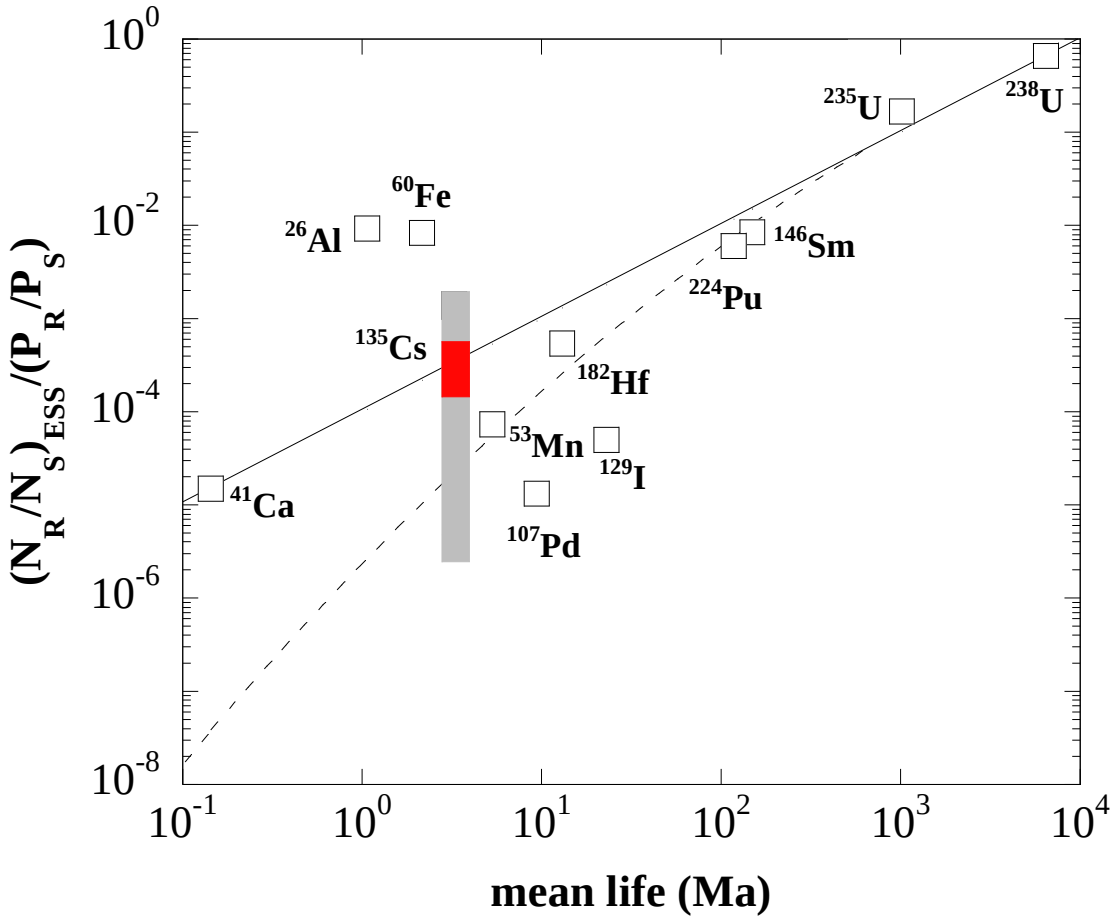

Fig. 10. The correlation diagram between the average ratios of extinct short-lived radioactive isotopes (R) to their stable reference isotope (S) in the early solar system $(N_R/N_S)_{ESS}$ normalized by the production ratios of these isotopes (P_R/P_S) and their mean life (Ma) on a logarithmic scale. The data shown in this figure are based on previous studies (Wasserburg et al., 1996; Busso et al., 1999). The production ratio of $^{135}Cs/^{133}Cs$ was obtained from the previous study (Harper, 1996). The gray zone in the figure is the range of values estimated from the abundance of $^{135}Cs/^{133}Cs$ in previous studies (McCulloch and Wasserburg, 1978; Hidaka et al., 2001, 2003; Hidaka and Yoneda, 2011, 2013; Brennecka and Kleine, 2017). The red symbol means the range of the abundance of $^{135}Cs/^{133}Cs$ estimated in this study. This figure is based on Hidaka and Yoneda (2013).

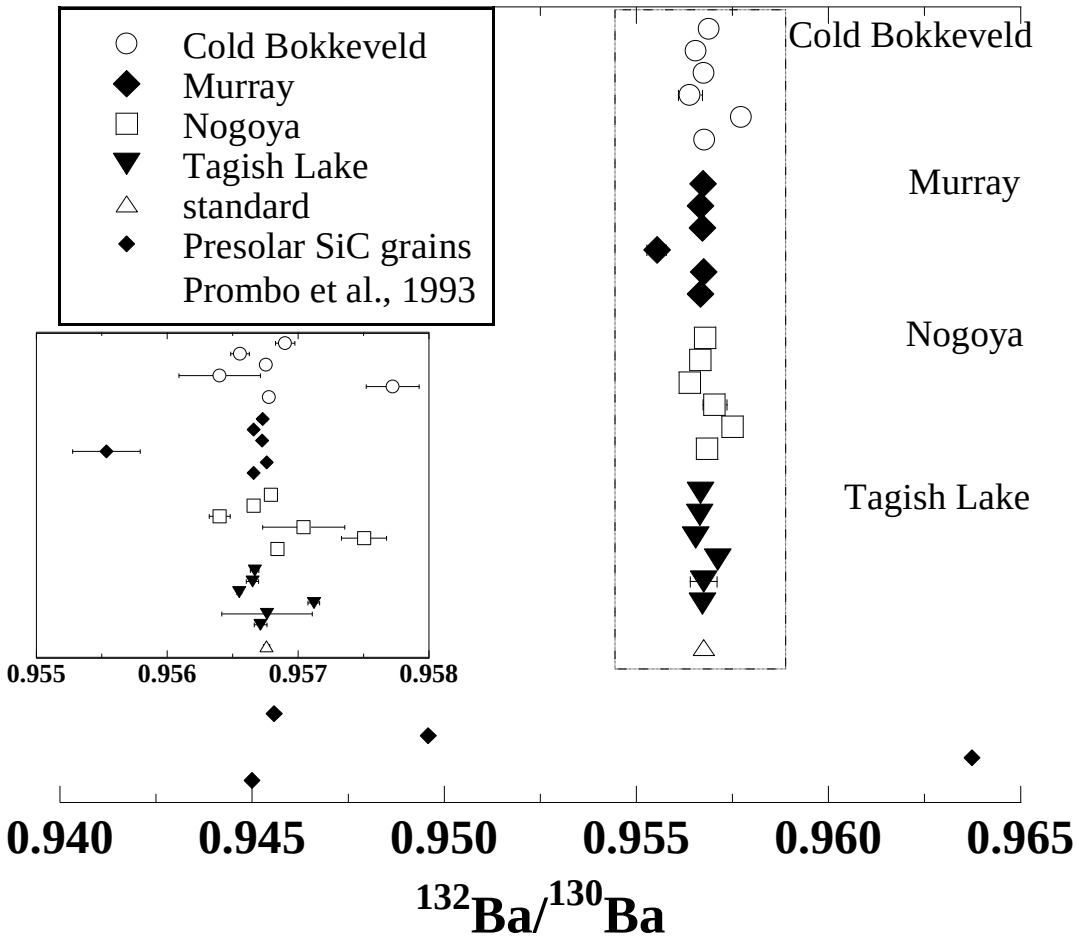

Fig. 11. Calculated $^{132}Ba/^{130}Ba$ ratio from this study and previously reported Ba isotopic data from presolar SiC grains (Prombo et al., 1993).

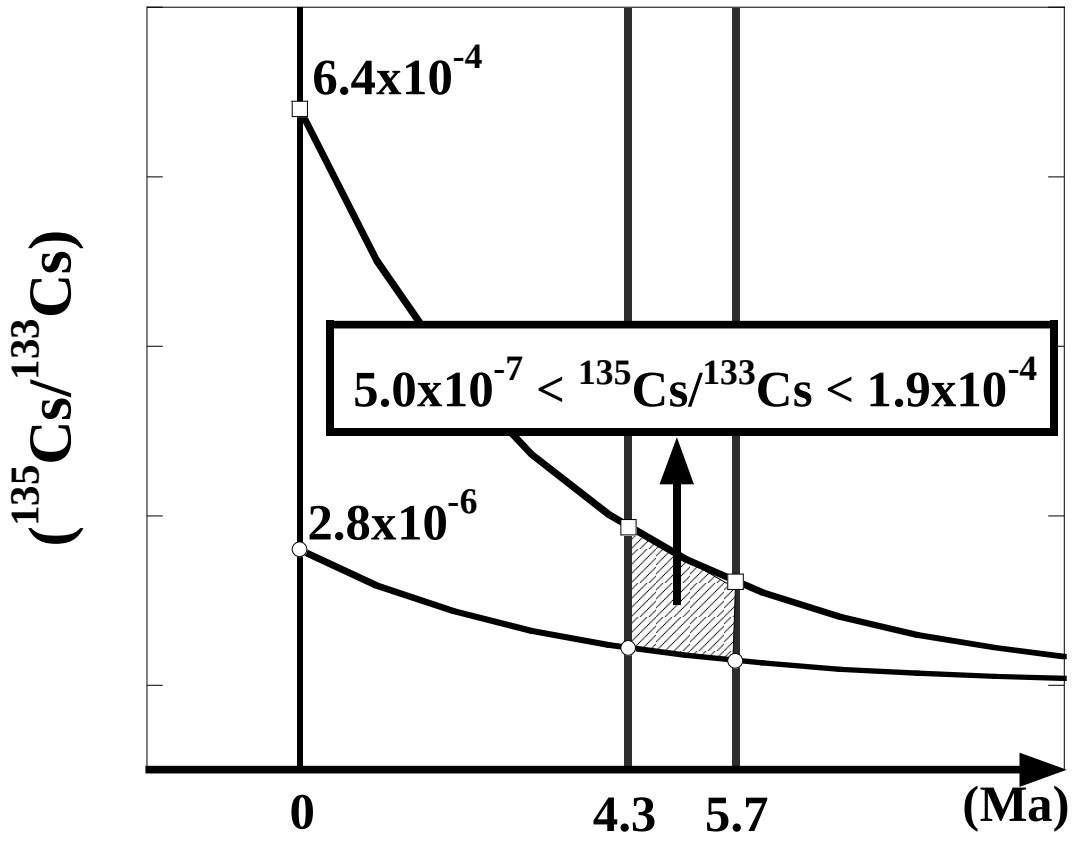

Fig. 12. Variation in the isotopic abundance of ^{135}Cs due to the time course after the formation of CAIs (0). The range of Cs abundance in the early solar system is the maximum and minimum of the values estimated in previous studies (Hidaka and Yoneda, 2013; Brennecka and Kleine, 2017). The shaded zone in the figure indicates the abundance of ^{135}Cs during aqueous alteration in the carbonaceous chondrite parent bodies after the formation of CAIs based on previous studies (Fujiya et al., 2012, 2013).

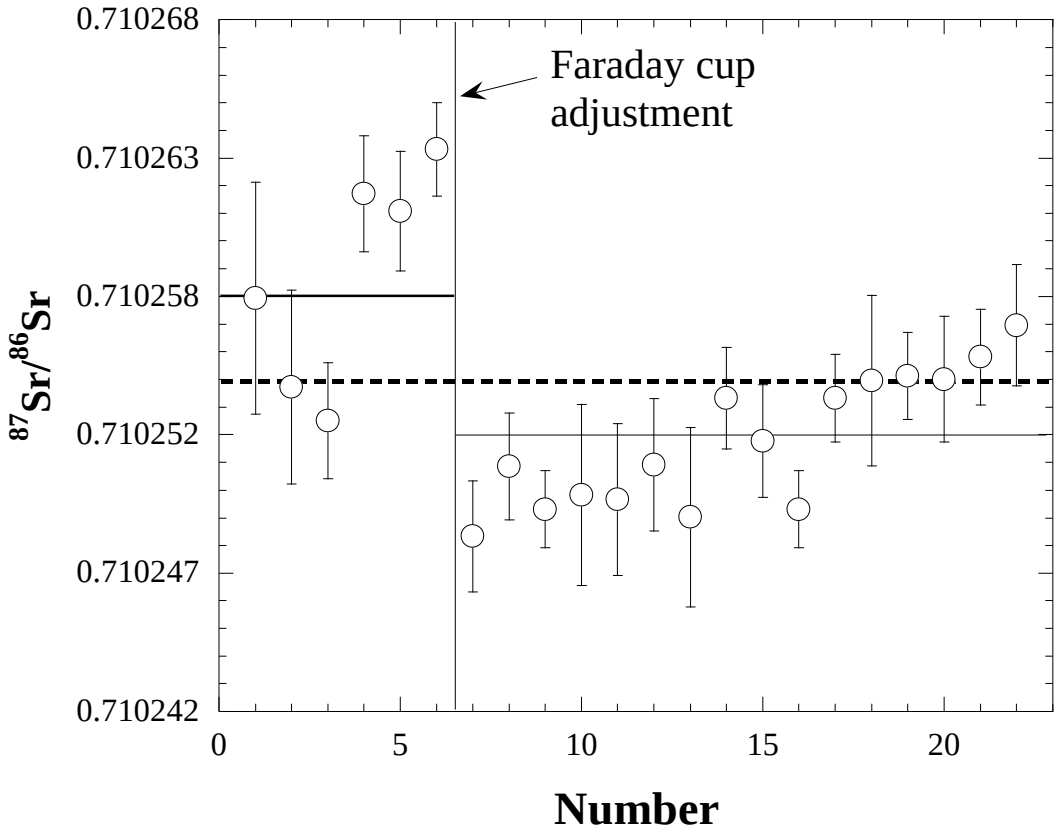

Fig. s1. $^{87}Sr/^{86}Sr$ isotope ratio during the measurement period. The vertical axis is the $^{87}Sr/^{86}Sr$ ratio of the standard sample (NIST 987), and shows the results of isotope analysis of 24 standard samples conducted during the measurement period. The line in the figure indicates the center value, the solid line indicates the value before ($^{87}Sr/^{86}Sr_{NIST}$ = 0.710258 ± 8, 2SE = 11 ppm (n = 6)) and after ($^{87}Sr/^{86}Sr_{NIST}$ = 0.710252 ± 5, 2SE = 7 ppm (n = 16)) adjustment of the detector, and the dottted line indicates the value during the measurement period ($^{87}Sr/^{86}Sr_{NIST}$ = 0.710254 ± 8, 2SE = 11 ppm (n = 22)).

Table 1. List of used samples.

Sample	Type	Mass (g)	Fall/Find	Cosmic ray exposure age (Ma)	Weathering grade
Cold Bokkeveld	CM2.2[a]	0.945	Fall	0.32 ± 0.04[b]	W0-1[a]
Murray	CM2.4/2.5[a]	0.595	Fall	2 ~ 6[c]	W1-2[a]
Nogoya	CM2.2[a]	0.740	Fall	0.14 ± 0.08[b]	W0[a]
NWA4428	CM2 anomalous	1.005	Find	-	-
Tagish Lake	C2-ungrouped	0.389	Fall	5.5 ± 0.7[d]	-

[a] Rubin et al. (2007).

[b] Heyman et al. (1967).

[c] Herzog et al. (1997).

[d] Nakamura et al. (2003).

Table 2. Scheme of chemical separation and purification for Sr and Ba.

	Acid	Volume (mL)
Step1: Separation of Sr and Ba and matrix removal		
AG50WX8, 200–400 mesh, H^+ form (50 mm length × 4.0 mm diameter)		
Resin cleaning	6 M HCl	2.5
	Ultrapure water	2.5
	2 M HNO_3	2.5
	Ultrapure water	2.5
Conditioning	2 M HCl	2.5
Loading	2 M HCl	0.5
Matrix elution	2 M HCl	3.5
Elution Sr	2 M HCl	3.5
Elution Ba	2 M HNO_3	3.0
Elution REE	6 M HCl	4.5
Step2: Purification of Sr		
Eichrom, Sr resin, particle size of 100–150 μm (50 mm length × 4.0 mm diameter)		
Resin cleaning	Ultrapure water	2.5
Conditioning	3 M HNO_3	2.5
Loading	3 M HNO_3	~0.05
Matrix elution	3 M HN O_3	2.5
Elution Sr	Ultrapure water (~60℃)	3.0
Step3: Purification of Ba		
Resin cleaning	Ultrapure water	2.5
	7.5 M HNO_3	2.5
	Ultrapure water	2.5
Conditioning	3 M HNO_3	2.5
Loading	3 M HNO_3	~0.05
Matrix elution	3 M HNO_3	3.5
Elution Ba	7.5 M HNO_3	6.5

Table 3. Faraday cup configuration and zoom optics for Ba and Sr isotopic measurements by the TRITON plus.

Ba isotopic measurements

	Collector									Zoom optics	
	L4	L3	L2	L1	C	H1	H2	H3	H4	Focus (V)	Dispersion (V)
Isotope	^{130}Ba	^{132}Ba	^{134}Ba	^{135}Ba	^{136}Ba	^{137}Ba	^{138}Ba	(^{139}La)	(^{140}Ce)	-7.5	31.0

Sr isotopic measurements

	Collector									Zoom optics	
	L4	L3	L2	L1	C	H1	H2	H3	H4	Focus (V)	Dispersion (V)
Isotope				^{84}Sr	(^{85}Rb)	^{86}Sr	^{87}Sr	^{88}Sr		0	0

Table 4. Trace Elemental Abundances (ppb) in the Chemical separates (L1–L5) and the Whole Rock (WR) of carbonaceous chondrites.

	Cold Bokkeveld																				
	L1			L2			L3			L4			L5			WR			sum		
Rb	730	±	4	149	±	3	232	±	5	42.3	±	1.0	8.64	±	0.37	1,070	±	20	1,162	±	7
Sr	4,610	±	30	1,990	±	10	1,450	±	10	161	±	1	254	±	1	7,840	±	30	8,472	±	29
Cs	32.8	±	0.3	12.1	±	0.7	54.1	±	1.7	22.2	±	1.0	18.7	±	0.7	133	±	3	139.9	±	2.2
Ba	637	±	17	552	±	14	1,450	±	50	194	±	7	50.2	±	0.8	2,710	±	50	2,884	±	53
La	11.2	±	0.3	30.8	±	0.5	231	±	2	24.8	±	0.2	50.2	±	0.8	316	±	3	348.0	±	2.1
Ce	22.8	±	0.5	66.5	±	0.7	590	±	3	65.7	±	0.5	149	±	1	843	±	8	894.0	±	3.3
Pr	3.14	±	0.04	8.97	±	0.22	88.8	±	0.7	10.09	±	0.02	25.4	±	0.2	123	±	1	136.4	±	0.8
Nd	16.8	±	0.5	45.0	±	0.1	446	±	2	51.0	±	0.9	141	±	1	642	±	8	698.9	±	2.7
Sm	5.09	±	0.08	12.5	±	0.4	144	±	1	14.8	±	0.3	52.0	±	0.3	215	±	1	228.9	±	1.4
Eu	2.99	±	0.05	6.5	±	0.3	81.9	±	1.5	7.9	±	0.2	4.8	±	0.2	97.1	±	1.0	104.2	±	1.5
Gd	6.96	±	0.54	17.4	±	0.3	193	±	2	27.4	±	0.7	84.93	±	0.02	301	±	4	330.2	±	1.8
Tb	0.54	±	0.07	2.66	±	0.12	34.6	±	0.4	4.3	±	0.2	16.0	±	0.1	51.6	±	0.8	58.16	±	0.49
Dy	6.08	±	0.25	22.5	±	0.2	238	±	1	32.7	±	0.6	110	±	1	371	±	2	409.1	±	1.9
Ho	1.36	±	0.19	4.42	±	0.21	51.0	±	0.1	7.79	±	0.34	24.7	±	0.9	80.1	±	0.6	89.25	±	1.02
Er	3.85	±	0.14	13.4	±	0.2	157	±	1	21.0	±	0.4	83.1	±	0.3	242.9	±	0.1	278.4	±	1.1
Tm	0.550	±	0.019	2.02	±	0.05	26.1	±	0.1	3.37	±	0.11	10.0	±	0.3	38.5	±	1.8	42.06	±	0.38
Yb	3.71	±	0.09	13.2	±	0.2	172	±	1	23.1	±	0.2	63.2	±	0.3	248	±	2	274.9	±	1.2
Lu	0.44	±	0.06	1.58	±	0.04	22.4	±	0.4	3.76	±	0.45	12.7	±	0.5	36.4	±	0.1	40.90	±	0.76

Analytical errors are shown in 1 S.D. (standard deviations) of runs.

Table 4. continued.

	Murray																				
	L1			L2			L3			L4			L5			WR			sum		
Rb	710	±	4	226	±	2	262	±	6	51.2	±	1.3	178	±	2	1,430	±	50	1,427	±	8
Sr	4,700	±	40	2,790	±	30	2,490	±	30	122	±	4	680	±	3	10,650	±	30	10,790	±	50
Cs	37.4	±	0.8	12.8	±	0.4	37.1	±	1.7	9.7	±	1.2	16.9	±	0.7	114	±	12	113.9	±	2.4
Ba	1,040	±	30	934	±	16	2,350	±	30	161	±	7	998	±	8	5,250	±	170	5,486	±	43
La	15.2	±	0.5	72.0	±	0.1	215	±	3	16.0	±	0.5	123	±	2	453	±	8	441.2	±	3.6
Ce	24.6	±	0.9	150	±	1	508	±	3	40.8	±	1.0	329	±	1	1,070	±	10	1,052.0	±	3.6
Pr	3.51	±	0.36	21.1	±	0.4	71.6	±	1.3	5.75	±	0.10	53.0	±	0.9	150	±	3	155.0	±	1.7
Nd	20.4	±	0.7	98.5	±	1.5	339	±	2	27.1	±	0.9	272	±	2	737	±	6	756.7	±	3.2
Sm	5.43	±	0.11	26.1	±	0.5	95.6	±	0.5	7.79	±	0.47	95.7	±	1.8	227	±	4	230.6	±	2.0
Eu	3.85	±	0.11	17.6	±	0.3	66.5	±	0.4	3.58	±	0.24	10.0	±	0.1	99.1	±	1.0	101.4	±	0.5
Gd	7.85	±	0.50	31.2	±	0.9	117	±	1	13.4	±	0.7	133	±	1	293	±	4	302.5	±	2.2
Tb	1.03	±	0.13	5.72	±	0.07	21.6	±	0.8	2.13	±	0.14	25.1	±	0.2	54.3	±	2.1	55.58	±	0.81
Dy	6.36	±	0.29	38.6	±	0.6	134	±	1	13.1	±	0.4	170	±	1	356	±	2	361.30	±	1.74
Ho	1.37	±	0.19	7.49	±	0.20	30.3	±	0.7	3.07	±	0.24	39.7	±	0.9	79.4	±	1.9	81.96	±	1.22
Er	4.68	±	0.18	22.5	±	0.2	88.0	±	1.1	11.1	±	0.4	128.7	±	0.5	246	±	4	255.08	±	1.26
Tm	0.493	±	0.049	3.37	±	0.25	14.0	±	0.2	1.49	±	0.30	16.4	±	0.3	40.1	±	2.0	35.71	±	0.55
Yb	3.08	±	0.17	21.4	±	0.4	102.4	±	0.4	9.8	±	0.5	105.1	±	0.8	225	±	3	241.72	±	1.07
Lu	0.66	±	0.14	2.59	±	0.33	13.3	±	0.3	1.74	±	0.12	18.7	±	0.4	36.8	±	1.7	36.89	±	0.59

Analytical errors are shown in 1 S.D. (standard deviations) of runs.

Table 4. continued.

	Nogoya																				
	L1			L2			L3			L4			L5			WR			sum		
Rb	858	±	3	245	±	4	290	±	3	70.5	±	1.2	27.5	±	1.1	1,490	±	30	1,490	±	6
Sr	3,700	±	30	3,083	±	3	2,130	±	20	218	±	5	266	±	1	9,220	±	30	9,396	±	39
Cs	32.6	±	2.0	14.8	±	0.7	56.0	±	1.6	16.8	±	0.4	11.6	±	0.2	132	±	14	131.8	±	2.7
Ba	506	±	32	613	±	22	1,290	±	10	176	±	8	90.2	±	3.9	2,660	±	70	2,670	±	43
La	6.3	±	0.2	22.0	±	0.2	214	±	1	20.8	±	0.3	34.1	±	0.3	293	±	1	297.7	±	0.9
Ce	12.3	±	0.3	42.7	±	0.6	533	±	2	55.1	±	0.3	99.3	±	0.2	741	±	9	742.4	±	1.9
Pr	2.26	±	0.11	6.9	±	0.5	84.4	±	1.2	8.69	±	0.25	17.3	±	0.4	122	±	3	119.5	±	1.4
Nd	9.4	±	0.9	30.2	±	1.2	411	±	4	42.0	±	0.8	90.1	±	1.6	570	±	12	582.2	±	4.9
Sm	3.58	±	0.20	10.0	±	0.5	138	±	1	15.9	±	0.4	31.1	±	0.2	193	±	2	198.2	±	1.4
Eu	1.96	±	0.05	4.15	±	0.16	59.1	±	0.6	6.05	±	0.18	3.09	±	0.09	73.8	±	2.0	74.30	±	0.63
Gd	4.53	±	0.16	13.4	±	0.3	189	±	2	33.5	±	0.9	56.6	±	0.8	306	±	5	296.7	±	2.0
Tb	0.74	±	0.11	2.24	±	0.10	32.6	±	1.0	5.28	±	0.38	11.2	±	0.4	51.2	±	1.1	52.1	±	1.1
Dy	4.46	±	0.28	14.9	±	0.2	227	±	1	39.1	±	0.7	83.7	±	0.8	345	±	3	369.4	±	1.5
Ho	0.81	±	0.09	3.46	±	0.32	48.2	±	0.9	7.41	±	0.14	16.7	±	0.7	78.2	±	2.5	76.5	±	1.2
Er	2.88	±	0.16	10.1	±	0.2	147	±	0	20.7	±	0.7	44.5	±	0.5	222	±	2	225.3	±	1.0
Tm	0.515	±	0.090	1.37	±	0.06	22.8	±	0.5	2.83	±	0.22	6.6	±	0.3	30.2	±	1.4	34.20	±	0.61
Yb	3.41	±	0.21	8.41	±	0.24	159	±	2	19.4	±	0.4	36.2	±	0.7	220	±	4	225.9	±	1.9
Lu	0.37	±	0.08	1.16	±	0.10	21.3	±	0.3	3.63	±	0.21	6.02	±	0.16	32.5	±	1.4	32.43	±	0.43

Analytical errors are shown in 1 S.D. (standard deviations) of runs.

Table 4. continued.

	NWA 4428																	
	L1			L2			L3			L4			L5			WR			sum		
Rb	335	±	7	82.5	±	3.9	252	±	1	125	±	1	308	±	3	1,010	±	30	1,103	±	9
Sr	22,100	±	100	11,000	±	100	12,400	±	100	1,330	±	10	730	±	11	45,500	±	100	47,560	±	150
Cs	24.1	±	1.2	6.5	±	0.6	27.5	±	0.7	32.9	±	0.9	29.6	±	0.5	123	±	9	120.6	±	1.8
Ba	8,200	±	60	7,960	±	20	20,300	±	100	5,150	±	70	1,470	±	4.0	38,100	±	500	43,020	±	140
La	2.72	±	0.08	21.0	±	0.5	281	±	2	50.1	±	0.4	139	±	1	501	±	1	493.8	±	2.2
Ce	5.88	±	0.24	40.6	±	0.9	690	±	5	121	±	1	304	±	2	1,153	±	3	1,161	±	5
Pr	0.91	±	0.08	5.76	±	0.10	102	±	1	17.3	±	0.4	41.2	±	0.6	165	±	5	167.5	±	1.1
Nd	4.72	±	0.19	25.9	±	0.6	490	±	2	79.3	±	0.5	185	±	1	784	±	12	785.0	±	2.2
Sm	1.86	±	0.11	8.86	±	0.22	169	±	2	24.1	±	0.3	54.1	±	0.5	258	±	6	257.5	±	1.7
Eu	2.49	±	0.10	5.68	±	0.24	70.7	±	0.9	10.6	±	0.2	7.28	±	0.23	98.4	±	1.7	96.7	±	1.0
Gd	2.38	±	0.23	10.82	±	0.04	192	±	2	37.6	±	1.0	83.7	±	0.6	327	±	4	326.7	±	2.5
Tb	0.32	±	0.06	1.64	±	0.08	34.9	±	0.1	6.65	±	0.20	16.4	±	0.2	56.8	±	2.5	59.99	±	0.30
Dy	2.23	±	0.23	10.7	±	0.3	227	±	1	45.5	±	0.8	133	±	1	391	±	6	418.2	±	1.6
Ho	0.43	±	0.05	2.28	±	0.24	49.0	±	0.2	10.3	±	0.1	29.2	±	0.5	82.3	±	1.8	91.18	±	0.63
Er	1.62	±	0.10	7.79	±	0.16	149.1	±	0.3	30.9	±	0.2	79.80	±	0.02	245	±	3	269.2	±	0.4
Tm	0.178	±	0.022	1.19	±	0.04	23.8	±	0.3	5.15	±	0.21	9.8	±	0.3	36.1	±	0.7	40.09	±	0.43
Yb	1.23	±	0.11	7.5	±	0.2	152	±	1	35.3	±	0.2	54.0	±	0.7	244	±	2	249.7	±	1.1
Lu	0.252	±	0.016	0.87	±	0.08	21.2	±	0.8	5.13	±	0.19	9.96	±	0.11	34.8	±	0.2	37.43	±	0.84

Analytical errors are shown in 1 S.D. (standard deviations) of runs.

Table 4. continued.

	Tagish Lake																			
	L1			L2			L3			L4			L5			WR			sum		
Rb	1,440	±	30	319	±	5	329	±	2	141	±	1	640	±	3	3,016	±	2	2,869	±	31
Sr	5,970	±	40	2,270	±	10	1,090	±	10	112	±	2	2,048	±	6	11,730	±	10	11,490	±	40
Cs	56.8	±	0.7	23.4	±	0.4	49.0	±	0.4	15.0	±	0.5	15.1	±	0.2	161.3	±	0.3	159.3	±	1.0
Ba	1,430	±	10	1,280	±	20	1,670	±	20	250	±	7	13,590	±	20	10,670	±	10	18,220	±	40
La	27.2	±	1.7	22.5	±	1.1	263	±	9	6.2	±	0.7	45.5	±	2.8	295	±	6	364.3	±	9.6
Ce	52.6	±	0.8	53.5	±	3.8	694	±	5	16.5	±	0.1	60.3	±	3.5	795	±	11	876.9	±	7.2
Pr	7.82	±	0.59	8.2	±	0.1	108	±	2	2.02	±	0.25	10.5	±	1.1	115	±	7	136.3	±	2.4
Nd	45.9	±	5.1	39.3	±	0.9	537	±	11	10.9	±	1.9	42.5	±	3.6	615	±	28	676.1	±	12.4
Sm	12.8	±	1.5	12.5	±	0.6	167	±	4	3.6	±	0.5	7.5	±	1.4	189	±	15	203.4	±	4.3
Eu	5.54	±	0.64	5.55	±	0.79	66.1	±	0.5	1.33	±	0.18	2.32	±	0.30	73.6	±	6.0	80.9	±	1.2
Gd	19.2	±	0.5	20.3	±	0.4	219	±	2	5.5	±	0.5	9.4	±	1.1	277	±	14	273.4	±	2.4
Tb	2.59	±	0.88	3.80	±	0.28	38.1	±	2.1	0.98	±	0.34	1.7	±	0.3	46.3	±	7.4	47.10	±	2.34
Dy	14.6	±	1.6	26.9	±	0.4	267	±	3	6.8	±	0.6	11.4	±	1.1	329	±	3	326.49	±	3.58
Ho	3.01	±	0.72	6.39	±	0.16	55.8	±	3.6	1.28	±	0.32	3.6	±	0.7	66	±	13	70.10	±	3.77
Er	7.01	±	0.20	18.1	±	0.5	170	±	3	5.2	±	0.2	11.5	±	0.7	196	±	4	211.92	±	2.96
Tm	0.86	±	0.28	2.61	±	0.18	26.1	±	1.9	0.57	±	0.10	1.8	±	0.8	29.7	±	8.1	31.87	±	2.10
Yb	7.28	±	0.22	17.3	±	0.3	175	±	5	4.6	±	0.3	11.5	±	1.1	202	±	7	216.0	±	5.0
Lu	0.85	±	0.42	2.18	±	0.27	25.5	±	1.4	0.66	±	0.43	2.23	±	0.34	30.4	±	0.8	31.46	±	1.56

Analytical errors are shown in 1 S.D. (standard deviations) of runs.

Table 5 (a). Ba isotopic data of L1—L5 and WR of carbonaceous chondrites.

Samples	$^{130}Ba/^{136}Ba$	$^{132}Ba/^{136}Ba$	$^{135}Ba/^{136}Ba$	$^{137}Ba/^{136}Ba$	$^{138}Ba/^{136}Ba$
Cold Bokkeveld					
L1	0.0134807 ± 0.0000021	0.0128997 ± 0.0000021	0.839530 ± 0.000007	1.429306 ± 0.000014	9.13037 ± 0.00012
L2	0.0134875 ± 0.0000020	0.0129015 ± 0.0000023	0.839529 ± 0.000009	1.429288 ± 0.000017	9.13028 ± 0.00016
L3	0.0134847 ± 0.0000005	0.0129015 ± 0.0000005	0.839534 ± 0.000002	1.429276 ± 0.000005	9.13014 ± 0.00005
L4	0.0134884 ± 0.0000088	0.0129003 ± 0.0000088	0.839508 ± 0.000020	1.429343 ± 0.000036	9.13056 ± 0.00034
L5	0.0133102 ± 0.0000056	0.0127475 ± 0.0000059	0.831409 ± 0.000013	1.421938 ± 0.000027	9.11173 ± 0.00026
WR	0.0134798 ± 0.0000004	0.0128972 ± 0.0000005	0.839342 ± 0.000002	1.429087 ± 0.000005	9.12954 ± 0.00005
Murray					
L1	0.0134830 ± 0.0000010	0.0128996 ± 0.0000010	0.839433 ± 0.000004	1.429194 ± 0.000009	9.12985 ± 0.00008
L2	0.0134839 ± 0.0000008	0.0128996 ± 0.0000008	0.839448 ± 0.000004	1.429109 ± 0.000008	9.12913 ± 0.00007
L3	0.0134840 ± 0.0000005	0.0129005 ± 0.0000006	0.839425 ± 0.000002	1.429202 ± 0.000005	9.12980 ± 0.00005
L4	0.0134980 ± 0.0000073	0.0128978 ± 0.0000073	0.839384 ± 0.000018	1.429242 ± 0.000041	9.13021 ± 0.00038
L5	0.0134685 ± 0.0000005	0.0128861 ± 0.0000006	0.838787 ± 0.000003	1.428592 ± 0.000006	9.12825 ± 0.00005
WR	0.0134808 ± 0.0000004	0.0128965 ± 0.0000005	0.839332 ± 0.000002	1.429000 ± 0.000005	9.12869 ± 0.00004

Analytical errors are shown in 2σ of the means.

Table 5 (a). continued.

Samples	$^{130}Ba/^{136}Ba$	$^{132}Ba/^{136}Ba$	$^{135}Ba/^{136}Ba$	$^{137}Ba/^{136}Ba$	$^{138}Ba/^{136}Ba$
Nogoya					
L1	0.0134840 ± 0.0000008	0.0129013 ± 0.0000008	0.839468 ± 0.000003	1.429288 ± 0.000007	9.13017 ± 0.00006
L2	0.0134867 ± 0.0000010	0.0129022 ± 0.0000011	0.839481 ± 0.000004	1.429292 ± 0.000008	9.13035 ± 0.00007
L3	0.0134867 ± 0.0000022	0.0128987 ± 0.0000020	0.839503 ± 0.000007	1.429253 ± 0.000015	9.13012 ± 0.00014
L4	0.0134851 ± 0.0000088	0.0129058 ± 0.0000081	0.839453 ± 0.000019	1.429344 ± 0.000039	9.13095 ± 0.00039
L5	0.0133719 ± 0.0000048	0.0128036 ± 0.0000044	0.834289 ± 0.000012	1.424560 ± 0.000023	9.11791 ± 0.00022
WR	0.0134781 ± 0.0000010	0.0128964 ± 0.0000012	0.839294 ± 0.000005	1.429118 ± 0.000010	9.12968 ± 0.00008
NWA 4428					
L1	0.0134802 ± 0.0000005	0.0128981 ± 0.0000005	0.839297 ± 0.000002	1.429092 ± 0.000005	9.12969 ± 0.00005
L2	0.0134808 ± 0.0000005	0.0128978 ± 0.0000005	0.839329 ± 0.000002	1.429028 ± 0.000005	9.12907 ± 0.00005
L3	0.0134797 ± 0.0000005	0.0128975 ± 0.0000004	0.839319 ± 0.000002	1.429055 ± 0.000005	9.12951 ± 0.00005
L4	0.0134803 ± 0.0000005	0.0128980 ± 0.0000005	0.839295 ± 0.000002	1.429104 ± 0.000005	9.12974 ± 0.00005
L5	0.0134780 ± 0.0000006	0.0128954 ± 0.0000006	0.839155 ± 0.000003	1.428906 ± 0.000006	9.12913 ± 0.00006
WR	0.0134800 ± 0.0000005	0.0128969 ± 0.0000005	0.839275 ± 0.000002	1.429105 ± 0.000005	9.12972 ± 0.00005

Analytical errors are shown in 2σ of the means.

Table 5 (a). continued.

Samples	$^{130}Ba/^{136}Ba$	$^{132}Ba/^{136}Ba$	$^{135}Ba/^{136}Ba$	$^{137}Ba/^{136}Ba$	$^{138}Ba/^{136}Ba$
Tagish Lake					
L1	0.0134816 ± 0.0000009	0.0128978 ± 0.0000009	0.839299 ± 0.000003	1.429085 ± 0.000007	9.12942 ± 0.00007
L2	0.0134904 ± 0.0000013	0.0129058 ± 0.0000012	0.839563 ± 0.000005	1.429323 ± 0.000009	9.12994 ± 0.00009
L3	0.0134860 ± 0.0000006	0.0129014 ± 0.0000006	0.839547 ± 0.000003	1.429295 ± 0.000006	9.12987 ± 0.00005
L4	0.0134905 ± 0.0000013	0.0129043 ± 0.0000013	0.839597 ± 0.000004	1.429374 ± 0.000010	9.13018 ± 0.00009
L5	0.0134921 ± 0.0000097	0.0129136 ± 0.0000097	0.839519 ± 0.000022	1.429327 ± 0.000043	9.13052 ± 0.00041
WR	0.0134765 ± 0.0000014	0.0128938 ± 0.0000013	0.839078 ± 0.000007	1.428888 ± 0.000013	9.12881 ± 0.00012

Analytical errors are shown in 2σ of the means.

Table 5 (b). Ba isotopic deviation of L1–L5 and WR of CM chondrites.

Samples	ε^{130}Ba	ε^{132}Ba	ε^{135}Ba	ε^{137}Ba	ε^{138}Ba
Cold Bokkeveld					
L1	0.21 ± 1.63	1.69 ± 1.75	2.48 ± 0.09	1.70 ± 0.11	0.91 ± 0.15
L2	5.21 ± 1.57	3.09 ± 1.83	2.46 ± 0.11	1.57 ± 0.13	0.81 ± 0.19
L3	3.13 ± 0.63	3.08 ± 0.68	2.52 ± 0.05	1.48 ± 0.06	0.66 ± 0.08
L4	5.88 ± 6.54	2.13 ± 6.84	2.21 ± 0.25	1.96 ± 0.25	1.12 ± 0.37
L5	-126.30 ± 4.20	-116.36 ± 4.58	-94.28 ± 0.16	-49.86 ± 0.19	-19.51 ± 0.29
WR	-0.45 ± 0.59	-0.26 ± 0.66	0.24 ± 0.05	0.17 ± 0.06	0.00 ± 0.08
Murray					
L1	1.62 ± 0.96	1.79 ± 0.99	1.25 ± 0.07	1.10 ± 0.09	0.69 ± 0.12
L2	2.35 ± 0.85	1.81 ± 0.91	1.43 ± 0.06	0.51 ± 0.08	-0.09 ± 0.11
L3	2.38 ± 0.72	2.51 ± 0.77	1.15 ± 0.05	1.16 ± 0.07	0.63 ± 0.09
L4	12.78 ± 5.45	0.46 ± 5.72	0.66 ± 0.22	1.44 ± 0.29	1.09 ± 0.42
L5	-9.14 ± 0.71	-8.65 ± 0.79	-6.45 ± 0.06	-3.11 ± 0.07	-1.06 ± 0.10
WR	0.03 ± 0.67	-0.06 ± 0.71	0.04 ± 0.05	-0.27 ± 0.07	-0.59 ± 0.09

Analytical errors are shown in 2σ of the means.

Table 5 (b). continued.

Samples	ε^{130}Ba	ε^{132}Ba	ε^{135}Ba	ε^{137}Ba	ε^{138}Ba
Nogoya					
L1	1.96 ± 0.78	2.38 ± 0.84	2.26 ± 0.05	1.33 ± 0.07	0.53 ± 0.10
L2	4.03 ± 0.90	3.09 ± 0.98	2.41 ± 0.06	1.36 ± 0.07	0.73 ± 0.10
L3	4.00 ± 1.73	0.33 ± 1.65	2.67 ± 0.09	1.09 ± 0.11	0.47 ± 0.17
L4	2.80 ± 6.56	5.84 ± 6.28	2.08 ± 0.23	1.72 ± 0.28	1.38 ± 0.43
L5	-81.17 ± 3.59	-73.36 ± 3.47	-59.45 ± 0.15	-31.76 ± 0.17	-12.90 ± 0.25
WR	-2.38 ± 0.90	-1.44 ± 1.06	0.19 ± 0.07	0.14 ± 0.08	-0.01 ± 0.11
NWA 4428					
L1	-0.86 ± 0.59	-0.16 ± 0.65	0.22 ± 0.04	-0.04 ± 0.06	0.00 ± 0.08
L2	-0.38 ± 0.59	-0.36 ± 0.64	0.60 ± 0.04	-0.49 ± 0.06	-0.68 ± 0.08
L3	-1.22 ± 0.59	-0.58 ± 0.63	0.48 ± 0.04	-0.30 ± 0.06	-0.20 ± 0.08
L4	-0.75 ± 0.59	-0.23 ± 0.66	0.20 ± 0.05	0.04 ± 0.06	0.05 ± 0.09
L5	-2.45 ± 0.65	-2.21 ± 0.72	-1.47 ± 0.05	-1.34 ± 0.06	-0.61 ± 0.09
WR	-0.95 ± 0.59	-1.02 ± 0.65	-0.04 ± 0.04	0.05 ± 0.06	0.03 ± 0.08

Analytical errors are shown in 2σ of the means.

Table 5 (b). continued.

Samples	ε^{130}Ba	ε^{132}Ba	ε^{135}Ba	ε^{137}Ba	ε^{138}Ba
Tagish Lake					
L1	6.52 ± 1.19	6.24 ± 1.18	3.15 ± 0.07	1.67 ± 0.08	0.58 ± 0.10
L2	3.26 ± 0.79	2.80 ± 0.83	2.96 ± 0.05	1.47 ± 0.07	0.49 ± 0.06
L3	6.59 ± 1.15	5.07 ± 1.21	3.56 ± 0.06	2.02 ± 0.09	0.84 ± 0.12
L4	7.81 ± 7.26	12.25 ± 7.52	2.62 ± 0.26	1.70 ± 0.30	1.21 ± 0.46
L5	-3.81 ± 1.24	-3.12 ± 1.24	-2.64 ± 0.09	-1.37 ± 0.10	-0.67 ± 0.15
WR	1.09 ± 1.17	1.27 ± 1.23	0.45 ± 0.06	0.19 ± 0.09	0.09 ± 0.12

Analytical errors are shown in 2σ of the means.

Table 5 (c). Sr isotopic data of L1–L5 and WR of carbonaceous chondrites.

samples	$\varepsilon^{84}Sr$	$^{84}Sr/^{86}Sr$	$^{87}Sr/^{86}Sr$
Cold Bokkeveld			
L1	0.57 ± 0.26	0.0564915 ± 0.0000011	0.732153 ± 0.000002
L2	0.68 ± 0.23	0.0564921 ± 0.0000009	0.724673 ± 0.000002
L3	0.29 ± 0.30	0.0564900 ± 0.0000014	0.718771 ± 0.000003
L4	1.27 ± 0.54	0.0564955 ± 0.0000029	0.734100 ± 0.000005
L5	-5.85 ± 0.56	0.0564552 ± 0.0000030	0.702536 ± 0.000004
WR	0.34 ± 0.32	0.0564902 ± 0.0000016	0.727275 ± 0.000003
Murray			
L1	0.75 ± 0.21	0.0564870 ± 0.0000007	0.727079 ± 0.000002
L2	1.00 ± 0.20	0.0564884 ± 0.0000006	0.725202 ± 0.000001
L3	0.93 ± 0.22	0.0564880 ± 0.0000008	0.729009 ± 0.000002
L4	-0.12 ± 0.42	0.0564820 ± 0.0000022	0.742027 ± 0.000004
L5	-3.09 ± 1.42	0.0564653 ± 0.0000080	0.710446 ± 0.000010
WR	0.46 ± 0.25	0.0564853 ± 0.0000010	0.726034 ± 0.000002
Nogoya			
L1	0.96 ± 0.20	0.0564882 ± 0.0000009	0.742720 ± 0.000002
L2	0.64 ± 0.20	0.0564864 ± 0.0000008	0.733003 ± 0.000002
L3	0.86 ± 0.20	0.0564876 ± 0.0000008	0.722380 ± 0.000002
L4	7.35 ± 0.51	0.0565234 ± 0.0000028	0.753165 ± 0.000005
L5	-1.44 ± 0.56	0.0564759 ± 0.0000031	0.710736 ± 0.000006
WR	0.53 ± 0.23	0.0564858 ± 0.0000010	0.734171 ± 0.000002

Analytical errors are shown in 2σ of the means.

Table 5 (c). continued.

samples	$\varepsilon^{84}Sr$	$^{84}Sr/^{86}Sr$	$^{87}Sr/^{86}Sr$
NWA 4428			
L1	-0.12 ± 0.19	0.0564844 ± 0.0000007	0.709356 ± 0.000002
L2	0.18 ± 0.19	0.0564861 ± 0.0000007	0.709303 ± 0.000002
L3	0.17 ± 0.20	0.0564860 ± 0.0000009	0.711952 ± 0.000002
L4	0.35 ± 0.49	0.0564870 ± 0.0000027	0.718025 ± 0.000004
L5	-2.36 ± 0.30	0.0564717 ± 0.0000015	0.713558 ± 0.000003
WR	-0.63 ± 0.20	0.0564815 ± 0.0000008	0.710329 ± 0.000002
Tagish Lake			
L1	0.35 ± 0.12	0.0564881 ± 0.0000009	0.737210 ± 0.000002
L2	0.40 ± 0.24	0.0564884 ± 0.0000010	0.725342 ± 0.000002
L3	1.75 ± 0.38	0.0564960 ± 0.0000019	0.729698 ± 0.000003
L4	0.04 ± 1.52	0.0564864 ± 0.0000085	0.782063 ± 0.000012
L5	-0.97 ± 2.22	0.0564806 ± 0.0000125	0.715547 ± 0.000017
WR	6.04 ± 8.01	0.0565203 ± 0.0000452	0.730789 ± 0.000052

Analytical errors are shown in 2σ of the means.

Table 6. The weighted average (WA) of isotopic deviations and isotopic deviations of whole rock (WR).

samples	$\varepsilon^{84}Sr$	$\varepsilon^{130}Ba$	$\varepsilon^{132}Ba$	$\varepsilon^{135}Ba$	$\varepsilon^{137}Ba$	$\varepsilon^{138}Ba$
Cold Bokkeveld						
WR	0.34 ± 0.32	-0.45 ± 0.59	-0.26 ± 0.66	0.24 ± 0.05	0.17 ± 0.06	0.00 ± 0.08
WA	0.37 ± 0.16	0.81 ± 0.72	0.63 ± 0.78	0.79 ± 0.04	0.69 ± 0.05	0.42 ± 0.07
Murray						
WR	0.46 ± 0.25	0.03 ± 0.67	-0.06 ± 0.71	0.04 ± 0.05	-0.27 ± 0.07	-0.59 ± 0.09
WA	0.60 ± 0.15	0.49 ± 0.58	0.24 ± 0.61	-0.18 ± 0.04	0.27 ± 0.05	0.23 ± 0.06
Nogoya						
WR	0.53 ± 0.23	-2.38 ± 0.90	-1.44 ± 1.06	0.19 ± 0.07	0.14 ± 0.08	-0.01 ± 0.11
WA	0.91 ± 0.12	0.66 ± 1.01	-0.77 ± 0.97	0.40 ± 0.05	0.13 ± 0.06	0.15 ± 0.09
NWA 4428						
WR	-0.63 ± 0.20	-0.95 ± 0.59	-1.02 ± 0.65	-0.04 ± 0.04	0.05 ± 0.06	0.03 ± 0.08
WA	0.00 ± 0.11	-0.98 ± 0.34	-0.48 ± 0.37	0.35 ± 0.03	-0.28 ± 0.03	-0.24 ± 0.04
Tagish Lake						
WR	6.04 ± 8.01	1.09 ± 1.17	1.27 ± 1.23	0.45 ± 0.06	0.19 ± 0.09	0.09 ± 0.12
WA	0.26 ± 0.40	0.91 ± 0.41	1.05 ± 0.42	0.38 ± 0.02	0.22 ± 0.03	0.02 ± 0.04

WA indicates a weighted average of isotopic deviations calculated based on the chemical separates of each sample.

WR indicates the measured isotopic data of the whole rock.

Analytical errors are shown in 2σ of the means.

Table 7. Maximum corrected value of ε^{135}Ba after subtraction of s- and n-process components from the total Ba isotopic components based on two models.

	model 1			model 2		
Cold Bokkeveld	12.93	±	0.82	12.94	±	0.55
Murray	0.36	±	0.30	0.36	±	0.17
Nogoya	8.45	±	0.72	8.43	±	0.49

The data of the model 1 and model 2 are calculated by the equations in the Appendix 1 and Appendix 2, respectively.

Table. s1. Ba isotope ratio of standard material for Ba measured during the entire analytical period.

Date	$^{130}Ba/^{136}Ba$	$^{132}Ba/^{136}Ba$	$^{135}Ba/^{136}Ba$	$^{137}Ba/^{136}Ba$	$^{138}Ba/^{136}Ba$
8/17/16	0.0134824 ± 0.0000009	0.0128997 ± 0.0000010	0.839315 ± 0.000003	1.429092 ± 0.000008	9.12946 ± 0.00007
8/17/16	0.0134816 ± 0.0000009	0.0128978 ± 0.0000009	0.839299 ± 0.000003	1.429085 ± 0.000007	9.12941 ± 0.00007
5/10/17	0.0134815 ± 0.0000009	0.0128984 ± 0.0000009	0.839321 ± 0.000004	1.429068 ± 0.000009	9.12935 ± 0.00008
7/6/17	0.0134833 ± 0.0000012	0.0128989 ± 0.0000013	0.839326 ± 0.000005	1.429047 ± 0.000010	9.12909 ± 0.00009
9/7/17	0.0134812 ± 0.0000008	0.0128992 ± 0.0000009	0.839303 ± 0.000004	1.429094 ± 0.000008	9.12966 ± 0.00007
11/16/17	0.0134811 ± 0.0000010	0.0128985 ± 0.0000010	0.839276 ± 0.000004	1.429116 ± 0.000009	9.12986 ± 0.00008
11/17/17	0.0134817 ± 0.0000008	0.0128990 ± 0.0000009	0.839325 ± 0.000003	1.429080 ± 0.000007	9.12966 ± 0.00007
11/20/17	0.0134810 ± 0.0000012	0.0128972 ± 0.0000012	0.839323 ± 0.000005	1.429071 ± 0.000010	9.12963 ± 0.00009
4/23/18	0.0134805 ± 0.0000007	0.0128976 ± 0.0000007	0.839322 ± 0.000003	1.429064 ± 0.000007	9.12954 ± 0.00006
4/23/18	0.0134805 ± 0.0000006	0.0128972 ± 0.0000006	0.839323 ± 0.000003	1.429081 ± 0.000006	9.12970 ± 0.00005
8/8/18	0.0134808 ± 0.0000008	0.0128972 ± 0.0000008	0.839329 ± 0.000004	1.429036 ± 0.000008	9.12922 ± 0.00007
8/10/18	0.0134814 ± 0.0000006	0.0128980 ± 0.0000007	0.839260 ± 0.000003	1.429079 ± 0.000006	9.12947 ± 0.00005
11/14/18	0.0134813 ± 0.0000006	0.0128983 ± 0.0000007	0.839279 ± 0.000003	1.429098 ± 0.000007	9.12969 ± 0.00006
11/18/18	0.0134803 ± 0.0000006	0.0128971 ± 0.0000007	0.839324 ± 0.000003	1.429026 ± 0.000006	9.12918 ± 0.00006

Analytical errors are shown in 2σ of the means.

Table. s2. Sr isotope ratio of standard material for Sr measured during the entire analytical period.

Date	$^{84}Sr/^{86}Sr$			$^{87}Sr/^{86}Sr$		
11/25/16	0.0564861	±	0.0000019	0.710258	±	0.000004
12/6/16	0.0564845	±	0.0000016	0.710254	±	0.000004
11/22/17	0.0564878	±	0.0000010	0.710253	±	0.000002
12/11/17	0.0564876	±	0.0000011	0.710261	±	0.000002
6/22/18	0.0564883	±	0.0000010	0.710261	±	0.000002
6/23/18	0.0564863	±	0.0000009	0.710263	±	0.000002
5/8/19	0.0564827	±	0.0000009	0.710249	±	0.000002
5/10/19	0.0564841	±	0.0000008	0.710251	±	0.000002
5/12/19	0.0564842	±	0.0000006	0.710250	±	0.000001
5/13/19	0.0564856	±	0.0000014	0.710250	±	0.000003
5/13/19	0.0564851	±	0.0000012	0.710250	±	0.000003
5/13/19	0.0564856	±	0.0000011	0.710251	±	0.000002
5/14/19	0.0564828	±	0.0000008	0.710254	±	0.000002
5/14/19	0.0564827	±	0.0000009	0.710252	±	0.000002
5/16/19	0.0564819	±	0.0000015	0.710249	±	0.000003
5/16/19	0.0564842	±	0.0000006	0.710250	±	0.000001
6/11/19	0.0564828	±	0.0000006	0.710254	±	0.000002
6/11/19	0.0564836	±	0.0000014	0.710254	±	0.000003
6/12/19	0.0564819	±	0.0000007	0.710255	±	0.000002
6/12/19	0.0564819	±	0.0000011	0.710255	±	0.000002
6/13/19	0.0564840	±	0.0000007	0.710255	±	0.000002
6/13/19	0.0564816	±	0.0000010	0.710256	±	0.000002
average				0.710254	±	0.000008
						(11 ppm)

Analytical errors are shown in 2σ of the means.